

**UCSF**

**UC San Francisco Electronic Theses and Dissertations**

**Title**

The Consequences of DNA Re-replication

**Permalink**

<https://escholarship.org/uc/item/86h6t4dr>

**Author**

Green, Brian Michael

**Publication Date**

2007-03-16

Peer reviewed|Thesis/dissertation

The Consequences of DNA Re-replication

by

Brian M. Green

DISSERTATION

Submitted in partial satisfaction of the requirements for the degree of

DOCTOR OF PHILOSOPHY

in

Biochemistry and Molecular Biology

in the

GRADUATE DIVISION

of the

UNIVERSITY OF CALIFORNIA, SAN FRANCISCO



**Dedicated to**

Frederic B. Stilmar

Catherine H. Stilmar

Michael P. Green

Dorothy H. Green

Heather B. Green

Elisabeth G. Green

## Acknowledgements

First I wish to thank my advisor, Dr. Joachim Li. I can honestly say that I would not have learned as much about how to be a scientist in any other laboratory. Joachim cares deeply about his students and trains them to be rigorous, careful and inventive thinkers. He has given me the freedom to learn from my mistakes while providing assistance whenever I needed it. Joachim and Anita have also been personally supportive and for all of that I am very grateful.

Thanks also to my thesis committee, who deserve exceptional gratitude for always being able to schedule committee meetings despite the fact that they were based on different campuses from mine. Dr. Thea Tlsty provided excellent suggestions regarding the directions of research that I should pursue and useful ideas about how to make my work more relevant to human disease. Dr. Dave Toczyski was very helpful with all aspects of my work, but particularly when my research required knowledge of DNA damage. Although not formally on my thesis committee, Dr. Dave Morgan was always willing to listen to my future plans and provide input into research directions.

I would next like to thank current and former members of the Li lab. Dr. Van Nguyen's work was the base on which I built my research and he helped me repeatedly with experimental assays. My fellow students Richard Morreale, Leslie Chu and Muluye Liku have been a lot of fun to go through graduate school with and have really helped with the details of my work. In particular, Rich has been a constant sounding board for my crazy ideas and I really appreciate his tireless willingness to talk about our research. Other Li lab members, including Erin Quan, Emily Wang, Bilge Ozaydin, Laura

Goodwin have all contributed ideas to my research. Marian Tse, Frank Castro, Saroya Pedamonte, Jeff Cheung and Ellen Dinglasian have made media, helped me with experiments or washed dishes and without their help, graduate school would have been much more challenging. Thanks also to members of the Toczyski and Morgan labs for their great help during our joint lab meetings.

Finally, I want to thank my family. My grandparents, Gramma and Grandfud, have supported my scientific inclinations from at least the seventh grade when I was testing the pH of leaf mulch. Every phone conversation, Grandfud asks, “How are the bugs treating you?” and their interest in my research has been really wonderful. My parents and sister have allowed me to follow my interests and been fantastically supportive and loving. And to Dr. Elisabeth Green, my absolutely amazing wife, I extend my deepest gratitude. Her love and help have enabled me to weather the ups and downs that are inherent to graduate school. Words cannot do justice to all that she means to me, but without her, this would not have been possible.

Chapters 2 and 6 of this dissertation are reprints of material as it appears in Green BM, Morreale RJ, Ozaydin B, Derisi JL, Li JJ (2006). Genome-wide mapping of DNA synthesis in *Saccharomyces cerevisiae* reveals that mechanisms preventing reinitiation of DNA replication are not redundant. *Mol Biol Cell* 17, 2401-14. Chapter 3 of this dissertation is a reprint of material as it appears in Green, BM and Li, JJ (2005). Loss of Rereplication Control in *Saccharomyces cerevisiae* Results in Extensive DNA Damage. *Mol Biol Cell* 16, 421-432. Chapters 4 and 7 of this dissertation are reprints of material which has been submitted for publication, Green, BM and Li, JJ (2007).

## **Contributions to Described Work**

The work in Chapters 2 and 6 was published in *Molecular Biology of the Cell* by me, Richard Morreale, Bilge Ozaydin, Joe DeRisi and Joachim Li. Richard Morreale and I were co first authors. I contributed to the design of all experiments and contributed to writing and editing the manuscript. I executed the experiments in Figures 2A, 2C, 4A, 4B, 5A, 5B, 5C, 5D, 6A, 6B, 6C, 6D and 7A. I wrote the computer program used to analyze and display Figures 1B, 1D, 2B, 2D, 3B, 4C, 4D, 5E, 6E, 7B and 7C. Richard Morreale executed the physical experiments for those figures with help from Bilge Ozaydin for Figures 4C, 4D and 6E. Richard Morreale executed the experiments in Figures 1A, 1C, 1E and 3A.

The work in Chapter 3 was published in *Molecular Biology of the Cell* by me and Joachim Li. I contributed to the design of all experiments, executed all experiments and contributed to writing and editing the manuscript.

The work in Chapters 4 and 7 has been submitted for publication. I contributed to the design of all experiments, executed all experiments and contributed to writing and editing the manuscript.

## The Consequences of DNA Re-replication

**Brian M. Green**

To maintain genomic stability, reinitiation of eukaryotic DNA replication within a single cell cycle is blocked by multiple mechanisms that inactivate or remove replication proteins after G1 phase. Joachim's lab had previously shown that simultaneous deregulation of three replication proteins, ORC, Cdc6, and Mcm2-7, was necessary to cause detectable bulk re-replication in G2/M phase in *Saccharomyces cerevisiae*. I have helped to refine this understanding and have identified a number of deleterious consequences of re-replication. First, we used microarray comparative genomic hybridization (CGH) to provide a more comprehensive and detailed analysis of re-replication. This genome-wide analysis suggests that reinitiation in G2/M phase primarily occurs at a subset of both active and latent origins, but is independent of chromosomal determinants that specify the use and timing of these origins in S phase. We also showed that very limited re-replication can be detected by microarray CGH when only two replication proteins are deregulated, suggesting that the mechanisms blocking re-replication are not redundant.

I was next interested in both the short and long term consequences of re-replication. I first focused on short term consequences and demonstrated that re-replication rapidly blocks cell proliferation and activates the classical DNA damage-induced checkpoint response. Strikingly, re-replicating cells accumulate



subchromosomal DNA breakage products, demonstrating that re-replication leads to DNA double strand breaks.

To address the long term consequences of re-replication, I decided to focus on gene amplification. Gene amplification, a stable increase in the copy number of a region of DNA, is frequently observed in tumors and is thought to be a driving force in tumorigenesis. There are numerous cases of tumor cells, however, with amplicons that are not readily explained by current models. I demonstrated that re-replication is a potent inducer of gene amplification that generates structures similar to these previously unexplained amplicons. The high frequency at which these amplification structures are generated is specific to re-replication, as similar structures are not observed when S phase DNA replication is impaired or DNA is directly damaged. I thus propose that re-replication arising from loss of replication control is a potential source of the genomic instability important for tumorigenesis.

## Table of Contents

	<u>page</u>
<b>CHAPTER 1</b> Introduction	1
<b>CHAPTER 2</b> Genome-wide mapping of DNA synthesis in <i>Saccharomyces cerevisiae</i> reveals that mechanisms preventing reinitiation of DNA replication are not redundant	21
<b>CHAPTER 3</b> Loss of Rereplication Control in <i>Saccharomyces cerevisiae</i> Results in Extensive DNA Damage	82
<b>CHAPTER 4</b> Loss of DNA Replication Control is a Potent Inducer of Gene Amplification	131
<b>CHAPTER 5</b> Conclusions	159
<b>CHAPTER 6</b> Supplemental data for Chapter 2	174
<b>CHAPTER 7</b> Supplemental data for Chapter 4	223

## List of Tables

	<u>page</u>	
<b>CHAPTER 2</b>		
Table 1	Plasmids used in Chapter 2	56
Table 2	Strains used in Chapter 2	57
Table 3	Oligonucleotides used in Chapter 2	60
<b>CHAPTER 3</b>		
Table 1	Strains used in Chapter 3	117
Table 2	Oligonucleotides used in Chapter 3	120
<b>CHAPTER 6</b>		
Table S1	CGH on spotted microarrays accurately identifies S phase replication origins	196
<b>CHAPTER 7</b>		
Table 1	Strains used in Chapter 4	228
Table 2	Plasmids used in Chapter 4	230
Table 3	Oligonucleotides used in Chapter 4	231

## List of Figures

	<u>page</u>
<b>CHAPTER 2</b>	
Figure 1	Use of comparative genomic hybridization (CGH) on spotted microarrays to assay DNA replication 62
Figure 2	Re-replication induced during G2/M phase when ORC, Mcm2-7, and Cdc6 are deregulated 65
Figure 3	Deregulation of ORC, Mcm2-7, and Cdc6 can induce re-replication in S phase 68
Figure 4	Re-replication induced upon release from a G1 arrest when ORC, Mcm2-7, and Cdc6 are deregulated 70
Figure 5	Re-replication can be induced when only ORC and Cdc6 are deregulated 73
Figure 6	Re-replication occurs primarily on a single chromosome when Mcm2-7 and Cdc6 are deregulated 76
Figure 7	The re-replication arising from deregulation of both Mcm2-7 and Cdc6 depends on ARS317 and Cdc7 79
<b>CHAPTER 3</b>	
Figure 1	Induction of rereplication rapidly blocks cell proliferation 121
Figure 2	Rereplication induces a RAD53-dependent checkpoint response 123

Figure 3	Subnuclear Ddc2p foci consistent with DNA damage are formed when rereplication is induced	125
Figure 4	The checkpoint response induced by rereplication is dependent on Rad9p and not Mrc1p.	127
Figure 5	Rereplication induces double-stranded breaks.	129
 <b>CHAPTER 4</b>		
Figure 1	Gene amplification assay	147
Figure 2	Re-replication induces segmental duplications	149
Figure 3	Re-replication leads to head to tail gene amplification	151
Figure 4	Underreplication does not lead to significant gene amplification	153
Figure 5	DNA damage does not lead to significant gene amplification	155
Figure 6	Model for re-replication induced gene amplification	157
 <b>CHAPTER 5</b>		
Figure 1	Potential mechanism of gene amplification induced by re-replication	172
 <b>CHAPTER 6</b>		
Figure S1	Example of raw data from a re-replication microarray experiment	197

Figure S2	Replication profiles generated by comparative genomic hybridization	199
Figure S3	The S phase replication profile of the re-replication competent OMC strain and the congenic wild-type strain are similar	201
Figure S4	Replication timing in the OMC re-replication competent mutant correlates with replication timing in the A364a background	203
Figure S5	Different strain backgrounds have very similar replication timing profiles	205
Figure S6	Replication timing in the S288c background strongly correlates with replication timing in the A364a background	207
Figure S7	Re-replication induced during G2/M phase when ORC, Mcm2-7 and Cdc6 are deregulated	209
Figure S8	The observed mean distance from re-replication peaks to pro-ARSs is highly significant	211
Figure S9	OMC cells can re-initiate and re-replicate within S phase	213
Figure S10	Re-replication induced upon release from a G1 arrest when ORC, Mcm2-7 and Cdc6 are deregulated	215
Figure S11	Re-replication can be induced when only ORC and Cdc6p are deregulated	217
Figure S12	Re-replication occurs primarily on a single chromosome when Mcm2-7 and Cdc6 are deregulated	219
Figure S13	MC <sub>2A</sub> - <i>cdc7</i> strain is competent to re-replicate at the	221

permissive temperature

**CHAPTER 7**

Figure S1	Breakage fusion bridge cycles	233
Figure S2	Re-replication induces segmental duplications at another locus	235

## **CHAPTER 1**

### **Introduction**



## Introduction

Eukaryotic DNA replication is tightly controlled such that every segment of the genome is replicated once and only once each cell cycle. Two seemingly incompatible conditions must be met for this to occur. First, because the genomes of eukaryotes are large and replication cannot efficiently occur from only one origin, replication has to nearly simultaneously initiate from hundreds to thousands of sites. Coordination of initiation of replication would be difficult enough without having the second condition: re-replication must be prevented. Once an origin initiates in S phase, the cell must prevent that origin, and any other replicated stretches of DNA, from reinitiating. This block must be maintained throughout the remainder of the cell cycle until the subsequent S phase.

Studies from many labs have led to a model for the block to re-initiation that is based on the division of the cell cycle into two mutually exclusive stages<sup>1-3</sup>. Essentially, cells prepare, but do not initiate, origins in one part of the cell cycle and initiate, but do not prepare, origins in the rest of the cell cycle. In the first stage, which is restricted to the G1 phase, pre-replicative complexes (preRCs, see below) assemble at origins of replication. In the second stage, which is restricted to the S, G2, and M phases, preRCs are activated to initiate DNA replication by two kinases, a cyclin-dependent kinase (CDK) and Cdc7 kinase. PreRC assembly is excluded from the S, G2, and M phases because the activation of CDKs prevents preRC assembly. Origin activation is excluded from the G1 phase, because the two kinases that trigger initiation are only activated after completion of that phase. In this way, a single cell cycle is coupled to exactly one round of replication.

### Initiation of DNA replication

The precise mechanisms required for initiation of eukaryotic DNA replication are beginning to be determined<sup>3</sup>. In short, a pre-replicative complex, or preRC, of replication components is assembled at origins of DNA replication during the G1 phase. The preRC consists of the DNA binding complex ORC, the putative replicative helicase, Mcm2-7, and two proteins thought to recruit Mcm2-7, Cdc6 and Cdt1. Once cells pass the G1 commitment point, Start, and cyclin dependent kinase (CDK) activities rise, additional proteins are recruited to the preRC and replication initiation occurs. Bidirectional replication forks are then established, which proceed away from the origin, and the preRC is disassembled.

In the budding yeast *Saccharomyces cerevisiae*, DNA replication initiation occurs from approximately 300 origins<sup>4</sup>. In *S. cerevisiae*, DNA replication occurs from well defined 100 to 150bp sequences with several 10 to 12bp A/T rich stretches<sup>5</sup>. In higher eukaryotes, there can be upwards of thousands of origins and the sequence specificity of initiation appears to be more permissive. Origins tend to be much larger, several kilobases, and consist of zones of initiation where replication can initiate from a number of different sequences<sup>6</sup>. Even more extreme is replication in the embryonic systems of *Drosophila melanogaster* and *Xenopus laevis*, where it appears that nearly any sequence of DNA will initiate efficiently<sup>6</sup>. Although there are a number of differences in the requirements for specific sequence elements, most of the protein components involved in DNA replication appear to be conserved from yeast to humans<sup>3</sup>.

In all eukaryotes, it appears that the origin recognition complex (ORC) binds to DNA and is initially required for the recruitment of all other preRC components<sup>3</sup>. This six subunit complex was originally identified in *S. cerevisiae* using genetic<sup>7</sup> and biochemical<sup>8</sup> means. Three of the six subunits of ORC (Orc1, Orc4 and Orc5) are members of the nucleotide binding AAA+ superfamily and ATP binding by ORC is required for sequence specific binding to origin DNA<sup>9</sup>. It has been shown in yeast that ORC does not exist merely as a landing pad for other preRC components, but that ORC hydrolysis of ATP is required for loading of multiple hexamers of the putative replicative helicase Mcm2-7 onto the DNA<sup>10</sup>.

Two proteins, Cdc6 and Cdt1, are thought to help ORC recruit Mcm2-7 to the preRC. Like ORC, Cdc6 is an AAA+ ATPase superfamily member that hydrolyzes ATP to complete multiple cycles of Mcm2-7 addition to the preRC<sup>11</sup>. A second protein involved in loading the Mcm2-7 complex is Cdt1. In contrast to most of the other preRC components, Cdt1 was first discovered, and is best characterized in, higher organisms<sup>3</sup>. However, *S. cerevisiae* does have a Cdt1 homolog and in the absence of this protein, Mcm2-7 is unable to associate with preRCs<sup>12</sup>.

The heterohexameric Mcm2-7 is thought to be the replicative helicase, despite difficulty in proving this hypothesis<sup>13</sup>. The Mcm2-7 complex consists of 6 different AAA+ ATPase proteins that have been shown to assemble at preRCs in the G1 phase and then travel with the replication fork during replication progression<sup>14</sup>. It has been difficult to show that the Mcm2-7 complex is the replicative helicase because only heterohexamers of a subset (Mcm4, Mcm6 and Mcm7) of the six proteins have been shown to have helicase activity in vitro<sup>15</sup>. This has led to speculation that perhaps a

subcomplex is the active complex, but this is somewhat unlikely since all Mcm2-7 proteins are required for replication initiation and, importantly, elongation in yeast<sup>16</sup>. Regardless of the precise action of the Mcm2-7 complex, it is clear that its recruitment to preRCs and replication forks is essential for replication initiation<sup>13</sup>. Once Cdc6 and Cdt1 help ORC assemble the Mcm2-7 complex onto origins of DNA replication, the preRC is complete and the origin is said to be licensed to initiate.

After cells pass through the cell cycle commitment point Start, the rise of cyclin dependent kinase (CDK) activity allows preRCs to be converted into replication forks. First, the DNA at the origin must be unwound and then the replication fork must be established. Phosphorylation of Sld2<sup>17</sup> and Sld3<sup>18,19</sup> by CDK is required for replication initiation. Additionally, activity of another protein kinase complex, Cdc7/Dbf4, is required, although the substrate of Cdc7 is not known<sup>3</sup>. A large number of proteins are required for the transition from preRC to replication fork, including Cdc45, Sld3, Sld2, Dpb11, the GINS complex and then RPA, PCNA and the DNA polymerases<sup>3,20</sup>. Once a preRC initiates replication, it is disassembled, preventing further initiation from that origin<sup>3</sup>.

### Preventing reinitiation

As discussed above, re-replication is prevented by restricting preRC formation to the G1 phase of the cell cycle. In *S. cerevisiae*, this block seems to be primarily enforced by CDK phosphorylation of a number of preRC components, although our lab has preliminary evidence that the replication fork itself might also be subject to regulation (data not shown). Metazoan cells have at least two additional, CDK-independent,

mechanisms to prevent re-replication<sup>21-23</sup>. Despite adhering to the general principle of two mutually independent replication states, the details by which different organisms prevent re-replication vary. I will first discuss the prevention of re-replication in yeast and then briefly mention the work done in other organisms.

In budding and fission yeast, CDKs appear to down regulate ORC through inhibitory phosphorylation of Orc2 and/or Orc6<sup>24,25</sup> as well as by direct binding to Orc6<sup>26</sup>. How phosphorylation of these ORC subunits leads to their inactivation is not well understood. In *S. cerevisiae*, ORC is bound to the DNA throughout the cell cycle<sup>3</sup>, and thus phosphorylation in the G2 and M phases of the cell cycle does not impact origin binding. Additionally, the direct binding to Orc6 by CDK is only minimally affected by phosphorylation<sup>26</sup>.

In addition to phosphorylating ORC, CDKs inhibit Cdc6 (or the *S. pombe* ortholog Cdc18) by promoting Cdc6/Cdc18 degradation<sup>27-30</sup>, by reducing *CDC6* transcription<sup>31</sup>, and by directly inhibiting Cdc6/Cdc18 through phosphorylation<sup>30</sup> or binding<sup>32</sup>. Some of the early reports relating to CDK control of Cdc6/Cdc18<sup>33-35</sup> were confounded by the fact that overexpression of Cdc6/Cdc18 inhibits CDK activity. Therefore, rather than identifying the key substrates of the CDK, the activity of CDK on other targets was suppressed. Later work, including that done in our lab and this dissertation, was performed with an allele of Cdc6 that does not inhibit the CDK<sup>36</sup>.

Finally, CDKs also promote the nuclear exclusion of Mcm2-7 and Cdt1 in budding yeast<sup>12,37,38</sup>. A number of reports have focused on the question of how CDK activity leads to net export of the Mcm2-7 complex from the nucleus. The most complete analysis of this was done in our lab, and demonstrated that this regulation was due, in

part, to direct phosphorylation of Mcm3<sup>39</sup>. This phosphorylation appears to modulate the activity of both a nuclear localization signal (NLS) and a nuclear export signal (NES) on the Mcm2-7 complex. The localization of the Mcm2-7 complex and Cdt1 is known to be interdependent<sup>12</sup>. In fact, much of the early work perturbing the regulation of the Mcm2-7 complex likely also resulted in disruption of Cdt1 localization.

The contribution of several of these mechanisms to the re-replication block has been confirmed by showing that their disruption can lead to re-replication. Obtaining clear evidence of re-replication within a single cell cycle has generally required the simultaneous disruption of multiple mechanisms, leading to the presumption that these mechanisms are redundant<sup>2,21</sup>. In budding yeast, for example, simultaneous deregulation of ORC phosphorylation, Mcm2-7 localization, and Cdc6 protein levels is needed to easily detect re-replication in the G2/M phase<sup>25</sup>. Similarly, in fission yeast, regulation of Cdc6/Cdc18 expression and phosphorylation, regulation of Cdt1 expression, and Orc2 phosphorylation have been proposed to act redundantly to prevent re-replication<sup>24,40,41</sup>. We will show in Chapters 2 and 6 that re-replication can be detected in *S. cerevisiae* when only two mechanisms are deregulated, but at the time I began my work, many people assumed that these regulations were redundant.

In metazoans, deregulation of multiple mechanisms that prevent re-replication is also normally required to detect loss of replication control. For example, CDKs have been implicated in Orc1 degradation, Cdt1 degradation and Cdc6 nuclear exclusion<sup>2</sup>. Metazoan cells also have a CDK-independent mechanism involving the protein geminin, which binds to Cdt1 and can prevent it from recruiting Mcm2-7 during the S, G2, and M phases<sup>21</sup>. Recent experiments in *Xenopus* and human cells have identified another CDK-

independent mechanism that degrades Cdt1 during the S phase<sup>22,23</sup>. Typically, several of these mechanisms must be deregulated to detect re-replication using current assays<sup>22,42-44</sup>.

The only examples where precise disruption of a single replication control mechanism has led to re-replication are provided by depletion of geminin in certain metazoan cell lines<sup>45-47</sup>. Even in these cases, other unknown factors may be contributing to the observed re-replication as: (1) many cells in the affected cell lines do not exhibit re-replication<sup>46,47</sup>; (2) not all geminin depleted cell lines experience detectable re-replication<sup>48</sup>; and (3) geminin depletion in whole metazoan organisms either does not cause overt re-replication<sup>49,50</sup> or is limited to prolonging DNA synthesis primarily in cell types that normally undergo endoreduplication or gene amplification<sup>51</sup>. None the less, these results support the notion, discussed further in Chapters 2 and 6, that re-replication controls are not redundant and rather provide overlapping protection against accidental and sporadic re-replication.

#### The consequence of re-replication

While re-replication has been proposed to be a source of genome rearrangements for years<sup>52</sup>, it is only recently that the experimental systems have existed to directly test this hypothesis. In fact, although I describe in Chapters 4 and 7 that re-replication leads to gene amplification, at the time of this writing there were no published studies on the long term genomic consequences of re-replication. The most relevant papers to the long term consequences of re-replication do not even discuss re-replication<sup>53,54</sup>. In these manuscripts, it is reported that overexpression of Cdt1 can lead to tumors in mice. In

human cells, overexpression of Cdt1 can lead to re-replication<sup>55</sup> so it is plausible, but unproven, that re-replication might lead to tumorigenesis.

More work has been done on the immediate consequences of re-replication. My contribution to this understanding is described in Chapter 3<sup>56</sup>, but other manuscripts have also helped to elucidate the short term stresses to the cell after induction of re-replication. In yeast, re-replication leads to a loss of viability and a significant DNA damage checkpoint response<sup>26,56-58</sup>. We directly demonstrate chromosomal fragmentation after re-replication in Chapter 3.

Two groups have reported that the induction of re-replication in human cells also induces a checkpoint response. The first group initially reported that re-replication induced by over expression of Cdc6 and Cdt1 activates a DNA damage response<sup>55</sup>, but have subsequently observed that overexpression of Cdc6 alone can induce this response in the absence of any detectable re-replication<sup>45</sup>. Instead, they now report that re-replication induced by geminin depletion leads to what they suspect is a stalled fork response<sup>45</sup>. A second group observes similar events during geminin depletion, which they attribute to either a DNA damage or replication stress response<sup>47</sup>. Both groups report a loss of cell viability after induction of re-replication.

Finally, a very recent paper in *Xenopus* proposes a mechanism to explain DNA damage seen after re-replication<sup>59</sup>. In this manuscript the authors propose that a re-replication event leads to a replication fork that slows or stalls. A second reinitiation event at the same origin will result in another replication fork “chasing” the first fork. If a collision occurs, it will result in a linear fragment being extruded from replication bubble, and the parental strands of DNA will remain intact. While the authors do an



excellent job demonstrating that very small DNA fragments observed after re-replication in their system are due to this extrusion, they fail to convincingly show that the parental DNA is truly intact. Additionally, since the *Xenopus* system permits reinitiation from nearly any sequence, it remains to be determined how well this mechanism can be generalized.

### Gene amplification

When the first reviews were written discussing the consequences of re-replication<sup>52</sup>, gene amplification was proposed to be a possible outcome. This is a reasonable supposition since re-replication leads to extra DNA that could conceivably be stably integrated into the genome. There is a great deal of interest in the mechanisms that generate gene amplification events because of their importance in tumorigenesis. Gene amplification is observed in many tumors, likely contributes to tumor progression and is associated with poor prognosis<sup>60,61</sup>.

Even with the great interest in this problem, the mechanisms behind many gene amplification events are poorly understood<sup>60</sup>. Gene amplifications can be intrachromosomal or extrachromosomal and the amplified structures can be quite diverse. The most popular model for intrachromosomal gene amplification is the breakage-fusion-bridge (BFB) model, but it best explains amplification events exhibiting the following three structural features: (1) amplicons in inverted orientation, (2) deletion of DNA telomeric to the amplified region, and (3) mitotic bridges arising from bipolar tension on dicentric chromosomes<sup>62</sup>. Such structural hallmarks have been documented most

carefully in cell culture systems where gene amplification is induced by drug selection, but some of these have also been observed in tumors <sup>60,61</sup>.

An increasing numbers of tumors, however, have been shown to contain amplified structures incompatible with the BFB model. For example, some of the classic examples of amplified oncogenes in tumors, such as MYCN in neuroblastomas <sup>63</sup> and ERBB2 in breast, ovarian and gastric cancers <sup>64</sup> are arrayed in direct repeats. Although most of the copies of MYCN in neuroblastomas are found at sites other than the starting locus, in at least some cases, there are some situations where an in place, head to tail gene amplification event can be detected <sup>65</sup>. The wide range of structures of gene amplifications in tumors suggests that there may be many mechanisms that lead to these genomic changes.

#### Gene duplication in evolution

Increases in gene copy number are not just important in gene amplification and tumorigenesis, they are also seen to be increasingly critical for evolution and phenotypic variation, which provides the substrate for evolutionary selection. During evolution, gene duplication allows for divergence of the duplicates and formation of new functions <sup>66</sup>, and an estimated 30 to 60% of eukaryotic genes arose from gene duplication events <sup>67</sup>. While some of these duplication events are likely to have occurred during whole genome duplications, many are thought to be due to increases in copy number of a smaller fragment of DNA <sup>66</sup>.

Copy number increases (as well as decreases) have also been suggested as a source of phenotypic variation, following the recent observation that as much as 12% of

the human genome displays copy number variation <sup>68</sup>. The mechanism by which many of these CNVs are generated is completely unknown, since precise structures for most have not been determined. It is, however, intriguing to note that there appears to be enrichment for repetitive sequences near the endpoints of many CNVs. I was interested in determining if sporadic re-replication should be considered as a possible driving force in evolution and phenotypic variation as well as tumorigenesis.

### Dissertation overview

In this dissertation I will describe our efforts to more completely understand re-replication in *S. cerevisiae*. I begin with an analysis of re-replication – what regions of DNA reinitiate during different portions of the cell cycle, what regions reinitiate when different control are perturbed and what combinations of perturbations result in re-replication (Chapters 2 and 6) <sup>69</sup>. I have been primarily interested in the consequences of the loss of replication control and in Chapter 3 <sup>56</sup> I address the immediate consequences of re-replication – demonstrating that re-replication leads to DNA damage. Finally, despite considerable speculation that re-replication might lead to genome instability, Chapters 4 and 7 (submitted for publication) will be the first demonstrations that gene amplification is, in fact, a long term consequence of re-replication.

### **References**

1. Machida, Y. J., Hamlin, J. L. & Dutta, A. Right place, right time, and only once: replication initiation in metazoans. *Cell* **123**, 13-24 (2005).

2. Diffley, J. F. Regulation of early events in chromosome replication. *Curr Biol* **14**, R778-86 (2004).
3. Bell, S. P. & Dutta, A. DNA replication in eukaryotic cells. *Annu Rev Biochem* **71**, 333-74 (2002).
4. Raghuraman, M. K. et al. Replication dynamics of the yeast genome. *Science* **294**, 115-21 (2001).
5. Bell, S. P. Eukaryotic replicators and associated protein complexes. *Curr Opin Genet Dev* **5**, 162-7 (1995).
6. Gilbert, D. M. In search of the holy replicator. *Nat Rev Mol Cell Biol* **5**, 848-55 (2004).
7. Li, J. J. & Herskowitz, I. Isolation of ORC6, a component of the yeast origin recognition complex by a one-hybrid system. *Science* **262**, 1870-4 (1993).
8. Bell, S. P., Kobayashi, R. & Stillman, B. Yeast origin recognition complex functions in transcription silencing and DNA replication. *Science* **262**, 1844-9 (1993).
9. Klemm, R. D., Austin, R. J. & Bell, S. P. Coordinate binding of ATP and origin DNA regulates the ATPase activity of the origin recognition complex. *Cell* **88**, 493-502 (1997).
10. Bowers, J. L., Randell, J. C., Chen, S. & Bell, S. P. ATP hydrolysis by ORC catalyzes reiterative Mcm2-7 assembly at a defined origin of replication. *Mol Cell* **16**, 967-78 (2004).

11. Randell, J. C., Bowers, J. L., Rodriguez, H. K. & Bell, S. P. Sequential ATP hydrolysis by Cdc6 and ORC directs loading of the Mcm2-7 helicase. *Mol Cell* **21**, 29-39 (2006).
12. Tanaka, S. & Diffley, J. F. Interdependent nuclear accumulation of budding yeast Cdt1 and Mcm2-7 during G1 phase. *Nat Cell Biol* **4**, 198-207 (2002).
13. Forsburg, S. L. Eukaryotic MCM proteins: beyond replication initiation. *Microbiol Mol Biol Rev* **68**, 109-31 (2004).
14. Aparicio, O. M., Weinstein, D. M. & Bell, S. P. Components and dynamics of DNA replication complexes in *S. cerevisiae*: redistribution of MCM proteins and Cdc45p during S phase. *Cell* **91**, 59-69 (1997).
15. Ishimi, Y. A DNA helicase activity is associated with an MCM4, -6, and -7 protein complex. *J Biol Chem* **272**, 24508-13 (1997).
16. Labib, K., Tercero, J. A. & Diffley, J. F. Uninterrupted MCM2-7 function required for DNA replication fork progression. *Science* **288**, 1643-7 (2000).
17. Masumoto, H., Muramatsu, S., Kamimura, Y. & Araki, H. S-Cdk-dependent phosphorylation of Sld2 essential for chromosomal DNA replication in budding yeast. *Nature* **415**, 651-5 (2002).
18. Zegerman, P. & Diffley, J. F. Phosphorylation of Sld2 and Sld3 by cyclin-dependent kinases promotes DNA replication in budding yeast. *Nature* **445**, 281-5 (2007).
19. Tanaka, S. et al. CDK-dependent phosphorylation of Sld2 and Sld3 initiates DNA replication in budding yeast. *Nature* **445**, 328-32 (2007).

20. Takayama, Y. et al. GINS, a novel multiprotein complex required for chromosomal DNA replication in budding yeast. *Genes Dev* **17**, 1153-65 (2003).
21. Blow, J. J. & Dutta, A. Preventing re-replication of chromosomal DNA. *Nat Rev Mol Cell Biol* **6**, 476-86 (2005).
22. Arias, E. E. & Walter, J. C. Replication-dependent destruction of Cdt1 limits DNA replication to a single round per cell cycle in *Xenopus* egg extracts. *Genes Dev* **19**, 114-26 (2005).
23. Takeda, D. Y., Parvin, J. D. & Dutta, A. Degradation of Cdt1 during S phase is Skp2-independent and is required for efficient progression of mammalian cells through S phase. *J Biol Chem* **280**, 23416-23 (2005).
24. Vas, A., Mok, W. & Leatherwood, J. Control of DNA rereplication via Cdc2 phosphorylation sites in the origin recognition complex. *Mol Cell Biol* **21**, 5767-77 (2001).
25. Nguyen, V. Q., Co, C. & Li, J. J. Cyclin-dependent kinases prevent DNA re-replication through multiple mechanisms. *Nature* **411**, 1068-73 (2001).
26. Wilmes, G. M. et al. Interaction of the S-phase cyclin Clb5 with an "RXL" docking sequence in the initiator protein Orc6 provides an origin-localized replication control switch. *Genes Dev* **18**, 981-91 (2004).
27. Drury, L. S., Perkins, G. & Diffley, J. F. The cyclin-dependent kinase Cdc28p regulates distinct modes of Cdc6p proteolysis during the budding yeast cell cycle. *Curr Biol* **10**, 231-40 (2000).
28. Drury, L. S., Perkins, G. & Diffley, J. F. The Cdc4/34/53 pathway targets Cdc6p for proteolysis in budding yeast. *Embo J* **16**, 5966-76 (1997).

29. Elsasser, S., Chi, Y., Yang, P. & Campbell, J. L. Phosphorylation controls timing of Cdc6p destruction: A biochemical analysis. *Mol Biol Cell* **10**, 3263-77 (1999).
30. Jallepalli, P. V., Brown, G. W., Muzi-Falconi, M., Tien, D. & Kelly, T. J. Regulation of the replication initiator protein p65cdc18 by CDK phosphorylation. *Genes Dev* **11**, 2767-79 (1997).
31. Moll, T., Tebb, G., Surana, U., Robitsch, H. & Nasmyth, K. The role of phosphorylation and the CDC28 protein kinase in cell cycle-regulated nuclear import of the *S. cerevisiae* transcription factor SWI5. *Cell* **66**, 743-58 (1991).
32. Mimura, S., Seki, T., Tanaka, S. & Diffley, J. F. Phosphorylation-dependent binding of mitotic cyclins to Cdc6 contributes to DNA replication control. *Nature* **431**, 1118-23 (2004).
33. Muzi Falconi, M., Brown, G. W. & Kelly, T. J. cdc18+ regulates initiation of DNA replication in *Schizosaccharomyces pombe*. *Proc Natl Acad Sci U S A* **93**, 1566-70 (1996).
34. Nishitani, H. & Nurse, P. p65cdc18 plays a major role controlling the initiation of DNA replication in fission yeast. *Cell* **83**, 397-405 (1995).
35. Thomer, M., May, N. R., Aggarwal, B. D., Kwok, G. & Calvi, B. R. *Drosophila* double-parked is sufficient to induce re-replication during development and is regulated by cyclin E/CDK2. *Development* **131**, 4807-18 (2004).
36. Elsasser, S., Lou, F., Wang, B., Campbell, J. L. & Jong, A. Interaction between yeast Cdc6 protein and B-type cyclin/Cdc28 kinases. *Mol Biol Cell* **7**, 1723-35 (1996).

37. Nguyen, V. Q., Co, C., Irie, K. & Li, J. J. Clb/Cdc28 kinases promote nuclear export of the replication initiator proteins Mcm2-7. *Curr Biol* **10**, 195-205 (2000).
38. Labib, K., Diffley, J. F. & Kearsley, S. E. G1-phase and B-type cyclins exclude the DNA-replication factor Mcm4 from the nucleus. *Nat Cell Biol* **1**, 415-22 (1999).
39. Liku, M. E., Nguyen, V. Q., Rosales, A. W., Irie, K. & Li, J. J. CDK Phosphorylation of a Novel NLS-NES Module Distributed between Two Subunits of the Mcm2-7 Complex Prevents Chromosomal Rereplication. *Mol Biol Cell* **16**, 5026-39 (2005).
40. Gopalakrishnan, V. et al. Redundant control of rereplication in fission yeast. *Proc Natl Acad Sci U S A* **98**, 13114-9 (2001).
41. Yanow, S. K., Lygerou, Z. & Nurse, P. Expression of Cdc18/Cdc6 and Cdt1 during G2 phase induces initiation of DNA replication. *Embo J* **20**, 4648-56 (2001).
42. McGarry, T. J. & Kirschner, M. W. Geminin, an inhibitor of DNA replication, is degraded during mitosis. *Cell* **93**, 1043-53 (1998).
43. Yoshida, K., Takisawa, H. & Kubota, Y. Intrinsic nuclear import activity of geminin is essential to prevent re-initiation of DNA replication in *Xenopus* eggs. *Genes Cells* **10**, 63-73 (2005).
44. Li, A. & Blow, J. J. Cdt1 downregulation by proteolysis and geminin inhibition prevents DNA re-replication in *Xenopus*. *Embo J* **24**, 395-404 (2005).



45. Zhu, W., Chen, Y. & Dutta, A. Rereplication by depletion of geminin is seen regardless of p53 status and activates a G2/M checkpoint. *Mol Cell Biol* **24**, 7140-50 (2004).
46. Mihaylov, I. S. et al. Control of DNA replication and chromosome ploidy by geminin and cyclin A. *Mol Cell Biol* **22**, 1868-80 (2002).
47. Melixetian, M. et al. Loss of Geminin induces rereplication in the presence of functional p53. *J Cell Biol* **165**, 473-82 (2004).
48. Nishitani, H., Lygerou, Z. & Nishimoto, T. Proteolysis of DNA replication licensing factor Cdt1 in S-phase is performed independently of geminin through its N-terminal region. *J Biol Chem* **279**, 30807-16 (2004).
49. McGarry, T. J. Geminin deficiency causes a Chk1-dependent G2 arrest in *Xenopus*. *Mol Biol Cell* **13**, 3662-71 (2002).
50. Yanagi, K. et al. *Caenorhabditis elegans* geminin homologue participates in cell cycle regulation and germ line development. *J Biol Chem* **280**, 19689-94 (2005).
51. Quinn, L. M., Herr, A., McGarry, T. J. & Richardson, H. The *Drosophila* Geminin homolog: roles for Geminin in limiting DNA replication, in anaphase and in neurogenesis. *Genes Dev* **15**, 2741-54 (2001).
52. Schimke, R. T. Gene amplification in cultured animal cells. *Cell* **37**, 705-13 (1984).
53. Seo, J. et al. Cdt1 transgenic mice develop lymphoblastic lymphoma in the absence of p53. *Oncogene* **24**, 8176-86 (2005).
54. Arentson, E. et al. Oncogenic potential of the DNA replication licensing protein CDT1. *Oncogene* **21**, 1150-8 (2002).

55. Vaziri, C. et al. A p53-dependent checkpoint pathway prevents rereplication. *Mol Cell* **11**, 997-1008 (2003).
56. Green, B. M. & Li, J. J. Loss of rereplication control in *Saccharomyces cerevisiae* results in extensive DNA damage. *Mol Biol Cell* **16**, 421-32 (2005).
57. Archambault, V., Ikui, A. E., Drapkin, B. J. & Cross, F. R. Disruption of mechanisms that prevent rereplication triggers a DNA damage response. *Mol Cell Biol* **25**, 6707-21 (2005).
58. Ikui, A. E., Archambault, V., Drapkin, B. J., Campbell, V. & Cross, F. R. Cyclin and Cdk substrate requirements for preventing re-replication reveal the need for concomitant activation and inhibition. *Genetics* (2006).
59. Davidson, I. F., Li, A. & Blow, J. J. Deregulated replication licensing causes DNA fragmentation consistent with head-to-tail fork collision. *Mol Cell* **24**, 433-43 (2006).
60. Albertson, D. G. Gene amplification in cancer. *Trends Genet* **22**, 447-55 (2006).
61. Savelyeva, L. & Schwab, M. Amplification of oncogenes revisited: from expression profiling to clinical application. *Cancer Lett* **167**, 115-23 (2001).
62. McClintock, B. The Fusion of Broken Ends of Chromosomes Following Nuclear Fusion. *Proc Natl Acad Sci U S A* **28**, 458-63 (1942).
63. Herrick, J. et al. Genomic organization of amplified MYC genes suggests distinct mechanisms of amplification in tumorigenesis. *Cancer Res* **65**, 1174-9 (2005).
64. Kuwahara, Y. et al. Alternative mechanisms of gene amplification in human cancers. *Genes Chromosomes Cancer* **41**, 125-32 (2004).

65. Corvi, R., Savelyeva, L. & Schwab, M. Duplication of N-MYC at its resident site 2p24 may be a mechanism of activation alternative to amplification in human neuroblastoma cells. *Cancer Res* **55**, 3471-4 (1995).
66. Presgraves, D. C. Evolutionary genomics: new genes for new jobs. *Curr Biol* **15**, R52-3 (2005).
67. Ball, C. A. & Cherry, J. M. Genome comparisons highlight similarity and diversity within the eukaryotic kingdoms. *Curr Opin Chem Biol* **5**, 86-9 (2001).
68. Redon, R. et al. Global variation in copy number in the human genome. *Nature* **444**, 444-54 (2006).
69. Green, B. M., Morreale, R. J., Ozaydin, B., Derisi, J. L. & Li, J. J. Genome-wide mapping of DNA synthesis in *Saccharomyces cerevisiae* reveals that mechanisms preventing reinitiation of DNA replication are not redundant. *Mol Biol Cell* **17**, 2401-14 (2006).

## **CHAPTER 2**

**Genome-wide mapping of DNA synthesis in *Saccharomyces cerevisiae* reveals that mechanisms preventing reinitiation of DNA replication are not redundant**

## ABSTRACT

To maintain genomic stability, re-initiation of eukaryotic DNA replication within a single cell cycle is blocked by multiple mechanisms that inactivate or remove replication proteins after G1 phase. Consistent with the prevailing notion that these mechanisms are redundant, we previously showed that simultaneous deregulation of three replication proteins, ORC, Cdc6 and Mcm2-7, was necessary to cause detectable bulk re-replication in G2/M phase in *Saccharomyces cerevisiae*. In this study, we used microarray comparative genomic hybridization (CGH) to provide a more comprehensive and detailed analysis of re-replication. This genome-wide analysis suggests that re-initiation in G2/M phase primarily occurs at a subset of both active and latent origins, but is independent of chromosomal determinants that specify the use and timing of these origins in S phase. We demonstrate that re-replication can be induced within S phase, but differs in amount and location from re-replication in G2/M phase, illustrating the dynamic nature of DNA replication controls. Finally, we show that very limited re-replication can be detected by microarray CGH when only two replication proteins are deregulated, suggesting that the mechanisms blocking re-replication are not redundant. Therefore we propose that eukaryotic re-replication at levels below current detection limits may be more prevalent and a greater source of genomic instability than previously appreciated.

## INTRODUCTION

Eukaryotic cells must replicate each portion of their genome precisely once per cell cycle to faithfully transmit that genome to succeeding generations. This cell cycle control is enforced at the hundreds to thousands of replication origins where replication is initiated. As part of this regulation, cells must prohibit re-initiation within a single cell cycle at every origin for many successive generations. Even a small or occasional slip in this control will lead to re-replication, which can potentially compromise genome integrity. Hence, the block to re-initiation must be absolutely effective and reliable.

Studies from many labs have led to a model for the block to re-initiation that is based on the division of the initiation event into two mutually exclusive stages (reviewed in (Bell and Dutta, 2002; Diffley, 2004; Machida *et al.*, 2005)). In the first stage, which is restricted to G1 phase, potential origins are selected on chromosomal DNA by assembly of the Origin Recognition Complex (ORC), Cdc6, Cdt1, and the putative replicative helicase, Mcm2-7 into pre-replicative complexes (pre-RCs). In the second stage, which is restricted to S, G2, and M phases, potential origins are activated to initiate DNA replication by two kinases, a cyclin-dependent kinase (CDK) and Cdc7 kinase. Since CDK activity prevents pre-RC assembly in S, G2 and M phases and origins are not activated in G1 phase, passage through the cell cycle is coupled to exactly one round of replication.

Although this model provides a framework for understanding once and only once initiation, it does not explain how the block to re-initiation can be maintained with such high fidelity. This fidelity can be readily incorporated into the model if multiple overlapping mechanisms prevent pre-RC reassembly. In fact, multiple CDK-dependent

inhibitory mechanisms that target pre-RC components have been identified in a number of eukaryotic organisms. In budding and fission yeast, CDKs appear to down regulate ORC through inhibitory phosphorylation of Orc2 and/or Orc6 (Nguyen *et al.*, 2001; Vas *et al.*, 2001) as well as by direct binding to Orc6 (Wilmes *et al.*, 2004). Additionally, CDKs inhibit Cdc6 (or the *S. pombe* ortholog Cdc18) by promoting Cdc6/Cdc18 degradation (Drury *et al.*, 1997; Jallepalli *et al.*, 1997; Elsasser *et al.*, 1999; Drury *et al.*, 2000), by reducing *CDC6* transcription (Moll *et al.*, 1991), and by directly inhibiting Cdc6/Cdc18 through phosphorylation (Jallepalli *et al.*, 1997) or binding (Mimura *et al.*, 2004). Finally, CDKs also promote the nuclear exclusion of Mcm2-7 and Cdt1 in budding yeast (Labib *et al.*, 1999; Nguyen *et al.*, 2000; Tanaka and Diffley, 2002), in part by direct phosphorylation of Mcm3 (Liku *et al.*, 2005). In metazoans, CDKs have been implicated in Orc1 degradation, Cdt1 degradation and Cdc6 nuclear exclusion (reviewed in (Diffley, 2004)). In addition, metazoan cells have a CDK-independent mechanism involving the protein geminin, which binds to Cdt1 and can prevent it from recruiting Mcm2-7 during S, G2, and M phase (reviewed in (Blow and Dutta, 2005)).

Obtaining clear evidence of re-replication within a single cell cycle has generally required the simultaneous disruption of multiple mechanisms, leading to the presumption that these mechanisms are redundant (Diffley, 2004; Blow and Dutta, 2005). In budding yeast, for example, simultaneous deregulation of ORC phosphorylation, Mcm localization, and Cdc6 protein levels was needed to detect re-replication in G2/M phase (Nguyen *et al.*, 2001). Similarly, disruption of several regulatory mechanisms leads to re-replication in fission yeast (Gopalakrishnan *et al.*, 2001; Vas *et al.*, 2001; Yanow *et*

*al.*, 2001) and in *Xenopus* replication extracts (McGarry and Kirschner, 1998; Arias and Walter, 2005; Li and Blow, 2005; Yoshida *et al.*, 2005).

In addition to the issue of mechanistic redundancy, the model for the block to re-replication makes predictions that are best examined by a genome-wide analysis of re-replication. First, the re-replication that is induced by deregulating pre-RC assembly should initiate from the potential replication origins used during normal replication. Re-initiation from a few origins has been observed by 2-dimensional gel electrophoresis in both budding (Nguyen *et al.*, 2001) and fission (Yanow *et al.*, 2001) yeast, but genome-wide mapping of re-initiation sites is needed to confirm this prediction. Second, deregulation of pre-RC reassembly should be able to induce re-replication throughout the period from S to M phase. Although Cdt1 overexpression has been shown to prolong S phase in *Drosophila* embryos (Thomer *et al.*, 2004), direct evidence for re-replication within S phase is still lacking. Finally, full deregulation of pre-RC reassembly should allow more than one round of re-initiation and result in rampant re-replication. So far, precise deregulation of replication proteins has led to at most a doubling of genomic DNA content, suggesting that additional inhibitory mechanisms remain to prevent re-replication. A more comprehensive analysis of where re-replication occurs in the genome may provide clues to how re-replication is still inhibited.

We have developed a more sensitive and comprehensive assay for re-replication by adapting and streamlining previously published microarray-based assays for analyzing DNA replication in budding yeast. With this assay we present evidence that re-initiation occurs primarily at a subset of the potential origins normally established for S phase without being strongly affected by the chromosomal determinants that specify the



efficiency and timing of these origins in S phase. Our studies suggest that the limited re-replication observed may be due in part to the fewer initiation sites used for re-replication compared to S phase. Additionally, our studies indicate that some of the mechanisms preventing re-replication in G2/M phase also operate in S phase but that the block to re-replication in these two phases is not identical. Finally, we demonstrate that re-initiation from as few as a single origin is detectable when fewer mechanisms are disrupted, consistent with the notion that these mechanisms are not redundant but are each actively maintaining the high fidelity of the block to re-replication.

## **MATERIALS AND METHODS**

### Plasmids and Strains

All plasmids are described in Table 1, all strains are described in Table 2 and all oligonucleotides are described in Table 3. Supplemental Methods contains detailed description of plasmid and strain construction.

### Yeast media, growth and arrest

Cells were grown in YEP, synthetic complete (SC), or synthetic (S broth) medium (Guthrie and Fink, 1990) supplemented with 2% dextrose (wt/vol), 2% galactose (wt/vol), 3% raffinose (wt/vol), or 3% raffinose (wt/vol) + 0.05% dextrose (wt/vol). For S phase experiments cells were grown overnight in SDC (YJL5038) or SDC-Met,Ura (YJL3248 and YJL5834) and arrested in G1 phase with 50 ng/ml alpha factor (all strains were *bar1*) at 30°C. Cells were released by filtering, washing, and then resuspending in

prewarmed 30°C YEPD containing 100 µg/ml pronase, 100 mM hydroxyurea, and 15 µg/ml nocodazole.

To obtain reproducible induction of re-replication, cells were inoculated from a fresh unsaturated culture containing 2% dextrose into a culture containing 3% raffinose + 0.05% dextrose and grown for 12-15 h the night before the experiment. The *GALI* promoter (*pGALI*) was induced by addition of 2% galactose and the *MET3* promoter (*pMET3*) was repressed by the addition of 2 mM methionine. All experiments were performed at 30°C except where noted. For induction of re-replication in G2/M phase, cells grown overnight in SRaffC-Met,Ura + 0.05% dextrose were pelleted and resuspended in YEP Raff + 2 mM methionine and 15 µg/ml nocodazole. Once arrested (>90% large budded cells), galactose was added to a final concentration of 2%. In experiments with strains containing *cdc7-1*, cells were grown and arrested at 23°C. These cultures were split after arresting in G2/M phase and either kept at 23°C or shifted to 35°C for 1 hour followed by addition of 2% galactose to both cultures

For induction of re-replication during the release from G1 phase into a G2/M phase arrest, cells grown overnight in SRaffC-Met,Ura + 0.05% dextrose were arrested with 50 ng/ml alpha factor (all strains were *bar1*). Once arrested (>95% small budded cells), galactose was added to a final concentration of 2% for 30 minutes. Cells were released by filtering, washing, and then resuspending in prewarmed YEPGal + 2 mM methionine, 100 µg/ml pronase, and 15 µg/ml nocodazole. For the induction of re-replication during a release from G1 phase into S phase, cells arrested and released as described above were resuspended in prewarmed YEPGal + 2 mM methionine, 100 µg/ml pronase, and 100 mM hydroxyurea.

### Flow cytometry

Cells were fixed and stained with 1  $\mu$ M Sytox Green (Molecular Probes, Eugene, OR) as previously described (Haase and Lew, 1997).

### Pulsed Field Gel Electrophoresis (PFGE)

PFGE was performed as described in Green *et al.* (Green and Li, 2005). Probes for *ARS305*, *ARS607* and *ARS1413* were prepared as described in Nguyen *et al.* (Nguyen *et al.*, 2001).

### 2-D Gel Electrophoresis

Neutral-neutral two-dimensional (2-D) gel analysis was performed essentially as described at <http://fangman-brewer.genetics.washington.edu>. The DNA preparation described there is a slight modification of the one used in Huberman *et al.* (Huberman *et al.*, 1987). Modifications to the previous protocols can be found in Supplemental Methods.

### Microarray Assay

Microarrays containing 12,034 PCR products representing every ORF and intergenic region were prepared essentially as described (DeRisi *et al.*, 1997; Iyer *et al.*, 2001) (see Supplemental Methods). Genomic DNA was prepared, labeled and hybridized as described in Supplemental Methods.

### Data analysis

Raw Cy5/Cy3 ratios from scanned arrays were normalized to the DNA content per cell based on the flow cytometry data to determine absolute copy number of each DNA segment. Raw values were then binned and smoothed using Fourier Convolution Smoothing essentially as described (Raghuraman *et al.*, 2001). Peaks in the replication profiles that were both prominent and reproducible among repetitions of an experiment were identified as origins. Details of data analysis (Supplemental Methods) and examples of raw data (Figure S1) are contained in Supplemental Information. The data discussed in this publication have been deposited in NCBI's Gene Expression Omnibus (GEO, <http://www.ncbi.nlm.nih.gov/geo/>) and are accessible through GEO Series accession number GSE4181.

The “experiment variability” was determined using the equation for calculating one standard deviation. Since there were only two DNA preparations used, each of which was hybridized twice, the trials are not truly independent and thus we call these values “experiment variability” rather than standard deviation.

### Scatter Plot

For each pro-ARS (Wyrick *et al.*, 2001), the normalized Cy5/Cy3 ratio of that chromosomal locus during replication or re-replication was determined and plotted. See Supplemental Methods for more details.

## RESULTS

### A simplified microarray CGH assay for DNA replication

We have adapted and streamlined existing microarray assays (Raghuraman *et al.*, 2001; Yabuki *et al.*, 2002) to create a rapid and economical genome-wide assay for yeast DNA replication. Our simplified assay uses comparative genomic hybridization (CGH) to directly measure the increase in DNA copy number arising from replication or re-replication. During S phase replication, the copy number of each DNA segment reflects the timing of its replication because the earlier a DNA segment replicates, the greater the proportion of replicating cells containing a duplication of this segment. Origins, which replicate earlier than neighboring regions, can be localized to chromosomal segments where the copy number reaches a local maxima. Thus, use of microarray CGH to monitor copy number changes across the genome can provide a comprehensive view of the location and efficiency/timing of initiation sites during replication and re-replication.

Figure 1A shows a schematic of our microarray CGH replication assay. Genomic DNA from replicating (or re-replicating) and non-replicating cells is purified and differentially labeled with Cy5 and Cy3. The labeled probes are competitively hybridized to a spotted microarray and the raw Cy5/Cy3 values are normalized such that the average ratio corresponds to the DNA content determined by flow cytometry. Data are smoothed and origins are computationally identified by locating prominent and reproducible peaks in smoothed replication profiles.

Before using the microarray CGH assay to study re-replication, we assessed its reproducibility and its ability to identify known replication origins in the S phase of a wild type S288c strain (flow cytometry data in Figure 1C). Figure 1B and Figure S2

show the mean of the smoothed S phase replication profiles from four hybridizations plus or minus the “experiment variability” (see Methods) for chromosome X. The small variability demonstrates that this technique is highly reproducible. An overlay of our replication profiles with those generated from previously published data (Raghuraman *et al.*, 2001; Yabuki *et al.*, 2002) shows considerable agreement in both peak positions, which reflects origin locations, and peak heights, which reflects origin timing/efficiency. When our peak finding algorithm was applied to our profiles, we obtained origin numbers (212) comparable to those obtained by Raghuraman *et al.* (332) (Raghuraman *et al.*, 2001) and Yabuki *et al.* (260) (Yabuki *et al.*, 2002). Additionally, the alignment of peaks to origins systematically mapped by 2-D gel electrophoresis or ARS plasmid assay was similar to, or better than, published data (Table S1). Together, these data confirm that our streamlined assay is reproducible and accurate.

#### Re-replication competent mutant has a mostly normal S phase

We have previously demonstrated that simultaneous deregulation of three pre-RC components (ORC, Mcm2-7, and Cdc6) leads to limited re-replication in G2/M phase arrested cells (Nguyen *et al.*, 2001). These initiation proteins were deregulated by mutations that make the proteins refractory to CDK regulation. First, the CDK consensus phosphorylation sites of two subunits of the origin recognition complex, Orc2 and Orc6, were mutated, preventing Cdc28/Cdk1 phosphorylation of these subunits (*orc2-cdk6A*, *orc6-cdk4A*). Second, two copies of the SV40 nuclear localization signal were fused to *MCM7* (*MCM7-SVNLS<sub>2</sub>*) to prevent the Cdc28/Cdk1 promoted net nuclear export of the Mcm2-7 complexes. Finally, an extra copy of *CDC6*, containing a partially stabilizing

N-terminal deletion, was placed under control of the galactose inducible promoter (*pGAL1- $\Delta$ ntcdc6*). This strain re-replicates when  $\Delta$ ntcdc6 is induced by addition of galactose and will be referred to as the OMC re-replicating strain in reference to its deregulation of **ORC**, **Mcm2-7**, and **Cdc6**.

A major concern in any genetic analysis of replication control is the possibility that the mutations deregulating replication proteins also disrupt their replication activity. Such a nonspecific perturbation would complicate any interpretation of the resulting phenotype. We and others have previously reported that  $\Delta$ nt-cdc6 expressed under the *CDC6* promoter retains full replication initiation function (Drury *et al.*, 2000; Nguyen *et al.*, 2001). To determine whether the mutations deregulating Orc2, Orc6, and Mcm7 in the OMC strain also preserve their initiation function, we compared S phase of the OMC strain (*orc2-cdk6A orc6-cdk4A MCM7-2NLS pGAL1- $\Delta$ ntcdc6*), when re-replication was not induced, to S phase of the congenic wild-type A364a strain (*ORC2 ORC6 MCM7 pGAL1*). When cells were harvested at the same point in S phase (Figure 1E), the replication profiles for the two strains showed considerable overlap (Figures 1D, S3 and S4) although ORC and Mcm7 mutations cause subtle alterations in the initiation of DNA replication. Because two wild-type strains of different strain backgrounds show nearly identical replication profiles (Figures S5 and S6), we believe these differences reflect subtle alterations in the initiation activity of the mutant ORC and Mcm2-7. Nonetheless, we conclude that, overall, the mutant ORC and Mcm2-7 proteins in the OMC strain retain most of their normal initiation activity.

### Mapping re-initiating origins

A key prediction of the current model for eukaryotic replication control is that pre-RC reassembly and re-initiation should only occur where pre-RCs normally assemble, i.e., the potential origins or pro-ARSs identified by Wyrick *et al.* (Wyrick *et al.*, 2001). In our previous characterization of re-replication induced at G2/M phase in the OMC strain (*orc2-cdk6A orc6-cdk4A MCM7-2NLS pGAL1-Δntcdc6*), we observed three active S phase origins re-initiating by 2-D gel-electrophoresis (Nguyen *et al.*, 2001). To comprehensively examine this prediction throughout the genome, we performed microarray CGH on the re-replicating DNA from OMC cells. This re-replicating DNA (flow cytometry in Figure 2A) was competitively hybridized against DNA from a congenic non-re-replicating strain that lacks the inducible  $\Delta ntcdc6$  and will be referred to as the OM strain (*orc2-cdk6A orc6-cdk4A MCM7-2NLS pGAL1*). Another source of non-re-replicating control DNA is OMC DNA from G1 phase cells, and when this was used, virtually identical results were obtained (data not shown).

The OMC G2/M phase re-replication profiles are shown in Figure 2B and Figure S7. These data confirm that the incomplete re-replication observed by flow cytometry is distributed over all sixteen chromosomes, as was first suggested by their limited entry into the gel during pulsed-field gel electrophoresis (PFGE) ((Nguyen *et al.*, 2001) and Figure 2C). The re-replication profiles also show that individual chromosomes re-replicate very unevenly, with some segments preferentially re-replicating more than others do.

Application of a peak finding algorithm to OMC re-replication profiles identified 106 re-initiating origins. Most of these origins appear to correspond to chromosomal loci



that form pre-RCs in G1 phase as more than 80% of the re-initiating origins map to within 10 kb of a pro-ARS identified by Wyrick *et al.* (Wyrick *et al.*, 2001) as sites of pre-RC binding. The mean distance between the OMC re-initiating origins and the closest Wyrick pro-ARS (Wyrick *et al.*, 2001) is 7.0 kb. This value is highly significant ( $p < 5 \times 10^{-8}$ ) when compared to the mean distances calculated for equivalent numbers of randomly selected chromosomal loci, as a value of 12.3 kb would be expected by chance (Figure S8).

In an accompanying manuscript, Tanny *et al.* (Tanny *et al.*, 2006) have analyzed the re-replication profile of a strain similar to our OMC strain containing the additional perturbation of a mutation of an RXL motif in ORC6 that abrogates CDK binding and results in a slightly increased extent of re-replication. Although both manuscripts use slightly different data analysis and presentation, (our profiles are presented to preserve absolute copy number information at the cost of less distinctive peaks) the re-replication profiles are strikingly similar (compare Figure S7 to Tanny *et al.* (Tanny *et al.*, 2006) Figure S2). Like our results, 80% of the 123 re-replication origins identified by Tanny *et al.* (Tanny *et al.*, 2006) are within 10kb of a Wyrick *et al.* pro-ARS, further supporting the notion that re-replication occurs at normal sites of pre-RC formation. Overlap of origins identified in both studies is considerable, with 64% of the origins in this study within 10kb of an origin in Tanny *et al.* (Tanny *et al.*, 2006) (20% would be expected by chance). This overlap becomes even more striking, 80% overlap (expected value is also 20%), when the top 40 highest peaks in our analysis are compared to peaks identified in Tanny *et al.* (Tanny *et al.*, 2006). Together with our previous confirmation by 2-D gel electrophoresis that ARS305, ARS121, and ARS607 re-initiate (Nguyen *et al.*, 2001),

these genomic data suggest that re-initiation primarily occurs at a subset of potential S phase origins.

The efficiency with which these potential origins re-initiate in G2/M phase, however, does not correlate with the efficiency or timing with which they initiate in S phase. For example, only 38% of the active S phase origins re-initiate with enough efficiency to be identified as peaks during re-replication in G2/M phase. Moreover, some regions that normally replicate late in S phase, such as those near the telomeres of chromosome III, re-replicate very efficiently in G2/M phase, apparently from very inefficient or latent S phase origins in those regions. For a systematic comparison of re-replication efficiency versus replication timing of all potential S phase origins, we plotted the re-replication copy number versus the replication copy number for the set of pro-ARs identified by Wyrick *et al.* (Wyrick *et al.*, 2001) (Figure 2D). The absence of any significant correlation ( $R^2$  of 0.0002) indicates that the efficiency or timing of a replication origin in S phase does not determine its re-replication efficiency during G2/M phase.

#### Mechanisms that prevent re-replication at G2/M phase also act in S phase

The prevailing model for replication control depicts the prevention of re-replication in S, G2, and M phase as one continuous inhibitory period using a common strategy of preventing pre-RC reassembly. Since CDKs are active throughout this period, the model would predict that mechanisms used by CDKs to regulate replication proteins should prevent re-replication throughout S, G2, and M phase. To determine if CDK regulation of ORC, Mcm2-7, and Cdc6, which prevents re-replication within G2/M

phase, also prevents re-replication in S phase, we induced  $\Delta$ ntcdc6 in OMC cells (*orc2-cdk6A orc6-cdk4A MCM7-2NLS pGAL1- $\Delta$ ntcdc6*) as they entered S phase.

OMC cells were arrested in G1 phase with alpha factor, and half the cells were harvested to obtain G1 phase DNA. The remaining cells were induced to express  $\Delta$ ntcdc6 and then released from the G1 arrest into a low concentration of HU to delay their replication and allow us to collect them in S phase. Flow cytometry indicated that the released cells were harvested while still in S phase with a DNA content of 1.4 C (Figure 3A). The S phase and G1 phase DNA were competitively hybridized against the yeast genomic microarray to generate a combined replication/re-replication profile for S phase (Figure 3B and Figure S9).

Because normal S phase replication can account for an increase in DNA copy number from 1 to 2, only DNA synthesis beyond this copy number can be unequivocally attributed to re-replication. As seen in Figure 3B and Figure S9, many early origins acquired a DNA copy number greater than 2; in some cases reaching values greater than 3. In the same profiles other chromosomal regions had copy numbers significantly below 2, confirming that cells were indeed in the midst of S phase. In fact, early origins re-initiated while forks from their first round of replication were still progressing and before many late origins had fired. Similar re-replication profiles were observed for re-replicating cells synchronously harvested in S phase in the absence of hydroxyurea (data not shown). These findings thus directly establish that mechanisms used to prevent re-replication in G2/M phase also act within S phase.

### Cell cycle position can affect the extent and location of re-replication

To determine if the block to re-replication is modulated during progression through the cell cycle, we compared the re-replication profile of OMC cells (*orc2-cdk6A orc6-cdk4A MCM7-2NLS pGAL1-Δntdc6*) that were induced to re-replicate through a complete S phase with the profile associated with re-replication in G2/M phase. To obtain the former profile, both OMC and control OM cells (*orc2-cdk6A orc6-cdk4A MCM7-2NLS pGAL1*) were arrested in G1 phase with alpha factor followed by addition of galactose to induce  $\Delta$ ntdc6 in the OMC strain. Cells were then released from the G1 arrest, allowed to proceed through S phase, and collected at a G2/M arrest 3 hours after the release. DNA prepared from the OMC and OM strains were competitively hybridized to our yeast genomic microarray to obtain a "G1 release" re-replication profile for the OMC cells.

Flow cytometry showed that both the re-replicating OMC and the control OM strain were in the middle of S phase 1 hour after the release (Figure 4A). As expected for actively replicating chromosomes (Hennessy and Botstein, 1991), the chromosomes of these strains were retained in the wells during PFGE (Figure 4B). Two hours after the release, S phase was mostly complete in the control OM strain and its chromosomes reentered the gel during PFGE. In the OMC strain, however, the induction of re-replication prevented chromosomes from reentering the PFGE gel at both 2 and 3 hr timepoints. Because significant re-replication could be induced in OMC cells delayed in S phase, we believe that re-replication during the progression through S phase contributed to the re-replication seen in the G1 release experiment.

Re-replication induced during G1 release of OMC cells was more extensive than re-replication induced in G2/M phase. Despite comparable lengths of induction, flow cytometry reproducibly indicated that the former accumulated a DNA content of 3.2 C while the latter accumulated only 2.7 C (compare 3h time points in Figure 4A to Figure 2A). More extensive re-replication could also be seen by comparing the re-replication profiles induced during the G1 release (Figure 4C and Figure S10) and the G2/M phase arrest (Figure 2B and Figure S7). In general the peaks in the G1 release profiles were taller than the G2/M phase profiles, suggesting that more efficient or more rounds of re-initiation can occur when re-replication is induced during S phase. For example, *ARS305* reached a copy number of 6.6, indicating it re-initiated a second time, as a single round can only generate a maximum copy number of 4. Overall, multiple rounds of re-initiation were observed on more than half of the chromosomes when re-replication was induced during the G1 release. In contrast, multiple rounds of re-initiation occurred at much fewer loci and to a lesser extent when re-replication was induced in G2/M phase.

A peak finding algorithm identified 87 potential re-initiation sites when re-replication was induced during the G1 release experiment. Of these, 85% were located within 10 kb of a Wyrick pro-ARS Wyrick *et al.* (Wyrick *et al.*, 2001). These data suggest that re-replication induced during a G1 release occurs from S phase origins of DNA replication.

In addition to the extent of re-replication, another significant difference between re-replication induced during the G1 release and re-replication induced during G2/M phase was their pattern of origin usage. As discussed above, efficiency of re-replication in G2/M phase was not correlated with origin usage during S phase. In contrast, the

efficiency of re-replication induced during the G1 release exhibited a modest positive correlation with S phase origin timing (Figure 4D). Although we cannot rule out an intrinsic difference in the re-initiation efficiency of early versus late origins when re-replication is induced during the G1 release, the simplest explanation for this correlation is that earlier replicating origins are cleared of pre-RCs earlier, making them available sooner for reassembly of pre-RCs and re-initiation within S phase.

#### Limited re-replication is detectable with fewer genetic perturbations

Our previous analysis of budding yeast re-replication failed to detect re-replication when only two pre-RC components were deregulated in G2/M phase (Nguyen *et al.*, 2001). This observation is frequently cited as evidence that eukaryotic replication controls are highly redundant. Both the increased sensitivity of the microarray CGH assay and the enhanced re-replication observed during a G1 release provided opportunities to reexamine whether these controls are indeed redundant in budding yeast.

As a first step, we examined an "OC" strain (*orc2-cdk6A orc6-cdk4A pGAL1-Δntcdc6*), in which only ORC and Cdc6 are deregulated and compared it to a control "O" strain (*orc2-cdk6A orc6-cdk4A GAL1*), where only ORC is deregulated. In accordance with our previous results (Nguyen *et al.*, 2001), induction of  $\Delta$ ntcdc6 in G2/M phase generated no significant increase in DNA content by flow cytometry (Figure 5A) or chromosome immobilization during PFGE (Figure 5C). Similarly, microarray CGH of DNA prepared from the OC and O strains after three hours of galactose induction in G2/M phase detected no re-replication on fifteen out of sixteen chromosomes (Figure S11). However, limited re-replication could clearly be observed on both arms of

chromosome III (Figure 5E). Thus, the microarray CGH assay can detect re-replication missed by other assays.

We next asked whether we could detect more re-replication in the OC strain by inducing it during a G1 release. In contrast to the results obtained during a G2/M phase induction, significant re-replication was detected by flow cytometry and PFGE within 2 hours of the G1 release (Figure 5B and Figure 5D). The re-replication profile of the OC strain induced during a G1 release (Figure 5E and Figure S11) showed broad re-replication zones of approximately 200-500 kb in width on all chromosomes. These results, along with the re-replication induced during G2/M phase, establish that deregulating just ORC and Cdc6 is sufficient to induce re-replication and thus these inhibitory mechanisms are not truly redundant. The greater amount of re-replication induced during G1 release versus G2/M arrest underscores the dynamic character of the block to re-replication and, in this case, is likely due to the incomplete expulsion of Mcm proteins from the nucleus during S phase.

#### Microarray CGH can detect re-replication initiating primarily from a single origin

To further investigate the question of redundancy in replication control, we examined the consequences of deregulating just Mcm2-7 and Cdc6. We were not able to detect re-replication in the "MC" strain (*MCM7-2NLS pGAL1- $\Delta$ ntcdc6*) whether  $\Delta$ ntcdc6 was induced in G2/M phase or during a G1 release (data not shown). Hence, we further deregulated Cdc6 inhibition by mutating the two full CDK consensus phosphorylation sites on  $\Delta$ ntcdc6 to generate the MC<sub>2A</sub> strain (*MCM7-2NLS  $\Delta$ ntcdc6-cdk2A*). These additional mutations increase the stability of  $\Delta$ ntcdc6 (Perkins *et al.*, 2001).

Expression of  $\Delta$ ntdc6-cdk2A in the MC<sub>2A</sub> strain in either G2/M phase or during a G1 release did not cause a detectable increase in DNA content by flow cytometry (Figures 6A and 6B). However, PFGE suggested that chromosome III re-replicated in a small subset of MC<sub>2A</sub> cells when  $\Delta$ ntdc6-cdk2A was induced under either protocol (Figure 6C and 6D). Microarray CGH provided definitive evidence that re-replication occurred, in this strain, primarily on the right arm of chromosome III (Figure 6E and Figure S12).

To confirm that the very limited DNA re-replication in the MC<sub>2A</sub> strain arose from a canonical re-initiation event, we asked whether this re-replication depended on known origins and initiation proteins. Our peak finding algorithm implicated an initiation event at approximately 297 kb, close to *ARS317*, an inefficient S phase origin located at 291 kb. 2-dimensional gel analysis of *ARS317* (Figure 7A) detected bubble arcs, indicative of replication initiation, in the MC<sub>2A</sub> strain but not the control "M" strain (*MCM7-2NLS pGAL1*). The immediately adjacent origins, *ARS316* and *ARS318*, only displayed fork arcs (data not shown), suggesting that most of the re-replication on the right arm of chromosome III originates from *ARS317*. Deletion of *ARS317*, but not *ARS316* or *ARS318*, in the MC<sub>2A</sub> strain eliminated the bulk of the re-replication detected by microarray CGH (Figure 7B and data not shown), demonstrating that re-replication initiates primarily from a single S phase origin.

We next asked whether this re-replication is dependent on the essential initiation factor, Cdc7-Dbf4 kinase. Both MC<sub>2A</sub> and MC<sub>2A</sub> *cdc7-1* strains were induced to re-



replicate in G2/M phase under permissive (23 °C) and restrictive (35 °C) temperatures for the *cdc7-1* allele. Microarray CGH demonstrated that both strains re-replicated to a similar extent at 23°C (Figure S13), but at 35 °C there was little or no re-replication in the MC<sub>2A</sub> *cdc7-1* strain (Figure 7C). Together, the dependence on both *ARS317* and Cdc7-Dbf4 indicates that the very limited re-replication induced in the MC<sub>2A</sub> strain arises primarily from a single *bona fide* re-initiation event.

## **DISCUSSION**

### Use of microarray CGH as a routine genome-wide assay for budding yeast replication.

We have refined previously published genome-wide replication assays for budding yeast and made them more amenable for routine and widespread use in the study of eukaryotic DNA replication. The previous assays required significant effort and cost to generate a single replication profile and were only used to characterize the normal wild-type S phase (Raghuraman *et al.*, 2001; Yabuki *et al.*, 2002). We have obtained comparable replication profiles using a streamlined protocol, collection of a single time point and inexpensive spotted microarrays. Thus, it is feasible to use our streamlined assay to examine the genome-wide replication phenotypes associated with many different genotypes or physiological conditions.

Re-initiation induced in G2/M phase largely follows the rules of origin selection, but not the rules of origin activation, that govern S phase replication.

We have taken advantage of our microarray CGH assay to perform a genome wide analysis of eukaryotic re-replication. This comprehensive analysis has allowed us to examine several key tenets of the current model for replication control. One important tenet is that re-initiation that arises from deregulation of ORC, Mcm2-7, and Cdc6 occur from sites of pre-RC formation in S phase. The overall concordance of mapped re-replication origins with pro-ARSs suggests that the re-initiation occurs at sites that normally assemble pre-RCs for S phase replication. Although current limitations of the resolution of microarray data prevent a precise match of replication and re-replication origins, in the few cases where this has been directly tested by 2-D gel electrophoresis or deletion analysis (Figure 7 and (Nguyen *et al.*, 2001)), we have confirmed that this is, in fact, the case. Thus, the sequence determinants that select potential origins in S phase appear to be conserved during re-replication.

In contrast to the selection of potential origins, the activation of these origins during re-replication in G2/M phase differs considerably from origin activation during replication in S phase. During S phase replication, poorly understood chromosomal determinant specify which potential origins are activated early, which are activated late, and which remain latent. During re-replication in G2/M phase, all three classes are among the 106 origins that re-initiate, and there is no correlation between the time/efficiency pro-ARSs replicate in S phase and the efficiency with which they re-replicate in G2/M phase. These results suggest that the chromosomal determinants governing S phase origin activation are not preserved during G2/M phase re-replication.

Such a conclusion is consistent with the finding that the temporal program for origin firing in S phase is lost by G2/M phase and must be reestablished upon entry into each new cell cycle (Raghuraman *et al.*, 1997).

The block to re-replication uses a common fundamental strategy implemented in a dynamic manner across the cell cycle

Another important tenet of the replication control model is that the blocks to re-replication in S, G2, and M phase use the same fundamental strategy of preventing pre-RC reassembly. Deregulating the mechanisms that prevent this reassembly in any of these cell cycle phases should thus lead to re-replication. Studies in human, *Drosophila* and *C. elegans* that deregulate geminin (Melixetian *et al.*, 2004), Cdt1 (Thomer *et al.*, 2004), and Cul-4 (which stabilizes Cdt1) (Zhong *et al.*, 2003), respectively, have inferred that re-replication can occur within S phase based on evidence of a prolonged S phase. In this study, we directly demonstrate that cells can re-initiate replication at multiple origins while the first round of replication is still ongoing. Thus, we establish that mechanisms used to prevent re-replication in G2/M phase also prevent re-replication within S phase.

Despite sharing common mechanisms to carry out the same fundamental strategy, the block to re-replication in S phase and G2/M phase are not identical. Two differences are readily apparent when comparing cells re-replicating through S phase during a G1 release with cells re-replicating at a G2/M phase arrest. The first difference is the bias toward re-initiation of early origins that is only observed in the G1 release experiment. The simplest explanation for this bias is suggested by the S phase re-replication profiles, which show re-initiation at early origins occurring before late origins have had a chance

to fire. These observations suggest that early origins clear their replication pre-RCs sooner and are more available for pre-RC reassembly during S phase, although other explanations for this bias cannot be ruled out.

The second difference between the G1 release and G2/M phase re-replication is that the amount of re-replication induced during the G1 release was greater than the amount induced in G2/M phase in both the OMC and OC strains. This difference can be observed by flow cytometry but is most striking when G1 release and G2/M phase re-replication profiles are compared. There are a growing number of examples of mechanisms that vary in their efficacy across the cell cycle, such as Cdc6 degradation in budding yeast (Perkins *et al.*, 2001), Cdt1 degradation in *Xenopus* and humans (Nishitani *et al.*, 2004; Arias and Walter, 2005; Li and Blow, 2005; Yoshida *et al.*, 2005), and geminin inhibition in human cells (Ballabeni *et al.*, 2004). Together these results indicate that the block to re-replication is dynamic with the number and relative contribution of regulatory mechanisms implementing the block changing during the cell cycle.

#### What is limiting re-replication?

A key difference between re-replication and replication in the OMC strain is that a significantly smaller number of origins initiate efficiently during re-replication (106 versus 193). This reduction in origin firing likely contributes to the limited re-replication observed in the OMC strain and suggests that additional mechanisms are still restraining re-initiation. Consistent with both notions, additional mechanisms inhibiting ORC (by CDK binding to Orc6 (Wilmes *et al.*, 2004)) and Cdc6 (by CDK binding to the N-terminus of phosphorylated Cdc6, (Mimura *et al.*, 2004)) have recently been identified in

budding yeast. The latter mechanism is already disrupted in the OMC strain because of the N-terminal deletion of Cdc6. Disrupting the former mechanism in the OMC background moderately enhances re-replication, but this re-replication is still restrained (Wilmes *et al.*, 2004; Tanny *et al.*, 2006), suggesting that still more re-replication controls remain to be identified.

The reduced number of re-initiating pro-ARs, however, may not be the only factor limiting re-replication. Previous work suggests that a single replication fork should be able to replicate 100-200kb (Dershowitz and Newlon, 1993; van Brabant *et al.*, 2001). Our re-replicating profiles show that the amount of DNA synthesis associated with many re-initiating origins is significantly reduced 100-200 kb away from these origins (Figure S7). These data suggest that re-replicating forks may not be able to progress as far as replicating forks, although a more direct analysis of fork movement will be needed to confirm this hypothesis.

#### Multiple nonredundant mechanisms work in combination to reduce the probability of re-replication.

We previously showed that we could reliably detect G2/M phase re-replication by flow cytometry in the OMC strain when ORC, Mcm2-7, and Cdc6 are deregulated, but not when only two of the three proteins were deregulated (Nguyen *et al.*, 2001). Since then, there have been many other examples where multiple replication controls had to be disrupted to detect re-replication (reviewed in (Diffley, 2004; Blow and Dutta, 2005)). These observations have led to the presumption that the eukaryotic replication controls

are redundant. We favor an alternative view that replication controls are not redundant and that disruption of one or a few of controls can lead to low levels of re-replication.

Failure to detect this re-replication has been due to the insensitivity of standard replication assays. In support of the view, the more sensitive microarray CGH assay used in this study was able to detect G2/M phase re-replication in the OC and MC<sub>2A</sub> strains. We did not detect re-replication when only a single mechanism was disrupted, but we note that the microarray CGH assay has its own detection limits and may have difficulty detecting rare or sporadic replication events. The development of even more sensitive single-cell assays that can detect these rare re-replication events may reveal that the chance of re-replication occurring is increased when ORC, Mcm2-7, or Cdc6 is individually deregulated.

Our findings support a model in which the block to re-replication is provided by a patchwork of many mechanisms, each of which contributes to a portion of the block by reducing the probability that re-replication will occur within a cell cycle. The combined action of all these mechanisms is needed to reduce the probability to such low levels that re-replication events become exceedingly rare and virtually prohibited. Successive disruption of these mechanisms does not lead to a sudden collapse of the block after a threshold of deregulation is reached, but instead results in a gradual erosion of the block manifested by incrementally higher frequencies and/or levels of limited re-replication. Because all mechanisms contribute in some way to the block, more than one mechanism or combination of mechanisms can be overridden to generate detectable re-replication. Hence, the fact that disruption of a mechanism is sufficient to induce limited re-

replication does not make it the critical or dominant mechanism in the block to re-replication.

Levels of re-replication likely to contribute to genomic instability and tumorigenesis may not be detectable by most currently available assays.

Because genomic instability is associated with, and possibly facilitates, tumorigenesis, there has been much interest in understanding the derangements in DNA metabolism and cell cycle control that can cause genomic instability. Re-replication is a potential source of genomic instability both because it produces extra copies of chromosomal segments and because it generates DNA damage and/or replication stress (Melixetian *et al.*, 2004; Zhu *et al.*, 2004; Archambault *et al.*, 2005; Green and Li, 2005). Re-replication has also been potentially linked to tumorigenesis by the observation that overexpression of Cdt1, which can contribute to re-replication (reviewed in (Blow and Dutta, 2005)), can transform NIH3T3 into tumorigenic cells (Arentson *et al.*, 2002). However, two considerations have raised concerns about the biological relevance of these potential connections. First, if replication controls are highly redundant, the probability that a cell will spontaneously acquire the multiple disruptions needed to induce re-replicate will be extremely small. Second, we and others have shown that cells undergoing overt re-replication experience extensive inviability (Jallepalli *et al.*, 1997; Yanow *et al.*, 2001; Wilmes *et al.*, 2004; Green and Li, 2005) or apoptosis (Vaziri *et al.*, 2003; Thomer *et al.*, 2004), making cell death a more likely outcome than genomic instability or tumorigenesis.

Our results in this study counter the first concern by challenging the concept of redundancy in replication control and showing that very low levels of re-replication can still be observed when fewer controls are disrupted. We also have evidence that lower levels of re-replication induce lower levels of inviability (data not shown), diminishing the second concern. Consequently, we suggest that re-replication at levels well below current detection limits may occur with greater frequency than previously anticipated and that genomic instability may arise from these low, non-lethal levels of re-replication.

## **ACKNOWLEDGEMENTS**

We thank Adam Carroll, Emily Wang and Marian Tse for assistance in constructing the microarrays. We thank Hiten Madhani, Bruce Alberts, David Morgan, and David Toczyski for helpful discussions and comments on the manuscript and Steve Bell for discussion of results before publication. This work was supported by grants to J.J.L. from the Sandler Program in Biological Sciences, the ACS (RPG-99-169-01-CCG) and the NIH (RO1 GM59704). B.R.M. was supported by an NSF Predoctoral Fellowship (DGE-0202754) and a DOD Breast Cancer Predoctoral Fellowship (W81XWH-04-1-0409). R.J.M. was supported by an NIH Genetics and Cell Biology Training Grant (T32 GM07810).

## **REFERENCES**

Archambault, V., Ikui, A.E., Drapkin, B.J., and Cross, F.R. (2005). Disruption of mechanisms that prevent rereplication triggers a DNA damage response. *Mol Cell Biol* 25, 6707-6721.



- Arentson, E., Faloon, P., Seo, J., Moon, E., Studts, J.M., Fremont, D.H., and Choi, K. (2002). Oncogenic potential of the DNA replication licensing protein CDT1. *Oncogene 21*, 1150-1158.
- Arias, E.E., and Walter, J.C. (2005). Replication-dependent destruction of Cdt1 limits DNA replication to a single round per cell cycle in *Xenopus* egg extracts. *Genes Dev 19*, 114-126.
- Balakrishnan, R., Christie, K. R., Costanzo, M. C., Dolinski, K., Dwight, S. S., Engel, S. R., Fisk, D. G., Hirschman, J. E., Hong, E. L., Nash, R., Oughtred, R., Skrzypek, M., Theesfeld, C. L., Binkley, G., Lane, C., Schroeder, M., Sethuraman, A., Dong, S., Weng, S., Miyasato, S., Andrada, R., Botstein, D., and Cherry, J. M. "Saccharomyces Genome Database".
- Ballabeni, A., Melixetian, M., Zamponi, R., Masiero, L., Marinoni, F., and Helin, K. (2004). Human geminin promotes pre-RC formation and DNA replication by stabilizing CDT1 in mitosis. *Embo J 23*, 3122-3132.
- Bell, S.P., and Dutta, A. (2002). DNA replication in eukaryotic cells. *Annu Rev Biochem 71*, 333-374.
- Blow, J.J., and Dutta, A. (2005). Preventing re-replication of chromosomal DNA. *Nat Rev Mol Cell Biol 6*, 476-486.
- DeRisi, J.L., Iyer, V.R., and Brown, P.O. (1997). Exploring the metabolic and genetic control of gene expression on a genomic scale. *Science 278*, 680-686.
- Dershowitz, A., and Newlon, C.S. (1993). The effect on chromosome stability of deleting replication origins. *Mol Cell Biol 13*, 391-398.

- Diffley, J.F. (2004). Regulation of early events in chromosome replication. *Curr Biol* *14*, R778-786.
- Drury, L.S., Perkins, G., and Diffley, J.F. (1997). The Cdc4/34/53 pathway targets Cdc6p for proteolysis in budding yeast. *Embo J* *16*, 5966-5976.
- Drury, L.S., Perkins, G., and Diffley, J.F. (2000). The cyclin-dependent kinase Cdc28p regulates distinct modes of Cdc6p proteolysis during the budding yeast cell cycle. *Curr Biol* *10*, 231-240.
- Elsasser, S., Chi, Y., Yang, P., and Campbell, J.L. (1999). Phosphorylation controls timing of Cdc6p destruction: A biochemical analysis. *Mol Biol Cell* *10*, 3263-3277.
- Gopalakrishnan, V., Simancek, P., Houchens, C., Snaith, H.A., Frattini, M.G., Sazer, S., and Kelly, T.J. (2001). Redundant control of rereplication in fission yeast. *Proc Natl Acad Sci U S A* *98*, 13114-13119.
- Green, B.M., and Li, J.J. (2005). Loss of rereplication control in *Saccharomyces cerevisiae* results in extensive DNA damage. *Mol Biol Cell* *16*, 421-432.
- Guthrie, C., and Fink, G. (eds.) (1990). *Guide to Yeast Genetics and Molecular Biology*. Academic Press.
- Haase, S.B., and Lew, D.J. (1997). Flow cytometric analysis of DNA content in budding yeast. *Methods Enzymol* *283*, 322-332.
- Hennessy, K.M., and Botstein, D. (1991). Regulation of DNA replication during the yeast cell cycle. *Cold Spring Harb Symp Quant Biol* *56*, 279-284.
- Huberman, J.A., Spotila, L.D., Nawotka, K.A., el-Assouli, S.M., and Davis, L.R. (1987). The in vivo replication origin of the yeast 2 microns plasmid. *Cell* *51*, 473-481.

- Iyer, V.R., Horak, C.E., Scafe, C.S., Botstein, D., Snyder, M., and Brown, P.O. (2001).  
Genomic binding sites of the yeast cell-cycle transcription factors SBF and MBF.  
*Nature* *409*, 533-538.
- Jallepalli, P.V., Brown, G.W., Muzi-Falconi, M., Tien, D., and Kelly, T.J. (1997).  
Regulation of the replication initiator protein p65cdc18 by CDK phosphorylation.  
*Genes Dev* *11*, 2767-2779.
- Labib, K., Diffley, J.F., and Kearsley, S.E. (1999). G1-phase and B-type cyclins exclude  
the DNA-replication factor Mcm4 from the nucleus. *Nat Cell Biol* *1*, 415-422.
- Li, A., and Blow, J.J. (2005). Cdt1 downregulation by proteolysis and geminin inhibition  
prevents DNA re-replication in *Xenopus*. *Embo J* *24*, 395-404.
- Liku, M.E., Nguyen, V.Q., Rosales, A.W., Irie, K., and Li, J.J. (2005). CDK  
Phosphorylation of a Novel NLS-NES Module Distributed between Two Subunits  
of the Mcm2-7 Complex Prevents Chromosomal Rereplication. *Mol Biol Cell* *16*,  
5026-5039.
- Machida, Y.J., Hamlin, J.L., and Dutta, A. (2005). Right place, right time, and only once:  
replication initiation in metazoans. *Cell* *123*, 13-24.
- McGarry, T.J., and Kirschner, M.W. (1998). Geminin, an inhibitor of DNA replication, is  
degraded during mitosis. *Cell* *93*, 1043-1053.
- Melixetian, M., Ballabeni, A., Masiero, L., Gasparini, P., Zamponi, R., Bartek, J., Lukas,  
J., and Helin, K. (2004). Loss of Geminin induces rereplication in the presence of  
functional p53. *J Cell Biol* *165*, 473-482.

- Mimura, S., Seki, T., Tanaka, S., and Diffley, J.F. (2004). Phosphorylation-dependent binding of mitotic cyclins to Cdc6 contributes to DNA replication control. *Nature* *431*, 1118-1123.
- Moll, T., Tebb, G., Surana, U., Robitsch, H., and Nasmyth, K. (1991). The role of phosphorylation and the CDC28 protein kinase in cell cycle-regulated nuclear import of the *S. cerevisiae* transcription factor SWI5. *Cell* *66*, 743-758.
- Nguyen, V.Q., Co, C., Irie, K., and Li, J.J. (2000). Clb/Cdc28 kinases promote nuclear export of the replication initiator proteins Mcm2-7. *Curr Biol* *10*, 195-205.
- Nguyen, V.Q., Co, C., and Li, J.J. (2001). Cyclin-dependent kinases prevent DNA re-replication through multiple mechanisms. *Nature* *411*, 1068-1073.
- Nishitani, H., Lygerou, Z., and Nishimoto, T. (2004). Proteolysis of DNA replication licensing factor Cdt1 in S-phase is performed independently of geminin through its N-terminal region. *J Biol Chem* *279*, 30807-30816.
- Perkins, G., Drury, L.S., and Diffley, J.F. (2001). Separate SCF(CDC4) recognition elements target Cdc6 for proteolysis in S phase and mitosis. *Embo J* *20*, 4836-4845.
- Raghuraman, M.K., Brewer, B.J., and Fangman, W.L. (1997). Cell cycle-dependent establishment of a late replication program. *Science* *276*, 806-809.
- Raghuraman, M.K., Winzeler, E.A., Collingwood, D., Hunt, S., Wodicka, L., Conway, A., Lockhart, D.J., Davis, R.W., Brewer, B.J., and Fangman, W.L. (2001). Replication dynamics of the yeast genome. *Science* *294*, 115-121.
- Tanaka, S., and Diffley, J.F. (2002). Interdependent nuclear accumulation of budding yeast Cdt1 and Mcm2-7 during G1 phase. *Nat Cell Biol* *4*, 198-207.

- Tanny, R.E., MacAlpine, D.M., Blitzblau, H.G., and Bell, S.P. (2006). Genome-wide Analysis of Re-replication Reveals Inhibitory Controls that Target Multiple Stages of Replication Initiation. *Mol Biol Cell*, (under review).
- Thomer, M., May, N.R., Aggarwal, B.D., Kwok, G., and Calvi, B.R. (2004). *Drosophila* double-parked is sufficient to induce re-replication during development and is regulated by cyclin E/CDK2. *Development* *131*, 4807-4818.
- van Brabant, A.J., Buchanan, C.D., Charboneau, E., Fangman, W.L., and Brewer, B.J. (2001). An origin-deficient yeast artificial chromosome triggers a cell cycle checkpoint. *Mol Cell* *7*, 705-713.
- Vas, A., Mok, W., and Leatherwood, J. (2001). Control of DNA rereplication via Cdc2 phosphorylation sites in the origin recognition complex. *Mol Cell Biol* *21*, 5767-5777.
- Vaziri, C., Saxena, S., Jeon, Y., Lee, C., Murata, K., Machida, Y., Wagle, N., Hwang, D.S., and Dutta, A. (2003). A p53-dependent checkpoint pathway prevents rereplication. *Mol Cell* *11*, 997-1008.
- Wilmes, G.M., Archambault, V., Austin, R.J., Jacobson, M.D., Bell, S.P., and Cross, F.R. (2004). Interaction of the S-phase cyclin Clb5 with an "RXL" docking sequence in the initiator protein Orc6 provides an origin-localized replication control switch. *Genes Dev* *18*, 981-991.
- Wyrick, J.J., Aparicio, J.G., Chen, T., Barnett, J.D., Jennings, E.G., Young, R.A., Bell, S.P., and Aparicio, O.M. (2001). Genome-wide distribution of ORC and MCM proteins in *S. cerevisiae*: high-resolution mapping of replication origins. *Science* *294*, 2357-2360.

- Yabuki, N., Terashima, H., and Kitada, K. (2002). Mapping of early firing origins on a replication profile of budding yeast. *Genes Cells* 7, 781-789.
- Yanow, S.K., Lygerou, Z., and Nurse, P. (2001). Expression of Cdc18/Cdc6 and Cdt1 during G2 phase induces initiation of DNA replication. *Embo J* 20, 4648-4656.
- Yoshida, K., Takisawa, H., and Kubota, Y. (2005). Intrinsic nuclear import activity of geminin is essential to prevent re-initiation of DNA replication in *Xenopus* eggs. *Genes Cells* 10, 63-73.
- Zhong, W., Feng, H., Santiago, F.E., and Kipreos, E.T. (2003). CUL-4 ubiquitin ligase maintains genome stability by restraining DNA-replication licensing. *Nature* 423, 885-889.
- Zhu, W., Chen, Y., and Dutta, A. (2004). Rereplication by depletion of geminin is seen regardless of p53 status and activates a G2/M checkpoint. *Mol Cell Biol* 24, 7140-7150.

**Table 1.** Plasmids used in this study

Plasmid	Key Features	Source
pJL737	<i>ORC6 URA3</i>	Nguyen <i>et al.</i> 2001
pJL806	<i>pGAL1 URA3</i>	Nguyen <i>et al.</i> 2001
pJL1206	<i>MCM7-(NLS)2 URA3</i>	Nguyen <i>et al.</i> 2001
pJL1488	<i>pGAL1-<math>\Delta</math>ntcdc6-cdk2A URA3</i>	This study
pJL1489	<i>pGAL1-<math>\Delta</math>ntcdc6 URA3</i>	Nguyen <i>et al.</i> 2001
pKI1260	<i>MCM7-(svnls3A)2 URA3</i>	Nguyen <i>et al.</i> 2001
pMP933	<i>ORC2 URA3</i>	Nguyen <i>et al.</i> 2001
YIp22	<i>pMET3-HA3-CDC20 TRP1</i>	Uhlmann <i>et al.</i> 2000
pFA6a	<i>KanMX6</i>	Wach <i>et al.</i> 1994
pAG25	<i>NatMX4</i>	Goldstein <i>et al.</i> 1999
pPP117	<i>cdc7-1 URA3</i>	Hollingsworth <i>et al.</i> 1992

**Table 2.** Strains used in this study

Strain	Genotype	Source
YJL310	<i>leu2-3,112 ura3-52 trp1-289 bar1Δ::LEU2</i>	Detweiler and Li 1998
YJL3244	<i>orc2-cdk6A orc6-cdk4A leu2 ura3-52:: {pGAL1, URA3} trp1-289 ade2 ade3 MCM7-2NLS bar1Δ::LEU2 cdc20:: {pMET3-HA3-CDC20, TRP1}</i>	Nguyen <i>et al.</i> 2001
YJL3248	<i>orc2-cdk6A orc6-cdk4A ura3-52:: {pGAL1-Δntcdc6, URA3} trp1-289 leu2 ade2 ade3 MCM7-2NLS bar1Δ::LEU2 cdc20:: {pMET3-HA3-CDC20, TRP1}</i>	Nguyen <i>et al.</i> 2001
YJL3249	<i>orc2-cdk6A orc6-cdk4A ura3-52:: {pGAL1-Δntcdc6, URA3} trp1-289 leu2 ade2 ade3 MCM7-2NLS bar1Δ::LEU2 cdc20:: {pMET3-HA3-CDC20, TRP1}</i>	This study
YJL4486	<i>ORC2 ORC6 leu2 ura3-52:: {pGAL1, URA3} trp1-289 ade2 ade3 MCM7-2NLS bar1Δ::LEU2 cdc20:: {pMET3-HA3-CDC20, TRP1}</i>	This study
YJL4489	<i>ORC2 ORC6 ura3-52:: {pGAL1-Δntcdc6-cdk2A, URA3} trp1-289 leu2 ade2 ade3 MCM7-2NLS bar1Δ::LEU2 cdc20:: {pMET3-HA3-CDC20, TRP1}</i>	This study
YJL4832	<i>orc2-cdk6A orc6-cdk4A ura3-52:: {pGAL1, URA3} trp1-289 leu2 ade2 ade3 MCM7-2nls3A bar1Δ::LEU2</i>	This study



---

	<i>cdc20::pMET3-HA3-CDC20, TRP1}</i>	
YJL3240	<i>orc2-cdk6A orc6-cdk4A ura3-52::pGAL1-Δntcdc6, URA3} trp1-289 leu2 ade2 ade3 MCM7-2nls3A bar1Δ::LEU2 cdc20::pMET3-HA3-CDC20, TRP1}</i>	This study
YJL5038	<i>his3Δ::KanMX leu2Δ0 met15Δ0 ura3Δ0 bar1Δ::NatMX4 can1Δ::pMFA1-HIS3::pMFA1-LEU2</i>	This study
YJL5493	<i>orc2-cdk6A orc6-cdk4A leu2 ura3-52::pGAL1, URA3} trp1-289 ade2 ade3 MCM7-2NLS bar1Δ::LEU2 cdc20::pMET3-HA3-CDC20, TRP1}</i>	This study
YJL5834	<i>ORC2 ORC6 leu2 ura3-52::pGAL1, URA3} trp1-289 ade2 ade3 MCM7 bar1::LEU2</i>	This study
YJL5787	<i>ORC2 ORC6 ura3-52::pGAL1-Δntcdc6-cdk2A, URA3} trp1-289 leu2 ade2 ade3 MCM7-2NLS bar1Δ::LEU2 cdc20::pMET3-HA3-CDC20, TRP1} Δars316::KanMX6</i>	This study
YJL5858	<i>ORC2 ORC6 ura3-52::pGAL1-Δntcdc6-cdk2A, URA3} trp1-289 leu2 ade2 ade3 MCM7-2NLS bar1Δ::LEU2 cdc20::pMET3-HA3-CDC20, TRP1} Δars317::KanMX6</i>	This study
YJL5861	<i>ORC2 ORC6 ura3-52::pGAL1-Δntcdc6-cdk2A, URA3} trp1-289 leu2 ade2 ade3 MCM7-2NLS bar1Δ::LEU2 cdc20::pMET3-HA3-CDC20, TRP1} Δars318::KanMX4</i>	This study

---

---

YJL5816	<i>ORC2 ORC6 leu2 ura3-52::</i> {p <i>GAL1</i> , <i>URA3</i> } <i>trp1-289</i> <i>ade2 ade3 MCM7-2NLS bar1Δ::LEU2</i> <i>cdc20::</i> {p <i>MET3-HA3-CDC20</i> , <i>TRP1</i> } <i>cdc7-1</i>	This study
YJL5822	<i>ORC2 ORC6 ura3-52::</i> {p <i>GAL1-Δntcdc6-cdk2A</i> , <i>URA3</i> } <i>trp1-289 leu2 ade2 ade3 MCM7-2NLS</i> <i>bar1Δ::LEU2 cdc20::</i> {p <i>MET3-HA3-CDC20</i> , <i>TRP1</i> } <i>cdc7-1</i>	This study

---

**Table 3.** Oligonucleotides used in this study

Oligo	Purpose	Sequence
OJL1596	$\Delta$ ARS316	5'-TTAACTGACAATTCTTTTGAACAAAATTTAC ACTTCATCAAGAAAGATGCCGGATCCCCGGGT TAATTAA-3'
OJL1597	$\Delta$ ARS316	5'-TGATGACGAAGGATTCGTTGAAGTTGAAT GCACACAAAAAAGCTTGATACATCGATGAAT TCGAGCTCG-3'
OJL1639	$\Delta$ ARS317	5'-ATTAAACAATGTTTGATTTTTTAAATCGCA ATTTAATACCCGGATCCCCGGGTAAATTAA-3'
OJL1640	$\Delta$ ARS317	5'-ATTTTTATGGAAGATTAAGCTCATAACTTG GACGGGGATCCATCGATGAATTCGAGCTCG-3'
OJL1641	$\Delta$ ARS318	5'-CGATAAAGTTATTATTTAGATTACATGTCA CCAACATTTTCGGATCCCCGGGTAAATTAA-3'
OJL1642	$\Delta$ ARS318	5'-AGAGAAAATAGCTATTTACCTCAACATTTA AAGGTATTAACATCGATGAATTCGAGCTCG-3'
OJL1607	ARS317 <i>probe</i>	5'-ATCGATTATCTGTTTGGCAGG-3'
OJL1608	ARS317 <i>probe</i>	5'-GAATTCAAAGAAGTCAATCTTATG-3'
OJL1452	<i>bar1</i> $\Delta$	5'-ATTAAAAATGACTATATATTTGATATTTAT ATGCTATAAAGAAATTGTACTCCAGATTTCCAT

---

CGATGAATTCGAGCTCG-3'

OJL1454 *bar1Δ* 5'-AGTGGTTCGTATCGCCTAAAATCATACCA

AAATAAAAAGAGTGTCTAGAAGGGTCATATAC

GGATCCCCGGGTTAATTAA-3'

---

**Figure 1** Use of comparative genomic hybridization (CGH) on spotted microarrays to assay DNA replication.

**A)** Schematic representation of the CGH replication assay. Genomic DNA is purified from non-replicating and replicating cells, differentially labeled with Cy3 and Cy5, and competitively hybridized to a microarray containing 12,034 ORF and intergenic PCR products. Cy5/Cy3 ratios are normalized so that the average ratio of all elements equals the DNA content of the cells (as determined by flow cytometry). Normalized ratios are plotted against chromosomal position and mathematically smoothed to generate a replication profile. In most cases, two hybridizations are performed from each of two independent experiments. The resulting four replication profiles are averaged into one composite profile, and the locations of origins are identified using a peak finding algorithm. Chromosomal regions lacking data of sufficient quality are represented as gaps in the profiles.

**B)** CGH replication assay described for Figure 1A was performed on YJL5038, a wild-type yeast strain in the S288c background. G1 phase genomic DNA was hybridized against S phase genomic DNA obtained 120 min after cells were released from G1 phase into media containing hydroxyurea (HU). The composite replication profile (blue line) plus and minus the “experiment variability” (light gray band, see Methods) is shown for Chromosome X. Positions of origins annotated in the *Saccharomyces* Genome Database (SGD, (Balakrishnan)) (red triangles) and the centromere (black circle) are marked along the X-axis. Replication profiles derived from Raghuraman *et al.* (Raghuraman *et al.*, 2001) (violet line) and Yabuki *et al.* (Yabuki *et al.*, 2002) (orange line) are shown for comparison.

- C)** S phase progression assayed by flow cytometry for experiment described in Figure 1B at the indicated times following release from G1 phase. DNA content of 1.4 C was used to normalize the S288c replication profile.
- D)** The S phase replication profile of the re-replication competent OMC strain and the congenic wild-type strain are similar. S phase replication profiles were generated for the OMC strain YJL3248 (*MCM7-2NLS orc2-cdk6A orc6-cdk4A pGAL1-Δntcdc6 pMET3-HA3-CDC20*) and a congenic wild-type A364a strain YJL5834 (*pGAL1*) essentially as described in Figure 1B except S phase cells were harvested, respectively, at 135 min and 180 min after alpha factor release. The S phase replication profile for the OMC strain (green line) and the A364a strain (black line) for chromosome X is shown. SGD annotated origins (red triangles) and the centromere (black circle) are marked along the X-axis.
- E)** S phase progression assayed by flow cytometry for experiment described in Figure 1D at the indicated times following release from G1 phase. DNA contents of 1.35 C and 1.4 C, respectively, were used to normalize the OMC and A364a replication profiles.

Figure 1

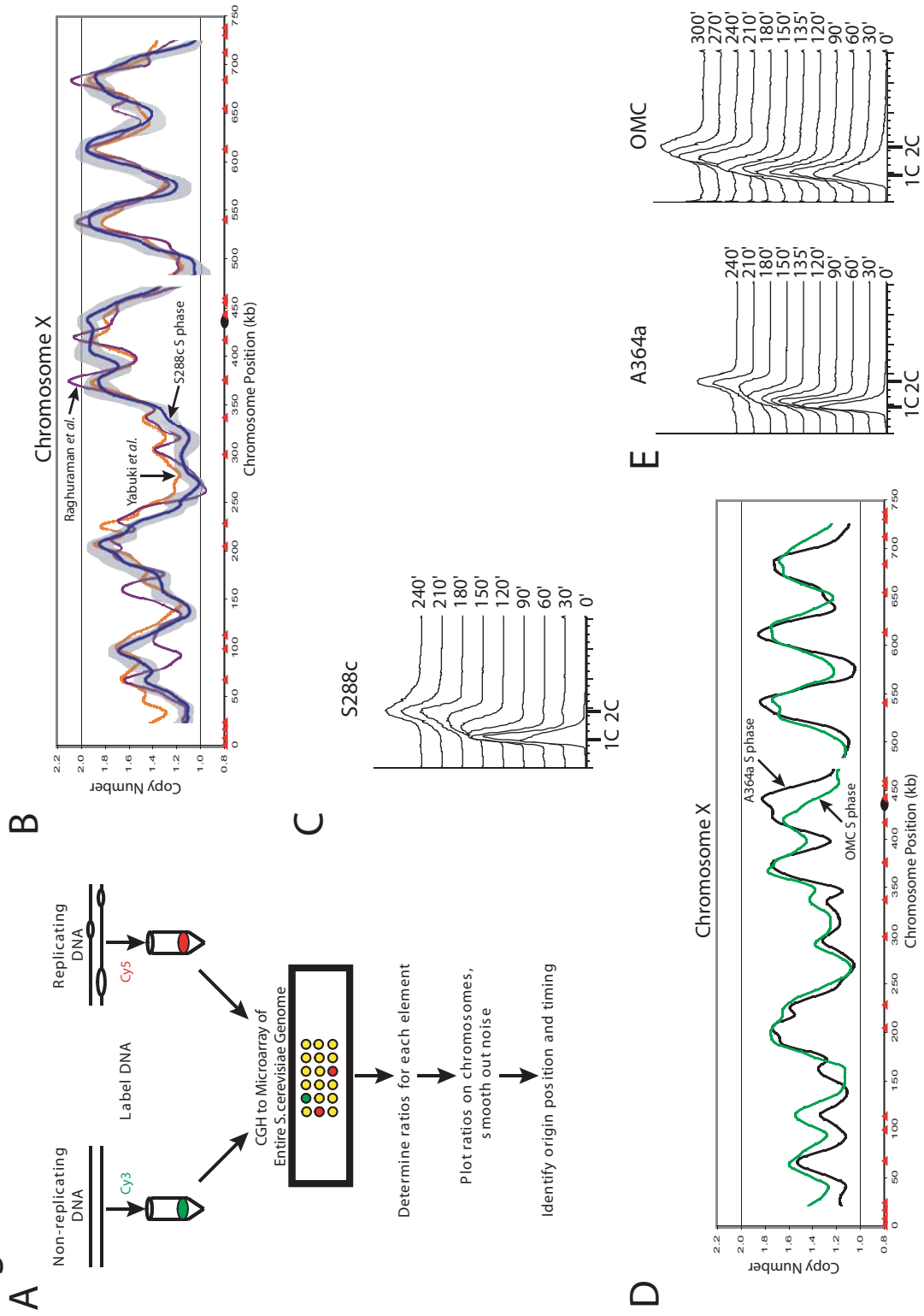


**Figure 2** Re-replication induced during G2/M phase when ORC, Mcm2-7 and Cdc6 are deregulated.

**A)** G2/M phase re-replication in the OMC strain is readily detectable by flow cytometry. The OMC strain YJL3248 (*orc2-cdk6A orc6-cdk4A MCM7-2NLS pGAL1-Δntcdc6 pMET3-HA3-CDC20*) and the control OM strain YJL3244 (*orc2-cdk6A orc6-cdk4A MCM7-2NLS pGAL1 pMET3-HA3-CDC20*) were arrested in G2/M phase. Once arrested, galactose was added, which induced re-replication in the OMC strain. Samples were taken for flow cytometry at the indicated points after galactose addition. The DNA content of 2.7 C at 3 hr was used to normalize the OMC re-replication profile in Figure 2B.

**B)** Genomic DNA was purified from the OMC strain and the control OM strain after 3 hr of galactose induction as described in Figure 2A and competitively hybridized against each other as described in Figure 1A. The OMC G2/M phase re-replication profiles (black lines, right axis), the OMC S phase replication profiles replotted from Figure 1D (gray lines, left axis), locations of pro-ARs mapped by Wyrick *et al.* (Wyrick *et al.*, 2001) (gray triangles) and the centromeres (black circles) are shown for chromosomes III, VI, and XIV.

**C)** Each chromosome participates when OMC cells are induced to re-replicate in G2/M phase. The OMC strain and the control OM strain from the experiment presented in Figure 2A were harvested for pulsed field gel electrophoresis (PFGE) at the indicated times. Southern blots of the gel were probed with fragments containing ARS305 to detect chromosome III, ARS607 to detect chromosome VI, and ARS1413 to detect

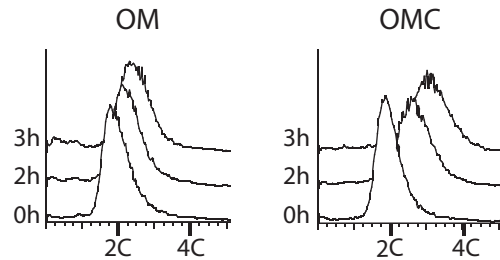


chromosome XIV. For each chromosome the Southern signal for both the gel well and the normal chromosomal position are shown.

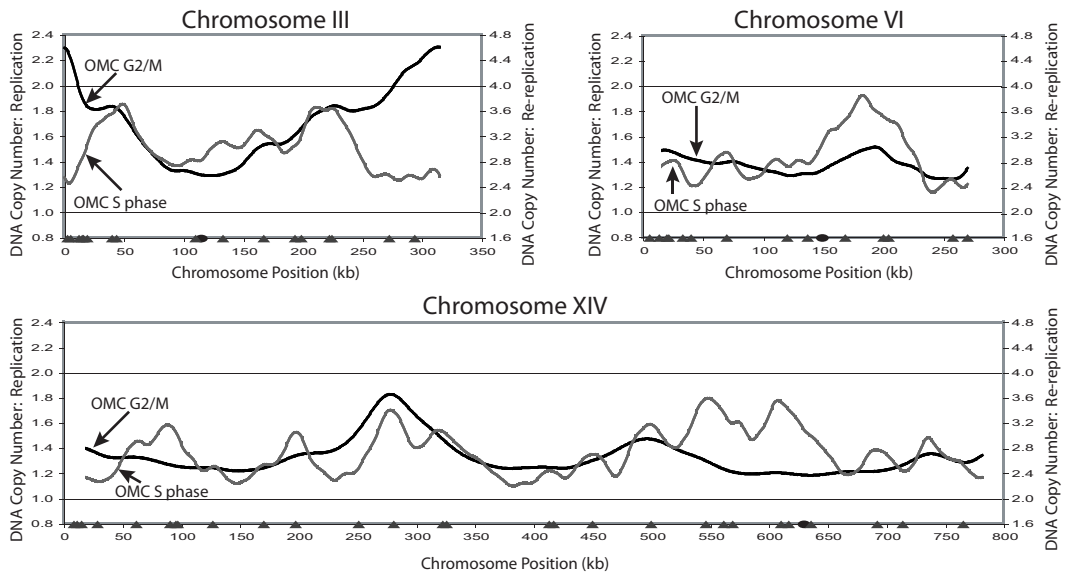
**D)** Replication timing does not correlate with efficiency of G2/M phase re-replication in the OMC strain. For each of the pro-ARSs defined by Wyrick *et al.* (Wyrick *et al.*, 2001), the DNA copy number from the OMC G2/M phase re-replication profile in Figure 2B was plotted versus the DNA copy number from the OMC S phase replication profile in Figure 2B. Line represents linear regression of plot.

Figure 2

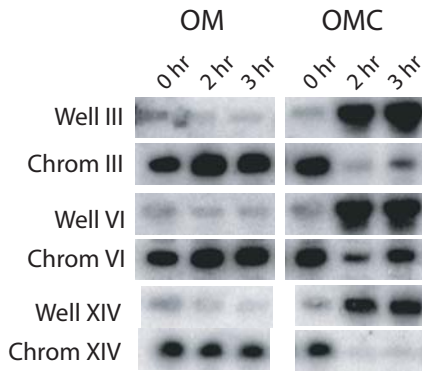
A



B



C



D

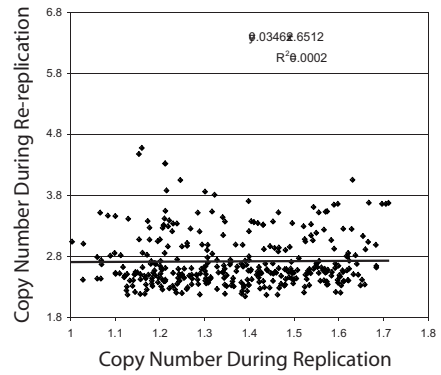


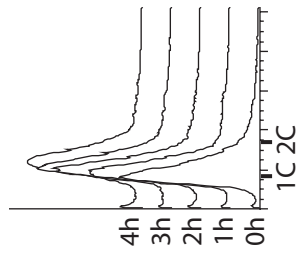
**Figure 3** Deregulation of ORC, Mcm2-7 and Cdc6 can induce re-replication in S phase.

**A)** Flow cytometry of OMC cells induced to re-replicate in S phase. The OMC strain YJL3249 (*orc2-cdk6A orc6-cdk4A MCM7-2NLS pGAL1- $\Delta$ ntcdc6 pMET3-HA3-CDC20*) was arrested in G1 phase, induced to express  $\Delta$ ntcdc6 by the addition of galactose, then released from the arrest into media containing HU to delay cells from exiting S phase. At 4 hr the cells were still in S phase with a DNA content of 1.4 C. This value was used to normalize the re-replication profile in 3B.

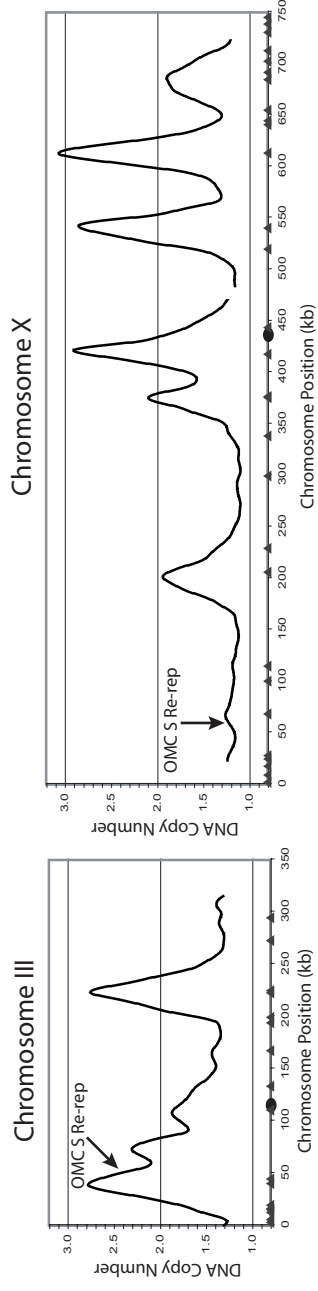
**B)** OMC cells can re-initiate and re-replicate within S phase. Genomic DNA was isolated at the 0 hr (G1 phase) and 4 hr (S phase) time points from the OMC strain YJL3249 as described in Figure 3A and competitively hybridized against each other. The resulting profiles shown for chromosomes III and X reflect copy number increases due to both replication and re-replication. Locations of pro-ARSs mapped by Wyrick *et al.* (Wyrick *et al.*, 2001) (gray triangles) and the centromeres (black circles) are plotted along the X-axis.

Figure 3

A



B



**Figure 4** Re-replication induced upon release from a G1 arrest when ORC, Mcm2-7 and Cdc6 are deregulated.

**A)** Robust re-replication of OMC cells following G1 release. The OMC strain YJL3248 (*orc2-cdk6A orc6-cdk4A MCM7-2NLS pGAL1- $\Delta$ ntcdc6 pMET3-HA3-CDC20*) and the control OM strain YJL3244 (*orc2-cdk6A orc6-cdk4A MCM7-2NLS pGAL1 pMET3-HA3-CDC20*) were arrested in G1 phase, exposed to galactose to induce  $\Delta$ ntcdc6 in the OMC strain, then released from the arrest into G2/M phase. Samples were taken for flow cytometry at the indicated times after release from the alpha factor arrest. The OMC re-replication profile in Figure 4C was normalized to the 3 hr DNA content of 3.2 C.

**B)** Cells that were induced to re-replicate in Figure 4A were harvested for PFGE at the indicated times. Southern blots of the gel were probed for chromosomes III, VI, and XIV as described in Figure 2C.

**C)** Re-replication profile of the OMC strain following G1 release. Genomic DNA was purified from the OMC strain and the control OM strain 3 hr after G1 release. The two DNA preparations were labeled and competitively hybridized against each other to generate the G1 release re-replication profiles shown for chromosomes III, VI, and XIV. Locations of pro-ARSs mapped by Wyrick *et al.* (Wyrick *et al.*, 2001) (gray triangles) and the centromeres (black circles) are plotted along the X-axis.

**D)** Re-replication induced in the OMC strain following a G1 release is slightly biased toward early replicating pro-ARSs. For each of the pro-ARSs defined by Wyrick *et al.* (Wyrick *et al.*, 2001), the DNA copy number from the OMC G1 release re-replication

profile in Figure 4C was plotted versus the DNA copy number from the OMC S phase replication profile in Figure 2B. Line represents linear regression of plot.

Figure 4

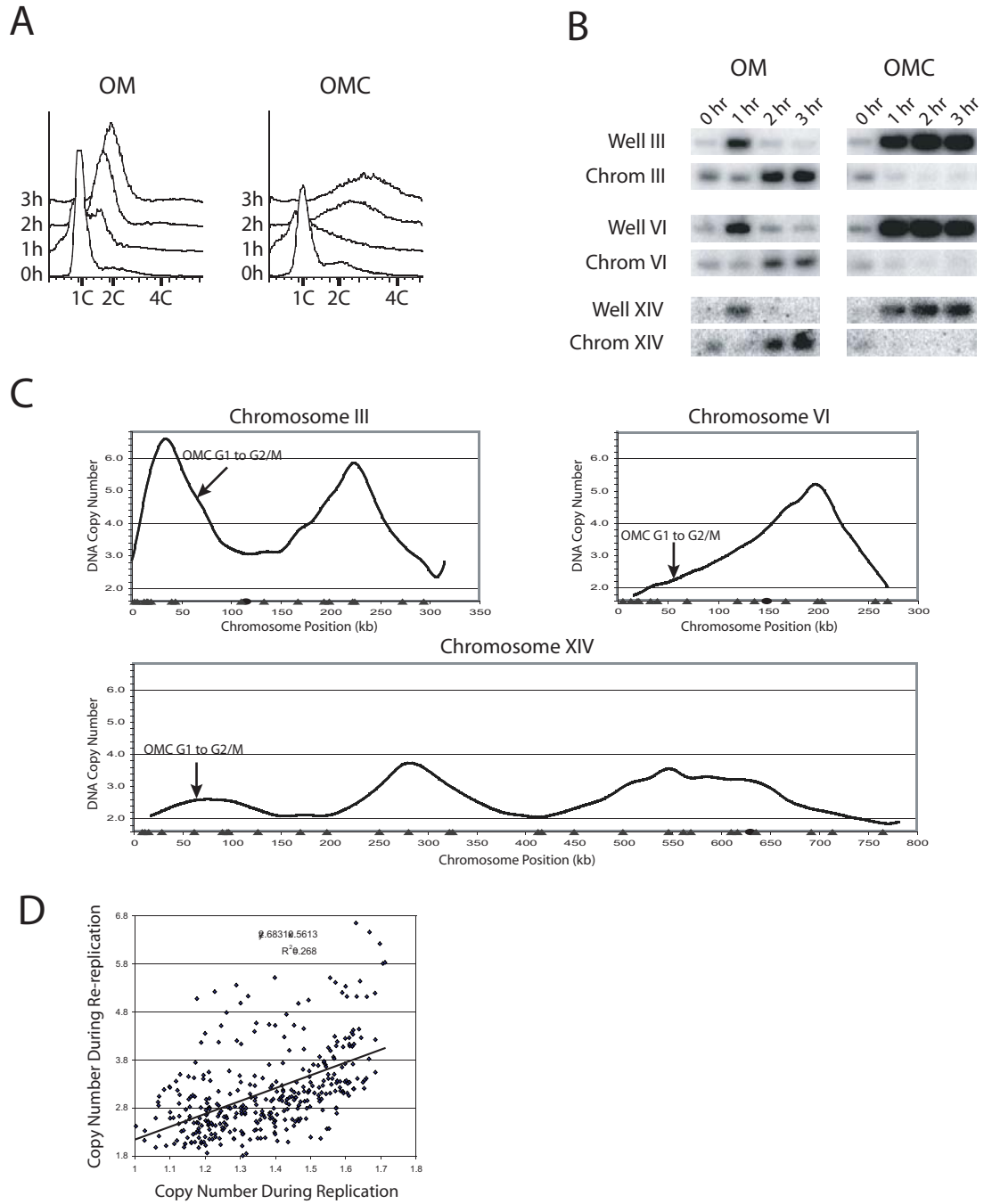


**Figure 5** Re-replication can be induced when only ORC and Cdc6 are deregulated.

**A)** Re-replication is undetectable by flow cytometry in OC cells in G2/M phase. The OC strain YJL3240 (*orc2-cdk6A orc6-cdk4A pGAL1- $\Delta$ ntcdc6 pMET3-HA3-CDC20*) and the control O strain YJL4832 (*orc2-cdk6A orc6-cdk4A pGAL1 pMET3-HA3-CDC20*) were arrested in G2/M phase and induced with galactose as described in Figure 2A.

Samples for flow cytometry were taken at the indicated times after galactose addition.

The OC G2/M re-replication profile in Figure 5E was normalized to the 3 hr DNA content of 2.0 C.

**B)** Significant re-replication can be induced in OC cells during a G1 release. The OC strain and the control O strain were induced with galactose and released from a G1 arrest as described in Figure 4A. Samples for flow cytometry were taken at the indicated times after G1 release. The OC G1 release re-replication profile in Figure 5E was normalized to the 3 hr DNA content of 2.6 C.

**C)** Re-replication is not readily detected by PFGE in OC cells in G2/M phase. Strains that were induced to re-replicate in Figure 5A were harvested for PFGE at the indicated times. Southern blots of the gel were probed for chromosomes III, VI, and XIV as described in Figure 2C.

**D)** Some but not all copies of each chromosome participate when OC cells are induced to re-replicate in G2/M phase. Strains that were induced to re-replicate in Figure 5B were harvested for PFGE at the indicated times. Southern blots of the gel were probed for chromosomes III, VI, and XIV as described in Figure 2C.

**E)** Cell cycle position significantly affects the extent of re-replication in the OC strain. The OC strain and the control O strain were induced to re-replicate in G2/M phase



or during a G1 release as described, respectively, in Figures 5A and 5B. For each induction protocol, OC and O strain genomic DNA were prepared and competitively hybridized against each other. Shown for chromosomes III, VI, and XIV are OC G2/M phase re-replication profiles (black lines), OC G1 release re-replication profiles (gray lines), locations of pro-ARSs mapped by Wyrick *et al.* (Wyrick *et al.*, 2001) (gray triangles), and the centromeres (black circles).

Figure 5

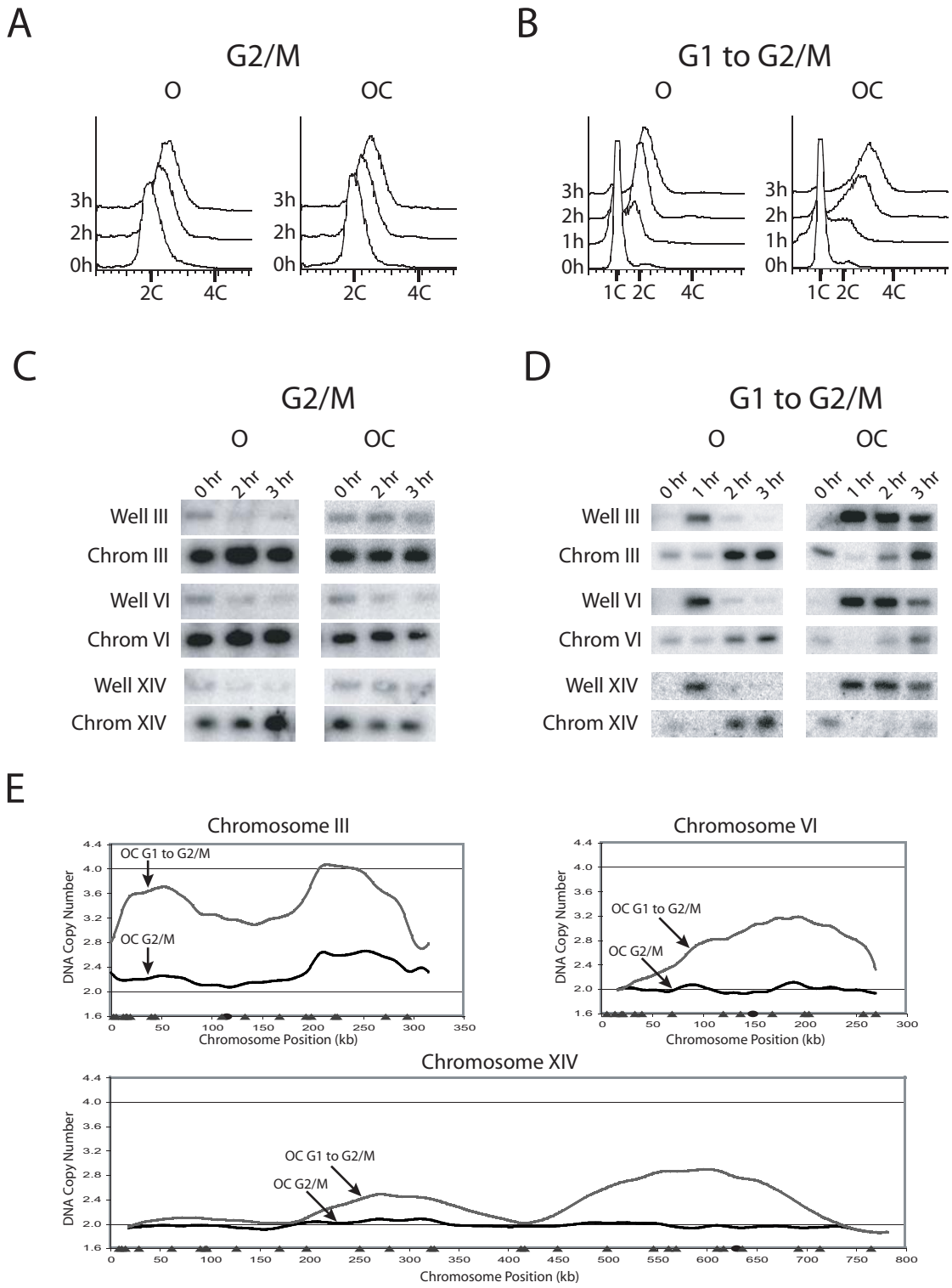


**Figure 6** Re-replication occurs primarily on a single chromosome when Mcm2-7 and Cdc6 are deregulated

**A)** Re-replication is undetectable by flow cytometry in MC<sub>2A</sub> cells in G2/M phase. The MC<sub>2A</sub> strain YJL4489 (*MCM7-NLS pGAL1-Δntcdc6-cdk2A pMET3-HA3-CDC20*) and the control M strain YJL4486 (*MCM7-2NLS pGAL1 pMET3-HA3-CDC20*) were arrested in G2/M phase and induced with galactose as described in Figure 2A. Samples for flow cytometry were taken at the indicated times after galactose addition. The MC<sub>2A</sub> G2/M re-replication profile in Figure 6E was normalized to the 3 hr DNA content of 2.0 C.

**B)** Re-replication is undetectable by flow cytometry in MC<sub>2A</sub> cells during a G1 release. The MC<sub>2A</sub> strain and the control M strain were induced with galactose and released from a G1 arrest as described in Figure 4A. Samples for flow cytometry were taken at the indicated times. The MC<sub>2A</sub> G1 release re-replication profile in Figure 6E was normalized to the 3 hr DNA content of 2.0 C.

**C)** A portion of the population of chromosome III molecules participate when MC<sub>2A</sub> cells are induced to re-replicate in G2/M phase. The strains that were induced to re-replicate in Figure 6A were harvested for PFGE at the indicated times. Southern blots of the gel were probed for chromosomes III, VI, and XIV as described in Figure 2C.

**D)** A portion of the population of chromosome III molecules participate when MC<sub>2A</sub> cells are induced to re-replicate during a G1 release. The strains that were induced to re-replicate in Figure 6B were harvested for PFGE at the indicated times. Southern blots of the gel were probed for chromosomes III, VI, and XIV as described in Figure 2C.

**E)** Re-replication in the MC<sub>2A</sub> strain occurs primarily on chromosome III. The MC<sub>2A</sub> strain and the control M strain were induced to re-replicate in G2/M phase or during a G1 release as described, respectively, in Figures 6A and 6B. For each induction protocol, MC<sub>2A</sub> and M strain genomic DNA were prepared and competitively hybridized against each other. Shown for chromosomes III, VI, and XIV are MC<sub>2A</sub> G2/M phase re-replication profiles (black lines), MC<sub>2A</sub> G1 release re-replication profiles (gray lines), locations of pro-ARs mapped by Wyrick *et al.* (Wyrick *et al.*, 2001) (gray triangles) and the centromeres (black circles).

Figure 6

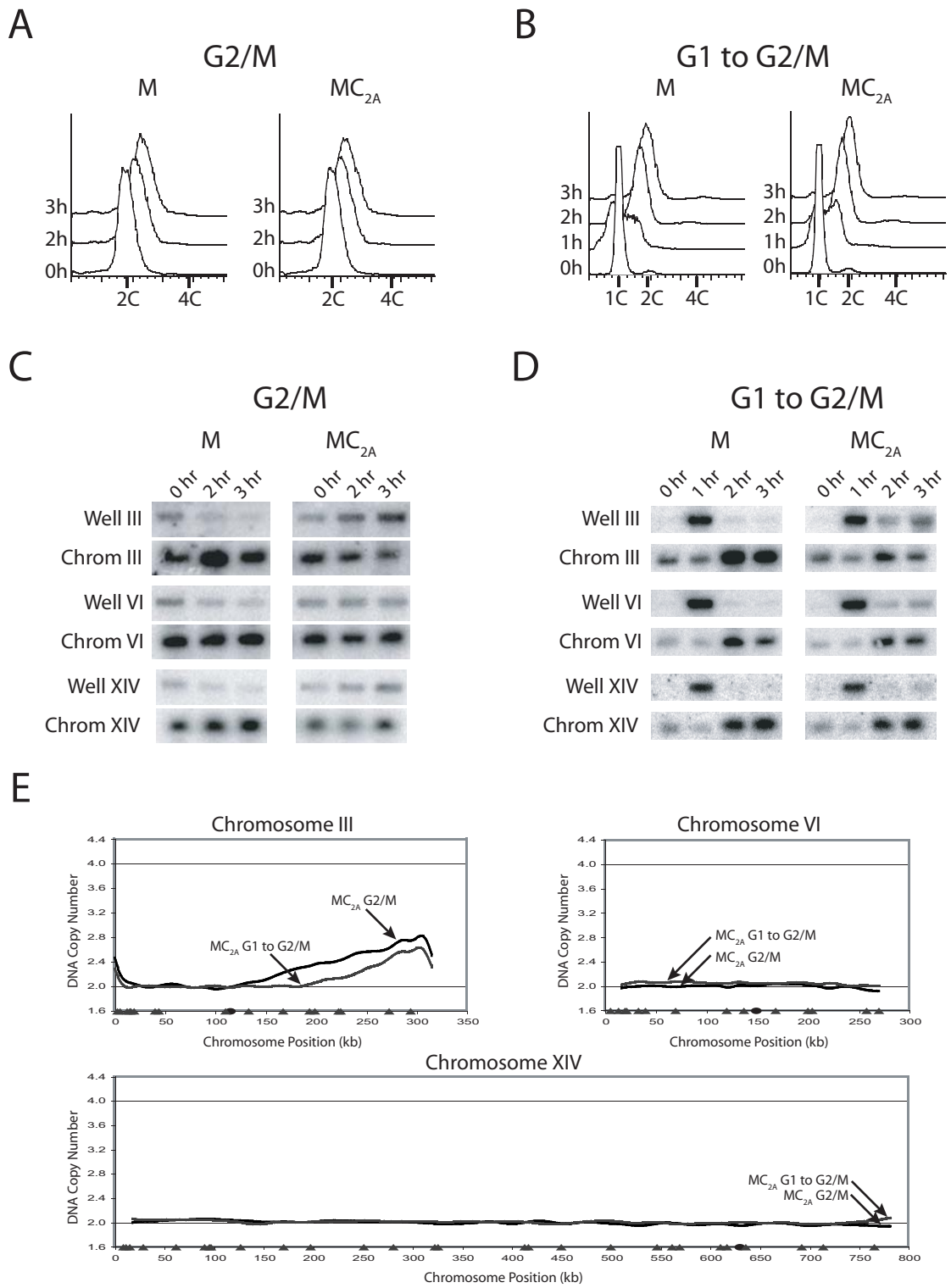


**Figure 7** The re-replication arising from deregulation of both Mcm2-7 and Cdc6 depends on *ARS317* and Cdc7.

**A)** Re-initiation bubbles are induced at *ARS317* when MC<sub>2A</sub> re-replicates in G2/M phase. The MC<sub>2A</sub> strain YJL4489 (*MCM7-NLS pGAL1-Δntcdc6-cdk2A pMET3-HA3-CDC20*) and the control M strain YJL4486 (*MCM7-2NLS pGAL1 pMET3-HA3-CDC20*) were arrested in G2/M phase and induced with galactose as described in Figure 6A.

Genomic DNA was purified from each strain at both 0 and 2 hr after induction and subjected to neutral-neutral 2-dimensional gel electrophoresis. Southern blots of the gels were probed with an *ARS317* fragment. Black arrow indicates re-replication bubbles.

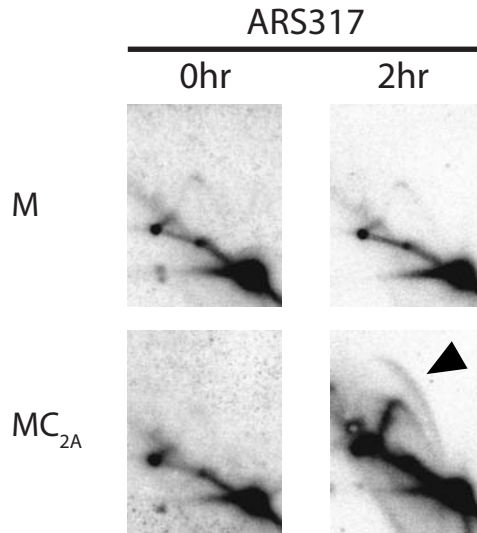
**B)** *ARS317* sequence is required for the bulk of re-replication induced in MC<sub>2A</sub> cells. The MC<sub>2A</sub>-*Δars317* strain YJL5858 (*MCM7-NLS pGAL1-Δntcdc6-cdk2A pMET3-HA3-CDC20 Δars317*) and the control M strain YJL4486 were arrested in G2/M phase and induced with galactose for 3 hours as described in Figure 6A. Genomic DNA from the two strains was competitively hybridized against each other to generate the MC<sub>2A</sub>-*Δars317* G2/M phase re-replication profile shown for chromosome III (gray line). The MC<sub>2A</sub> G2/M phase re-replication profile from Figure 5E is replotted for comparison (black line). The locations of pro-ARs mapped by Wyrick *et al.* (Wyrick *et al.*, 2001) (gray triangles), and the centromere (black circle) are plotted along the X-axis.

**C)** Cdc7 kinase is required for re-replication induced in MC<sub>2A</sub> cells. The MC<sub>2A</sub> strain YJL4489, the congenic MC<sub>2A</sub>-*cdc7* strain YJL5821 (*MCM7-2NLS pGAL1-Δntcdc6-2A pMET3-HA3-CDC20 cdc7-1*) and their respective controls, the M strain YJL4486 and the M-*cdc7* strain YJL5816 (*MCM7-2NLS pGAL1 pMET3-HA3-CDC20 cdc7-1*) were induced with galactose as described in Figure 6A, except the initial arrest

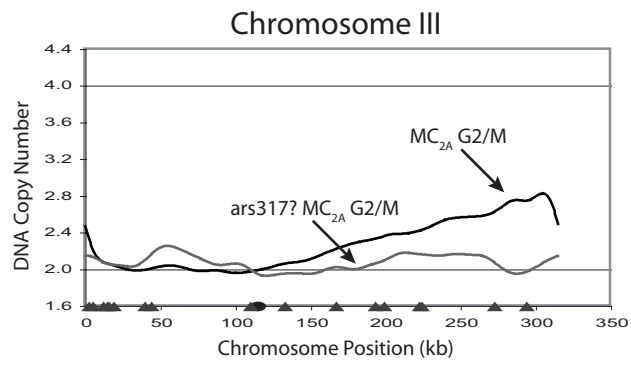
was performed at 23° C, and the arrested cells were shifted to 35° C for 1 hr, before the addition of galactose. Genomic DNA was isolated 4 hr after galactose addition and competitively hybridized (MC<sub>2A</sub> versus M and MC<sub>2A-cdc7</sub> versus M-*cdc7*) as described in Figure 1A. Re-replication profiles for the MC<sub>2A</sub> (black line) and MC<sub>2A-cdc7</sub> (gray line) strains are shown for chromosome III. Locations of pro-ARSs mapped by Wyrick *et al.* (Wyrick *et al.*, 2001) (gray triangles), and the centromere (black circle) are plotted along the X-axis.

Figure 7

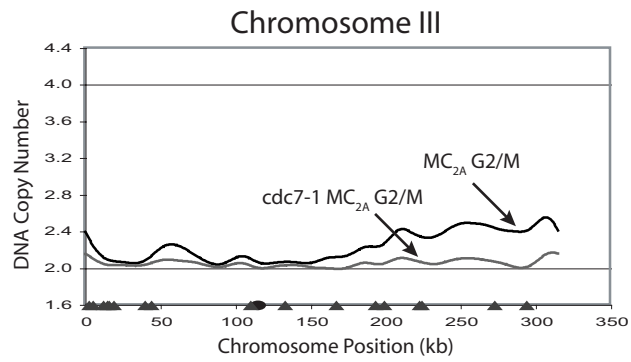
A



B



C





## **CHAPTER 3**

**Loss of Rereplication Control in *Saccharomyces cerevisiae***

**Results in Extensive DNA Damage**

## **Abstract**

To maintain genome stability, the entire genome of a eukaryotic cell must be replicated once and only once per cell cycle. In many organisms, multiple overlapping mechanisms block re-replication, but the consequences of deregulating these mechanisms are poorly understood. Here we show that disrupting these controls in the budding yeast *Saccharomyces cerevisiae* rapidly blocks cell proliferation. Re-replicating cells activate the classical DNA damage-induced checkpoint response, which depends on the BRCT checkpoint protein Rad9. In contrast, Mrc1, a checkpoint protein required for recognition of replication stress, does not play a role in the response to re-replication. Strikingly, re-replicating cells accumulate sub-chromosomal DNA breakage products. These rapid and severe consequences suggest that even limited and sporadic re-replication could threaten the genome with significant damage. Hence, even subtle disruptions in the cell cycle regulation of DNA replication may predispose cells to the genomic instability associated with tumorigenesis.

## **Introduction**

Eukaryotic DNA replication is tightly controlled such that every segment of the genome is replicated once and only once each cell cycle. This control is primarily exerted at the hundreds to thousands of replication origins where DNA replication initiates. Once an origin initiates in S phase, multiple mechanisms prevent it from re-initiating replication for the remainder of that cell cycle (Gopalakrishnan *et al.*, 2001;

Nguyen *et al.*, 2001; Vas *et al.*, 2001; Yanow *et al.*, 2001; Vaziri *et al.*, 2003). Such tight control suggests that even an occasional re-initiation event would be deleterious to cells, and it is readily apparent that, in principle, excessive synthesis of just small segments of the genome could eventually threaten its stable propagation. Nonetheless, a direct analysis of the consequences of re-replication is needed to understand whether and how re-replication contributes to genomic instability. *Saccharomyces cerevisiae* provides a powerful genetic system for such an analysis, especially as there is considerable understanding of both the mechanisms regulating replication and those protecting genome stability in this organism.

Eukaryotic replication initiation can be divided into two fundamental stages (reviewed in Bell and Dutta, 2002). In the first stage, which occurs in early G1 phase, a pre-replicative complex (pre-RC) is assembled at replication origins through the sequential loading of the initiation proteins ORC, Cdc6, Cdt1, and Mcm2-7. In the second stage, activation of two kinases, Dbf4-Cdc7 kinase and a cyclin-dependent kinase (CDK), triggers events that culminate in replication initiation and disassembly of the pre-replicative complex: additional replication proteins are recruited to the origin, the DNA is unwound, and replisomes are assembled at two nascent replication forks.

In addition to triggering initiation, CDKs also prevent re-initiation of eukaryotic DNA replication (Broek *et al.*, 1991; Dahmann *et al.*, 1995; Sauer *et al.*, 1995; Hua *et al.*, 1997). CDKs do this in part by down-regulating multiple components of the pre-RC, thereby preventing reassembly of these complexes at origins that have initiated. In budding yeast, CDKs promote the nuclear exclusion of Mcm2-7 (Labib *et al.*, 1999; Nguyen *et al.*, 2000), inhibit CDC6 transcription (Moll *et al.*, 1991) and promote its

degradation (Drury *et al.*, 1997; Elsasser *et al.*, 1999; Drury *et al.*, 2000), and appear to inactivate ORC through phosphorylation (Nguyen *et al.*, 2001). Making these three initiation factors refractory to CDK inhibition in metaphase arrested cells allows a subset of origins to re-initiate and portions of the genome to re-replicate (Nguyen *et al.*, 2001). The limited extent of re-initiation suggests that not all inhibitory mechanisms to block re-replication have been identified. Consistent with this, a recent study indicates that CDK binding to ORC provides an additional mechanism to inhibit pre-RC formation (Wilmes *et al.*, 2004).

Analogous CDK-dependent mechanisms antagonizing Cdc6, ORC, and Cdt1 have been shown to inhibit re-replication in other eukaryotes (Jallepalli *et al.*, 1997; Lopez-Girona *et al.*, 1998; Nishitani *et al.*, 2000; Vas *et al.*, 2001; Wuarin *et al.*, 2002; Zhong *et al.*, 2003). Moreover, a CDK-independent mechanism to prevent pre-RC assembly has been identified in metazoans. Central to this mechanism is the protein Geminin (McGarry and Kirschner, 1998; Tada *et al.*, 2001; Wohlschlegel *et al.*, 2002), which binds to Cdt1 and is thought to sterically inhibit its ability to recruit Mcm proteins to replication origins (Lee *et al.*, 2004; Saxena *et al.*, 2004). Inactivation of geminin can lead to partial re-replication, confirming its role in preventing re-initiation of DNA replication (Quinn *et al.*, 2001; Mihaylov *et al.*, 2002; Melixetian *et al.*, 2004; Zhu *et al.*, 2004).

The partial extent of re-replication that we and others have observed suggests that these re-replicating forks are stalled or damaged before they can completely re-replicate the entire genome. Such insults to the re-replicating genome could trigger one or both of the checkpoint pathways that monitor genome integrity (reviewed in Melo and Toczyski,

2002; Nyberg *et al.*, 2002). The replication stress pathway responds to slowed or stalled replication forks, such as those arising from inhibition of nucleotide incorporation. The DNA damage pathway responds to chromosomal insults such as double-stranded breaks generated by ionizing radiation or enzymatic cleavage. These pathways activate proteins that stabilize stalled replication forks and repair DNA damage, respectively. In addition, they provide critical time to complete the replication or repair of DNA by imposing arrests at key cell cycle transitions.

Distinguishing whether the replication stress and/or DNA damage pathway is activated is an important first step in understanding the immediate molecular response to re-replication. This distinction is difficult because many checkpoint proteins and events are shared between the two pathways. For example, in metazoans, both types of genomic insults lead to the induction of p21, p53, and PIG3 protein levels, the phosphorylation of histone H2AX, p53, Cdc2, and the checkpoint kinases, Chk1 and Chk2, and the organization of H2AX and Rad51 into subnuclear foci (Haaf *et al.*, 1995; Gottifredi *et al.*, 2001; Saintigny *et al.*, 2001; Ward and Chen, 2001; Brown and Baltimore, 2003). In a few of these responses the kinetics or degree of change may vary between the two pathways, but overall the events considered to be hallmarks of DNA damage are also observed with replication stress. Complicating the distinction between these two responses is the potential for stalled forks to degenerate into damaged forks, particularly if the stalled forks are not properly stabilized (reviewed in Nyberg *et al.*, 2002).

Two groups have recently reported that the induction of re-replication in human cells induces a checkpoint response. The first group initially reported that re-replication

induced by over expression of Cdc6 and Cdt1 activates a DNA damage response (Vaziri *et al.*, 2003), but have subsequently observed that overexpression of Cdc6 alone can induce this response in the absence of any detectable re-replication (Zhu *et al.*, 2004). Instead, they now report that re-replication induced by geminin depletion leads to what they suspect is a stalled fork response (Zhu *et al.*, 2004). Thus, they no longer assert that re-replication generates DNA damage. A second group observes similar events during geminin depletion, which they attribute to either a DNA damage or replication stress response (Melixetian *et al.*, 2004). Thus, although a clear assignment of pathways was not possible, the data is consistent with re-replication generating a replication stress-like response.

In *S. cerevisiae*, the DNA damage and replication stress responses can be genetically distinguished, because the DNA damage pathway is primarily dependent on the BRCT checkpoint protein Rad9 (reviewed in Toh and Lowndes, 2003), whereas the replication stress pathway is primarily dependent on Mrc1 (Alcasabas *et al.*, 2001; Osborn and Elledge, 2003). In this work we take advantage of this genetic distinction to unambiguously determine which response is activated upon re-replication. We present evidence that re-replication leads to significant inviability and the activation of a *RAD53* (budding yeast Chk2) dependent checkpoint response. The *RAD9* dependence of the signaling pathway suggests that re-replication is triggering a DNA damage response and is not inducing a replication stress pathway. Moreover, we present the first direct evidence for the accumulation of chromosomal damage as a consequence of re-replication. These data indicate that re-replication induces DNA damage and poses an immediate threat to both cell viability and genome integrity.

## Materials and Methods

### Strain Construction

All strains (Table 1) with the exception of YJL310 were derived from YJL1737 (*orc2-cdk6A orc6-cdk4A leu2 ura3-52 trp1-289 ade2 ade3 bar1Δ::LEU2*). The *orc2-cdk6A* and *orc6-cdk4A* alleles encode mutant proteins in which alanine is substituted for the phosphoacceptor serines or threonines in CDK consensus phosphorylation sites (S/T-P-X-K/R). For *orc2-cdk6A*, residues 16, 24, 70, 174, 188, and 206 were mutated and for *orc6-cdk4A*, residues 106, 116, 123, and 146 were mutated. The following plasmids were digested and integrated as follows: pJL806 (*pGAL1, URA3/StuI* (Nguyen *et al.*, 2001)), pJL1489 (*pGAL1-Δntcdc6, URA3/StuI* (Nguyen *et al.*, 2001)), pRS304Rad53HA-HIS (*RAD53-HA-HIS, TRP1/HpaI* (Emili, 1998)), YIp22 (*pMET3-HA3-CDC20, TRP1/MscI* (Uhlmann *et al.*, 2000)), and pBO1555 (*pMET3-HA3-CDC20, NatMX4/MscI*). pJL1206 (*MCM7-2NLS, URA3/AspI* (Nguyen *et al.*, 2001)) was used to replace *MCM7* with *MCM7-2NLS* by two-step gene replacement. The plasmid pBO1555 was generated by subcloning a BglII to Sall *pMET3-HA3-CDC20* fragment from YIp22 into pAG25 (Goldstein and McCusker, 1999) cut with BglII and Sall.

Genomic DNA from yJK7-2 (Melo *et al.*, 2001) was used as a template to generate a *DDC2-GFP, kanMX* PCR fragment using OJL1404 and OJL1405. Genomic DNA from U973 (*sml1Δ::TRP1 esr1-1*, Rothstein laboratory) was used as a template to generate a *sml1Δ::TRP1* PCR fragment using OJL1110 and OJL1111. Genomic DNA from the yeast haploid deletion collection (ResGen; Invitrogen) was used as a template to

generate a *rad9Δ::kanMX* PCR fragment using OJL1487 and OJL1488. The entire *RAD53* and *MRC1* open reading frames were deleted using PCR amplification of the *kanMX* from pAG25 with tagged primers using the oligonucleotides indicated in Table 2 (Goldstein and McCusker, 1999).

#### Yeast media

Cells were grown in YEP, synthetic complete (SC) or synthetic (S broth) medium (Guthrie and Fink, 1990) supplemented with 2% dextrose (w/v), 2% galactose (w/v), 3% raffinose (w/v) or 3% raffinose (w/v) plus 0.05% dextrose (w/v). In order to obtain reproducible induction of re-replication, cells were inoculated from a culture containing 2% dextrose into a culture containing 3% raffinose plus 0.05% dextrose and grown for 12 to 15 hours overnight before the experiment commenced.

#### Cell proliferation assay

Yeast cells were diluted in S broth to OD600 measurements of 0.2, then serially diluted 5 fold for six dilutions and spotted onto SDC-Ura or SGalC-Ura plates. For transient pulses of re-replication, cells grown overnight in SRaffC-Ura + 0.05% dextrose were pelleted and resuspended in YEPRaff + 15µg/ml nocodazole. Once >90% of the cells were arrested as large budded cells, galactose was added to a final concentration of 2%, samples were removed at various time points, diluted in SD broth and plated on SDC-Ura plates. Colonies were counted after 72 hours at 30°C. All platings were done in triplicate and two separate experiments were conducted. The mean and standard error of the mean are shown. Statistical significance was determined using a Student's t-test.



## Flow cytometry analysis

Cells grown overnight in SRaffC-Met,Ura + 0.05% dextrose were pelleted and resuspended in YEPRaff + 2mM methionine to arrest cells in metaphase by Cdc20p depletion. Once arrested (>90% large budded cells), nocodazole (15µg/ml) was added for an additional 30 minutes. Galactose was then added to a final concentration of 2% and samples were taken every hour. Cells were fixed and stained with 1µM Sytox Green (Molecular Probes) as described (Haase and Lew, 1997). Vertical lines indicate median DNA content after gating from 100 to 1,000, which captures all whole, unclumped cells.

## DDC2-GFP foci

Cells grown overnight in YEPRaff + 0.05% dextrose were pelleted and resuspended in YEPRaff + 15µg/ml nocodazole. Once >90% of the cells were arrested as large budded cells, galactose was added to 2% and samples were removed at various time points, washed twice in phosphate buffered saline (PBS) and visualized using an Olympus BX60 microscope. Pictures were recorded using a Hamamatsu Orca-ER camera and OpenLab3.1.7 software. Fluorescent images were taken in three z sections that bracketed the thickness of the cell, then projected into one image using ImageJ's maximum pixel intensity function. Between 60 and 120 cells were scored for zero, one, or two or more foci per cell, for each strain for each time point. To obtain HU treated cells for the experiment in Figure 3A, cells were grown in YEPD. They were then arrested in G1 (>95% unbudded cells) with 50ng/ml alpha factor and released into a HU

arrest with the addition of pronase to a final concentration of 100µg/ml and HU to a final concentration of 0.2M. Samples were processed for quantification as above. To obtain phleomycin treated cells for the experiment in Figure 3A, cells were grown in YEPD, arrested with 15µg/ml nocodazole (>95% large budded cells) and then treated with phleomycin at a final concentration of 20µg/ml (Cayla). Samples were processed for quantification as above.

#### Rad53p Immunoblot

Cells grown overnight in SRaffC-Ura + 0.05% dextrose were pelleted and resuspended in YEPRaff + 15µg/ml nocodazole. Once >90% of the cells were arrested as large budded cells, galactose was added to a final concentration of 2% and samples were removed at various time points. Cells (8.5ml) at OD600 0.5 to 1.0 were pelleted and lysed by vortex mixing and boiling with 300µl 0.5mm glass beads (Biospec Product, Bartlesville, OK) and 300µl SDS/PAGE loading buffer (8% glycerol (v/v), 100mM TrisHCl pH6.8, 1.6% SDS (w/v), 1.6x10<sup>-3</sup>% bromophenol blue (w/v), 100mM DTT, 1mM PMSF) with protease inhibitors (1µg/ml leupeptin, 1µg/ml pepstatin A, 1µg/ml chymostatin, 1mM benzamidine) and phosphatase inhibitors (1mM Na<sub>3</sub>VO<sub>4</sub>, 50mM NaF, 50mM Na β-glycerophosphate). The soluble protein was quantified using a Bradford assay (Bio-Rad) with bovine serum albumin (BSA) as a standard (Sigma). 40µg of each protein sample was electrophoresed on a 7.5% SDS/PAGE gel and transferred to nitrocellulose (Applied Scientific Protran BA85). The membrane was probed with anti-HA 16B12 (Covance) at 1:1000, followed by sheep anti-mouse HRP (Amersham NA931V) at 1:2000. Immunoblots were developed with the SuperSignal system (Pierce).

### Assaying induction of a metaphase arrest

Cells grown overnight in SRaffC-Met,Ura + 0.05% dextrose were pelleted and resuspended in YEPRaff + 2mM methionine to arrest cells in metaphase by Cdc20p depletion. Once arrested (>90% large budded cells), galactose was added to a final concentration of 2% for 2 hours, then the cells were filtered and washed with S broth and resuspended in SGalC-Met,Ura + 50ng/ml alpha factor. Samples were fixed in 67% ethanol (v/v), washed twice with PBS and resuspended in 50ng/ml 4'6-Diamidino-2-Phenylindole (DAPI). Cells were visualized by fluorescence microscopy on an Olympus BX60 microscope and quantified as pre or post metaphase based on nuclear morphology. At least 200 cells were scored for each strain for each time point and the experiment was executed twice. The mean percentage of post metaphase cells and the standard error of the mean from the two experiments is charted.

### Pulsed field gel electrophoresis (PFGE)

YJL3244 and YJL3248 cells grown overnight in SRaffC-Met,Ura + 0.05% dextrose were pelleted and resuspended in YEPRaff + 2mM methionine to arrest cells in metaphase by Cdc20p depletion. Once arrested (>90% large budded cells), nocodazole was added to a final concentration of 15 $\mu$ g/ml for 30 minutes, after which galactose was added to a final concentration of 2% at time zero. To obtain HU treated cells for the experiment in Figure 5, cells were grown in YEPD. They were then arrested in G1 (>95% unbudded cells) with 50ng/ml alpha factor and released into a HU arrest with the addition of pronase to a final concentration of 100 $\mu$ g/ml and HU to a final concentration

of 0.2M. To obtain phleomycin treated cells for the experiment in Figure 5, cells were grown in YEPD, arrested with 15µg/ml nocodazole (>95% large budded cells) and then treated with phleomycin at a final concentration of 20 or 200µg/ml (Cayla).

To make plugs for PFGE,  $6 \times 10^8$  cells were washed twice with ice cold 50mM EDTA and resuspended to 500µl with 50°C SCE (1M sorbitol, 0.1M Na citrate, 10mM EDTA). Lyticase was added to a final concentration of 150U/ml and 250µl of the sample was mixed with 250µl of molten, 50°C 1% SeaPlaque GTG LMP agarose (FMC Bioproducts) and then aliquoted into disposal plug molds (Bio-Rad 170-3713). The plug molds were allowed to solidify at 4°C, then placed in SCEM + lyticase (1M sorbitol, 0.1M Na citrate, 10mM EDTA, 5% β-mercaptoethanol (v/v), 160U/ml lyticase) for 24 hours at 37°C. Plugs were then washed 3 times in T<sub>10</sub>E<sub>1</sub> (10mM Tris pH8.0, 1mM EDTA) for 15 minutes each wash and resuspended in proteinase K solution (1% sarcosyl (w/v), 0.5M EDTA, 2mg/ml proteinase K) for 48 hours at 55°C. Finally, plugs were washed 3 times in T<sub>10</sub>E<sub>1</sub> for 15 minutes each wash and left overnight at 37°C in T<sub>10</sub>E<sub>1</sub> which removes background fluorescence during ethidium bromide visualization of the gel.

Plugs were cut in half and loaded on a 1% SeaKem LE agarose (w/v) gel in 0.5x TBE (45mM Tris, 45mM borate, 1mM EDTA). The gel was electrophoresed in 14°C 0.5xTBE on a CHEF DR-III system with initial switch time of 50 seconds, final switch time of 90 seconds, run time of 22 hours, voltage of 6V and angle of 120 degrees. The gel was stained with 0.5µg/ml ethidium bromide in 0.5xTBE for 1.5 hours, destained in deionized water for 2 hours and imaged with an AlphaImager. The DNA was then nicked in 0.5M HCl for 1 hour, denatured in 1.5M NaCl, 0.5M NaOH for 40 minutes and

neutralized in 3M NaCl, 55mM Tris base, 455mM TrisHCl for 40 minutes. The DNA was then transferred to a GeneScreen Plus nylon membrane and crosslinked with 0.12 joules of UV light in a Stratagene UV Stratalinker 1800. The membrane was probed with an ARS305 fragment (Nguyen et al. 2001) and imaged and quantified with a Molecular Dynamics Storm 840.

## Results

### Re-replication rapidly blocks cell proliferation

Previous work in our lab established yeast strains in which re-replication can be induced in metaphase arrested cells (Nguyen *et al.*, 2001). These yeast strains contain genetic alterations that make three replication initiation proteins refractory to the inhibitory effect of the cyclin-dependent kinase (CDK) Cdc28. The CDK phosphorylation of two subunits of the Origin Recognition Complex, Orc2p and Orc6p, was blocked by mutating their CDK consensus phosphorylation sites (*orc2-6A, orc6-4A*). Cdc28-directed nuclear exclusion of the Mcm2-7p complex (Labib *et al.*, 1999; Nguyen *et al.*, 2000) was prevented by fusing two tandem copies of the SV40 nuclear localization signal to Mcm7p (*MCM7-2NLS*). Finally, CDK regulation of Cdc6p was disrupted by integrating *pGAL1-Δntcdc6*, which expresses an N-terminally truncated and slightly stabilized Cdc6p (*Δntcdc6p*), under the control of the galactose inducible *GAL1* promoter (Drury *et al.*, 1997). In this re-replicating strain, re-replication is detectable only after *Δntcdc6p* is induced by growth in galactose containing medium. A parallel strain,

containing *pGAL1* instead of *pGAL1-Δntcdc6*, does not re-replicate and serves as a negative control strain (Figure 1A).

Further characterization of these strains initially revealed that sustained re-replication leads to a dramatic decrease plating efficiency (Figure 1B). Both the *pGAL1-Δntcdc6* re-replicating strain and *pGAL1* control strain grew with similar efficiency when plated on medium containing dextrose, which represses the *pGAL1* promoter. However, when cells were plated on medium containing galactose, the *pGAL1-Δntcdc6* re-replicating strain showed a decrease in plating efficiency by at least three orders of magnitude. In the absence of perturbations of ORC and MCM, expression of  $\Delta$ ntcdc6p had no effect on cell growth as assayed by colony size or plating efficiency on galactose containing medium (data not shown).

Significant inhibition of cell proliferation could also be seen with transient induction of re-replication (Figure 1C). Both the *pGAL1-Δntcdc6* re-replicating strain and *pGAL1* control strain were arrested in metaphase with nocodazole then exposed to galactose to induce re-replication. After varying amounts of time in galactose, cells were plated on dextrose containing medium to assess the number of cells that could give rise to viable colonies (colony forming units). Because  $\Delta$ ntcdc6p becomes undetectable within 30 minutes after galactose-induced cells are repressed by the addition of dextrose (Nguyen *et al.*, 2001), we expected re-initiation to end following cell plating. The *pGAL1* control strain showed only a slight decrease in colony forming units after three hours in galactose. In contrast, the *pGAL1-Δntcdc6* re-replicating strain showed a five-fold decrease in colony forming units after only 30 minutes in galactose and a nearly fifty-fold decrease after three hours, a statistically significant difference ( $p < 0.002$ ).

### Re-replication induces a *RAD53*-dependent metaphase checkpoint arrest

To determine how rapidly re-replicating cells cease dividing, we examined cells microscopically two days after transient exposure to galactose. Most re-replicating cells that did not give rise to colonies also did not rebud (data not shown), indicating that the cells could not progress beyond the G1 commitment point of the next cell cycle. To pinpoint where in the cell cycle these cells were blocked, we arrested cells in metaphase by depleting them of Cdc20, which is required for the metaphase-anaphase transition (Schwab *et al.*, 1997; Visintin *et al.*, 1997), induced re-replication with galactose for two hours, then restored Cdc20 expression to remove the original metaphase block. Alpha factor was added to trap any cells that progressed into G1 phase of the next cell cycle (Figure 2A). Cell and nuclear morphology were used to distinguish between cells that were in metaphase and cells that were post metaphase (anaphase/telophase or G1 phase). More than 90% of the *pGAL1* negative control cells proceeded past metaphase and accumulated in G1 phase. In contrast, less than 20% of the *pGAL1-Δntcdc6* re-replicating cells had exited metaphase five hours after Cdc20 expression was restored. Similar results were obtained when these cells were monitored after re-replication was induced for only one hour instead of two (data not shown). Since re-replication was barely detectable by flow cytometry after one hour of induction (Figure 1A), these data suggest that even limited re-replication induces a metaphase arrest.

In budding yeast, genotoxic stresses such as replication fork stalls or DNA damage induce a metaphase arrest that requires activation of the checkpoint kinase Rad53p (Allen *et al.*, 1994; Weinert *et al.*, 1994; Sanchez *et al.*, 1996; Sun *et al.*, 1996),

the homolog of Chk2 in mammalian cells and Cds1 in *Schizosaccharomyces pombe*. To determine whether re-replication might activate these pathways, we induced re-replication in a *rad53* $\Delta$  mutant background and monitored the ability of these cells to progress past metaphase. Flow cytometry demonstrated that re-replication was still induced in the presence of the *rad53* $\Delta$  mutation (Figure 1A), and vital staining with Phloxine B showed that most of the cells remained metabolically alive after three hours of induction (data not shown). The percentage of cells that could complete metaphase, however, increased from less than 20% to nearly 50%. This result suggests that a significant portion of the checkpoint proficient re-replicating cells were arrested solely in response to a *RAD53*-dependent checkpoint. The remaining 50% of the cells also appeared to activate this checkpoint (see below) but presumably stayed arrested because they were subjected to an additional *RAD53*-independent metaphase block (see discussion).

Additional evidence that re-replication activates a *RAD53*-dependent checkpoint response was obtained by examining Rad53p directly. Activation of Rad53p protein kinase is tightly correlated with its hyperphosphorylation (Allen *et al.*, 1994; Weinert *et al.*, 1994; Sanchez *et al.*, 1996; Sun *et al.*, 1996), a modification that retards Rad53p mobility during gel electrophoresis. After inducing re-replication with galactose in metaphase arrested cells, we monitored the phosphorylation state of Rad53p by immunoblotting total cell lysates (Figure 2B). In the *pGAL1* control strain, Rad53p remained hypophosphorylated for the duration of the galactose induction, consistent with the absence of any checkpoint arrest of the cell cycle. In the *pGAL1*- $\Delta$ *ntcdc6* re-replicating strain, however, Rad53p hyperphosphorylation was detected within 45



minutes of induction, and the majority of the protein became hyperphosphorylated by 120 minutes. Together, the metaphase arrest and Rad53p hyperphosphorylation indicate that Rad53p is activated as part of a checkpoint response triggered by re-replication. The nearly complete conversion of Rad53p to the hyperphosphorylated form (Figure 2B, Figure 4A) further suggests that this response was activated in almost all re-replicating cells.

#### Re-replication induces formation of Ddc2-GFP foci

Because the genome is only partial re-replicated in our strains, many re-replication forks cannot be properly terminating with a converging fork from the adjacent replicon. This suggests that many of the re-replication forks must be stalled or disrupted, potentially signaling replication stress, DNA damage, or both. Analysis of the Ddc2p response to re-replication provided an initial hint that re-replication elicits a checkpoint response to DNA damage. Like Rad53p, Ddc2p is required for the response to both DNA damage and replication stress. Ddc2p in complex with Mec1p is recruited to both sites of double-strand breaks (Kondo *et al.*, 2001; Melo *et al.*, 2001) and stalled replication forks (Katou *et al.*, 2003; Osborn and Elledge, 2003) as part of the sensing of these lesions by the checkpoint pathways. Previous studies established that Ddc2p relocalizes from a diffuse nuclear distribution to punctate subnuclear foci in response to DNA damage (Melo *et al.*, 2001). We observed that similar foci are not generated in response to hydroxyurea (HU) in our strains, thereby providing a possible way to distinguish between the two responses (Figure 3A).

This distinction was demonstrated in a *pGAL1-Δntcdc6* re-replicating strain where *DDC2* was replaced by *DDC2-GFP*. Initial experiments were performed in dextrose containing medium to ensure tight repression of *pGAL1-Δntcdc6*. The re-replicating strain was arrested in metaphase with nocodazole, exposed to 20μg/ml of the DNA damaging agent phleomycin, and examined by fluorescence microscopy. Within one hour, one or more subnuclear foci of Ddc2p-GFP were observed in most cells (Figure 3A), consistent with previously published observations. In contrast, when these cells were released from a G1 arrest into S phase in the presence of 0.2 M HU, there was little induction of Ddc2p-GFP subnuclear foci even three hours after imposition of the replication block (Figure 3A). If phleomycin is added to these cells, subnuclear Ddc2p-GFP foci appear within an hour, indicating that damage-induced foci are observable in HU arrested cells (data not shown). Similar results were observed in wild-type cells not containing any perturbations of ORC, Mcm2-7, or Cdc6.

To examine the localization of Ddc2p following re-replication, the *pGAL1-Δntcdc6* re-replicating and *pGAL1* control strains containing *DDC2-GFP* were arrested in metaphase, induced with galactose, and examined at 30 minute intervals by fluorescence microscopy. In the *pGAL1-Δntcdc6* strain, within one hour of induction of re-replication, there was a significant increase in Ddc2p-GFP subnuclear foci (Figure 3B). Within two hours the number of cells with foci and the number of foci per cell were quantitatively similar to the response observed with the addition of the DNA damaging agent phleomycin. Little increase in Ddc2p-GFP foci was observed in the *pGAL1* control strain. Thus, these findings suggest that re-replication induces a DNA damage checkpoint.

### Re-replication induces a DNA damage response

For a more definitive examination of whether re-replication was triggering a DNA damage response, a replication stress response, or both, we took advantage of the genetic distinction between these two checkpoint pathways in budding yeast. Both pathways converge on *RAD53* and induce a metaphase arrest. However, upstream of *RAD53*, the DNA damage response is predominantly dependent on *RAD9*, while the replication stress response is predominantly dependent on *MRC1*. We individually deleted each gene in the *pGAL1- $\Delta$ ntcdc6* re-replicating strain and the *pGAL1* control strain and investigated whether the metaphase arrest and Rad53p hyperphosphorylation induced by re-replication was dependent on either gene. Initial experiments established that re-replication was still induced on all chromosomes in the *mrc1 $\Delta$*  and *rad9 $\Delta$*  mutants (Figure 1A and data not shown).

As described above, the proportion of cells arrested in metaphase due to re-replication was approximately halved when *RAD53* was deleted. A slightly higher reduction was observed when *RAD9* was deleted, whereas a much smaller reduction was observed upon deletion of *MRC1* (Figure 2A). Thus, nearly half of the re-replicating cells that are arrested in metaphase are solely held at that arrest by a *RAD9* dependent pathway. The remainder, as discussed previously, appear to be subjected to an additional metaphase block. The hyperphosphorylation of Rad53p induced during re-replication (Figure 4A, lanes 1-5) was also dramatically reduced in a *rad9 $\Delta$*  mutant background (Figure 4A, lanes 11-15). The simplest interpretation of these results is that the Rad53p phosphorylation and *RAD53*-dependent metaphase arrest induced by re-

replication is primarily triggered through the *RAD9*-dependent DNA damage response pathway.

The virtually complete dependence of Rad53p hyperphosphorylation on *RAD9* suggests that re-replication generates little or no *MRC1*-dependent signaling of replication stress. Alternatively, one could hypothesize that the *rad9* $\Delta$  mutation, the metaphase state of the cell, or an insufficient number of re-replicating forks, somehow prevents the detection of replication stress in our re-replicating cells. For example, if Mrc1p did not properly assemble onto re-replication forks during re-initiation as it normally does at replication forks during normal initiation, the *rad9* $\Delta$  cells would be unable to signal the presence of stalled forks.

To demonstrate that we can indeed detect replication stress during re-replication in a *rad9* $\Delta$  mutant, the mutant strain was arrested in metaphase, split into three separate culture conditions, and each harvested for immunoblot analysis of Rad53p. Galactose was added to one culture to induce re-replication. As described above, there was little Rad53p hyperphosphorylation because of the *rad9* $\Delta$  mutation (Figure 4B, lanes 9-11). Galactose and HU were added to a second culture to induce replication stress during re-replication. In these cells, robust Rad53p hyperphosphorylation could now be observed (Figure 4B, lanes 6-8), presumably through activation of the *MRC1*-dependent replication stress response pathway. Finally, dextrose and HU were added to the third culture. Dextrose represses the *pGAL1* promoter and stifles any induction of re-replication. No Rad53p hyperphosphorylation was observed in this culture (Figure 4B, lanes 3-5), confirming that re-replication forks were generating the HU-induced replication stress response observed in the second culture. Thus, the *MRC1*-dependent replication stress

response pathway is capable of sensing stalled re-replication forks during a metaphase arrest in a *rad9Δ* background. The lack of any significant activation of this pathway in the absence of HU suggests that stalled re-replication forks are not triggering the checkpoint response observed in re-replicating cells. Consistent with this conclusion is the observation that the extent and kinetics of Rad53p hyperphosphorylation induced by re-replication are unchanged by deletion of *MRC1* (Figure 4A, lanes 6-10). Taken together, our data suggest that DNA damage, and not replication stress, is the predominant genotoxic insult accumulating as a consequence of re-replication.

#### Re-replication induces double-stranded breaks

Given the induction of a DNA damage response, we looked for direct evidence of DNA damage induced by re-replication. We assayed whether re-replication results in double-stranded breaks by monitoring the appearance of sub-chromosomal fragments by pulsed field gel electrophoresis (PFGE). To verify that PFGE can detect chromosome fragmentation, we examined yeast chromosomes from metaphase arrested cells treated with phleomycin, which generates double-stranded breaks. At high doses of phleomycin, all chromosomes were converted to a heterogeneous pool of sub-chromosomal fragments (Figure 5A, lanes 4-6). These results were confirmed by southern blot analysis of these gels, using ARS305 to probe for chromosome III (Figure 5A, lanes 15-17).

Similar chromosome fragmentation was not observed in cells arrested in S phase with HU (Figure 5A lanes 1-3 and 12-14). Replicating structures, such as replication bubbles and forks, are thought to significantly retard DNA mobility during PFGE, and whole chromosomes with many replicating structures are retained in gel loading wells

(Hennessy *et al.*, 1990). Nonetheless, the absence of any significant sub-chromosomal fragments even after prolonged HU arrest suggests that there is no rapid or widespread degeneration of stressed replication forks to double-stranded breaks.

Like HU treatment, re-replication caused the majority of each chromosome to be retained in the wells. However, re-replication also generated sub-chromosomal fragments, which appeared as a smear of DNA migrating from below the smallest chromosome up toward the well (Figure 5A, lanes 9-11). This could be seen more clearly by southern blot analysis which showed an accumulation of chromosome III fragments migrating faster than the smallest full length chromosome (Figure 5A, lanes 20-22) in amounts comparable to those generated by 20 $\mu$ g/ml of phleomycin (Figure 5B). This induction of sub-chromosomal fragments was specific to re-replicating cells, as no such induction was seen in the control strain (Figure 5A, lanes 18-19). Similar sub-chromosomal fragments were observed when the southern blots were probed for chromosome 4 and 7 (data not shown). Thus, re-replication, but not replication stressed by HU, generates double-stranded DNA breaks.

#### Checkpoint responses do not reduce the lethality induced by re-replication

By mobilizing a corrective response and delaying the cell cycle, checkpoint pathways help to protect cells from insults that would disrupt the proper transmission of genetic information. In some cases, however, recovery from the insult may not be possible despite the activation of a checkpoint. For example, degradation of Mcm proteins in the middle of S phase disrupts active replication forks and appears to activate the replication stress response: Rad53p is hyperphosphorylated and cells experience a

*RAD9*-independent metaphase arrest (Labib *et al.*, 2001). Despite the activation of this checkpoint, cells are unable to recover their ability to replicate after Mcm proteins are restored (Labib *et al.*, 2001), presumably because Mcm proteins cannot be reloaded onto the disrupted replication forks. In order to determine if the DNA damage response is able to protect cells from the amount and type of DNA lesions generated by re-replication, we examined the viability of re-replicating cells that harbor deletions in *RAD53*, *RAD9*, or *MRC1*. Strains deleted for any of these genes showed similar decreases in viability as checkpoint proficient strains when subjected to constitutive or transient ( $p > 0.35$  at three hours) re-replication (Figure 1B, 1C). This suggests that the extent of re-replication in these cells generates an amount or type of lethal genotoxic stress that is irreparable.

## **Discussion**

Eukaryotic cells employ multiple overlapping mechanisms to prohibit re-initiation of DNA replication within a single cell cycle. An obvious reason why cells might impose such extensive and layered safeguards is that even a low frequency and amount of extra DNA synthesis could eventually alter genome content. We report here that re-replication can induce an immediate and severe threat to the cell. Re-replicating cells rapidly and permanently cease cell division. They phosphorylate Rad53p in a *RAD9* dependent manner and arrest in metaphase. This checkpoint response is unlikely to be a novel “re-replication checkpoint.” Rather, we infer from the stereotypical DNA damage response that re-replication rapidly generates DNA lesions that are recognized by the cell as DNA damage. Thus, the use of multiple mechanisms to prevent re-replication not only

preserves genome content in the long-term, but also protects cells from lethal genomic insults in the short term.

Surprisingly, we have been able to demonstrate that re-replication triggers little or no replication stress response, even though re-replication forks fail to complete a full round of replication. The Rad53p phosphorylation observed during re-replication was almost exclusively dependent on *RAD9*, which signals DNA damage, and was independent of *MRC1*, which signals replication stress. Similarly, the metaphase arrest induced by re-replication was more dependent on *RAD9* than on *MRC1*. Importantly, the absence of a replication stress response was not due to an inability to respond to replication stress. In a *rad9* $\Delta$  mutant background, where re-replication by itself failed to induce Rad53p phosphorylation, the addition of HU to stress the re-replicating forks leads to robust and persistent Rad53p phosphorylation. The simplest interpretation of these data is that re-replicating forks fail to complete a full round of replication, not because they eventually stall, but because they somehow degenerate into DNA lesions that are recognized as DNA damage. These results contrast with those obtained in human cells depleted of geminin, where the resulting re-replication can be associated with the replication stress response (Melixetian *et al.*, 2004; Zhu *et al.*, 2004). Whether these contrasting results reflect differences in species or protocol for inducing re-replication remains to be addressed in the future.

A key question raised by these findings is how re-replication generates DNA lesions without inducing a stalled fork response. Because a prompt DNA damage response is observed in almost all cells in the presence of the microtubule depolymerizing agent nocodazole, the lesions are unlikely to be a consequence of spindle tension on



partially replicated chromosomes. Consistent with this, we can induce re-replication and observe the attendant DNA damage response during S phase (data not shown), suggesting that a mitotic state is not required to generate the lesion. Moreover, preliminary evidence suggests that elongation is restrained during re-replication (data not shown), raising the possibility that re-replicating replisomes encounter problems that could lead to DNA lesions. We therefore suspect that the lesions are generated by the act of re-replication itself.

Any molecular model for how these lesions are generated must explain why they are generated during re-replication and not during normal replication. One possible explanation is that the first round of replication structurally alters chromosomes in a manner that interferes with their re-replication within the same cell cycle; sister chromatid cohesion, which is established during DNA replication, provides precedence for such a replication-coupled change in chromosome state (reviewed in Nasmyth, 2001). Other possible explanations include hypothetical problems specific to re-replication such as poor coordination of histone synthesis and/or nucleosome assembly with re-replication (Verreault, 2003), re-replicating forks from later rounds of re-replication overtaking re-replicating forks from earlier rounds, or defective assembly of replisomes during re-initiation.

An important approach to understanding how re-replication generates DNA damage is to characterize the molecular structure of the primary lesions that are induced. Importantly, these primary lesions may not be the chromosomal breaks that we observed by PFGE. Other abnormal DNA structures that could trigger the DNA damage response might be generated earlier before degenerating into chromosomal breaks. Fork collapse,

for example, can generate “chicken feet” structures (Sogo *et al.*, 2002), which expose free double-stranded DNA ends without cleaving the chromosome. Further analysis of re-replicating DNA will hopefully yield more insight into the structure of these primary lesions and the molecular mechanisms by which they are generated.

Although re-replication induces a *RAD9* dependent checkpoint response, this response offers little protection against the lethal consequences of re-replication (Fig. 1B). This lack of protection is reminiscent of the futile induction of a *RAD9* independent checkpoint response following complete Mcm degradation in S phase (Labib *et al.*, 2001). Loss of Mcm proteins from replication forks is apparently irreparable even after resynthesis of the proteins, because there is no efficient mechanism to reload Mcm proteins at forks. Similarly, in our re-replicating cells the damage induced by re-replication may also be irreparable and overwhelm any possible protective effect of the DNA damage response. Additionally, other lethal problems may arise from re-replication that are not dependent on DNA damage and cannot be corrected by the DNA damage response. Such additional problems might account for the partial persistence of metaphase arrested cells when re-replication is induced in the absence of *RAD53* or *RAD9* (Figure 2A). Fully understanding the lethal consequences of re-replication will require further molecular characterization of the terminal phenotype of re-replicating cells.

The extra copies of genes that are generated by re-replication have long been considered a possible source of genomic instability. Our observation that DNA damage is generated during re-replication suggests an additional way by which re-replication might generate genomic changes. Interestingly, in mammalian cells, overexpression of a

single replication initiation protein Cdt1 can induce subtle re-replication (Vaziri *et al.*, 2003) and has been implicated in tumorigenesis (Arentson *et al.*, 2002). Thus, re-replication may be another potential source for the genomic instability associated with tumorigenesis.

### **Acknowledgements**

We thank Anita Sil, David Toczyski, David Morgan, Hiten Madhani, Carol Gross, and Alexander Johnson for helpful discussions and comments on the manuscript. We thank Alexander Johnson for use of his CHEF gel apparatus. We also thank Erin Quan and Emily Wang for help making initial observations of the checkpoint response. This work was supported by grants to J. Li from the ACS (RPG-99-169-01-CCG) and the NIH (RO1 GM59704). B. Green was supported by an NSF Predoctoral Fellowship (DGE-0202754) and a DOD Breast Cancer Predoctoral Fellowship (W81XWH-04-1-0409).

### **References**

Alcasabas, A.A., Osborn, A.J., Bachant, J., Hu, F., Werler, P.J., Bousset, K., Furuya, K., Diffley, J.F., Carr, A.M., and Elledge, S.J. (2001). Mrc1 transduces signals of DNA replication stress to activate Rad53. *Nat Cell Biol* 3, 958-965.

- Allen, J.B., Zhou, Z., Siede, W., Friedberg, E.C., and Elledge, S.J. (1994). The SAD1/RAD53 protein kinase controls multiple checkpoints and DNA damage-induced transcription in yeast. *Genes Dev* 8, 2401-2415.
- Arentson, E., Faloon, P., Seo, J., Moon, E., Studts, J.M., Fremont, D.H., and Choi, K. (2002). Oncogenic potential of the DNA replication licensing protein CDT1. *Oncogene* 21, 1150-1158.
- Bell, S.P., and Dutta, A. (2002). DNA replication in eukaryotic cells. *Annu Rev Biochem* 71, 333-374.
- Broek, D., Bartlett, R., Crawford, K., and Nurse, P. (1991). Involvement of p34cdc2 in establishing the dependency of S phase on mitosis [see comments]. *Nature* 349, 388-393.
- Brown, E.J., and Baltimore, D. (2003). Essential and dispensable roles of ATR in cell cycle arrest and genome maintenance. *Genes Dev* 17, 615-628.
- Dahmann, C., Diffley, J.F., and Nasmyth, K.A. (1995). S-phase-promoting cyclin-dependent kinases prevent re-replication by inhibiting the transition of replication origins to a pre-replicative state. *Curr Biol* 5, 1257-1269.
- Detweiler, C.S., and Li, J.J. (1998). Ectopic induction of Clb2 in early G1 phase is sufficient to block prereplicative complex formation in *Saccharomyces cerevisiae*. *Proc Natl Acad Sci U S A* 95, 2384-2389.
- Drury, L.S., Perkins, G., and Diffley, J.F. (1997). The Cdc4/34/53 pathway targets Cdc6p for proteolysis in budding yeast. *Embo J* 16, 5966-5976.

- Drury, L.S., Perkins, G., and Diffley, J.F. (2000). The cyclin-dependent kinase Cdc28p regulates distinct modes of Cdc6p proteolysis during the budding yeast cell cycle. *Curr Biol* 10, 231-240.
- Elsasser, S., Chi, Y., Yang, P., and Campbell, J.L. (1999). Phosphorylation controls timing of Cdc6p destruction: A biochemical analysis. *Mol Biol Cell* 10, 3263-3277.
- Emili, A. (1998). MEC1-dependent phosphorylation of Rad9p in response to DNA damage. *Mol Cell* 2, 183-189.
- Goldstein, A.L., and McCusker, J.H. (1999). Three new dominant drug resistance cassettes for gene disruption in *Saccharomyces cerevisiae*. *Yeast* 15, 1541-1553.
- Gopalakrishnan, V., Simancek, P., Houchens, C., Snaith, H.A., Frattini, M.G., Sazer, S., and Kelly, T.J. (2001). Redundant control of rereplication in fission yeast. *Proc Natl Acad Sci U S A* 98, 13114-13119.
- Gottifredi, V., Shieh, S., Taya, Y., and Prives, C. (2001). p53 accumulates but is functionally impaired when DNA synthesis is blocked. *Proc Natl Acad Sci U S A* 98, 1036-1041.
- Guthrie, C., and Fink, G. (eds.) (1990). *Guide to Yeast Genetics and Molecular Biology*. Academic Press.
- Haaf, T., Golub, E.I., Reddy, G., Radding, C.M., and Ward, D.C. (1995). Nuclear foci of mammalian Rad51 recombination protein in somatic cells after DNA damage and its localization in synaptonemal complexes. *Proc Natl Acad Sci U S A* 92, 2298-2302.
- Haase, S.B., and Lew, D.J. (1997). Flow cytometric analysis of DNA content in budding yeast. *Methods Enzymol* 283, 322-332.

- Hennessy, K.M., Clark, C.D., and Botstein, D. (1990). Subcellular localization of yeast *CDC46* varies with the cell cycle. *Genes and Development* 4, 2252-2263.
- Hua, X.H., Yan, H., and Newport, J. (1997). A role for Cdk2 kinase in negatively regulating DNA replication during S phase of the cell cycle. *J Cell Biol* 137, 183-192.
- Jallepalli, P.V., Brown, G.W., Muzi-Falconi, M., Tien, D., and Kelly, T.J. (1997). Regulation of the replication initiator protein p65cdc18 by CDK phosphorylation. *Genes Dev* 11, 2767-2779.
- Katou, Y., Kanoh, Y., Bando, M., Noguchi, H., Tanaka, H., Ashikari, T., Sugimoto, K., and Shirahige, K. (2003). S-phase checkpoint proteins Tof1 and Mrc1 form a stable replication-pausing complex. *Nature* 424, 1078-1083.
- Kondo, T., Wakayama, T., Naiki, T., Matsumoto, K., and Sugimoto, K. (2001). Recruitment of Mec1 and Ddc1 checkpoint proteins to double-strand breaks through distinct mechanisms. *Science* 294, 867-870.
- Labib, K., Diffley, J.F., and Kearsley, S.E. (1999). G1-phase and B-type cyclins exclude the DNA-replication factor Mcm4 from the nucleus. *Nat Cell Biol* 1, 415-422.
- Labib, K., Kearsley, S.E., and Diffley, J.F. (2001). MCM2-7 proteins are essential components of prereplicative complexes that accumulate cooperatively in the nucleus during G1-phase and are required to establish, but not maintain, the S-phase checkpoint. *Mol Biol Cell* 12, 3658-3667.
- Lee, C., Hong, B., Choi, J.M., Kim, Y., Watanabe, S., Ishimi, Y., Enomoto, T., Tada, S., and Cho, Y. (2004). Structural basis for inhibition of the replication licensing factor Cdt1 by geminin. *Nature* 430, 913-917.

- Lopez-Girona, A., Mondesert, O., Leatherwood, J., and Russell, P. (1998). Negative regulation of Cdc18 DNA replication protein by Cdc2. *Mol Biol Cell* *9*, 63-73.
- McGarry, T.J., and Kirschner, M.W. (1998). Geminin, an inhibitor of DNA replication, is degraded during mitosis. *Cell* *93*, 1043-1053.
- Melixetian, M., Ballabeni, A., Masiero, L., Gasparini, P., Zamponi, R., Bartek, J., Lukas, J., and Helin, K. (2004). Loss of Geminin induces rereplication in the presence of functional p53. *J Cell Biol* *165*, 473-482.
- Melo, J., and Toczyski, D. (2002). A unified view of the DNA-damage checkpoint. *Curr Opin Cell Biol* *14*, 237-245.
- Melo, J.A., Cohen, J., and Toczyski, D.P. (2001). Two checkpoint complexes are independently recruited to sites of DNA damage in vivo. *Genes Dev* *15*, 2809-2821.
- Mihaylov, I.S., Kondo, T., Jones, L., Ryzhikov, S., Tanaka, J., Zheng, J., Higa, L.A., Minamino, N., Cooley, L., and Zhang, H. (2002). Control of DNA replication and chromosome ploidy by geminin and cyclin A. *Mol Cell Biol* *22*, 1868-1880.
- Moll, T., Tebb, G., Surana, U., Robitsch, H., and Nasmyth, K. (1991). The role of phosphorylation and the CDC28 protein kinase in cell cycle-regulated nuclear import of the *S. cerevisiae* transcription factor SWI5. *Cell* *66*, 743-758.
- Nasmyth, K. (2001). Disseminating the genome: joining, resolving, and separating sister chromatids during mitosis and meiosis. *Annu Rev Genet* *35*, 673-745.
- Nguyen, V.Q., Co, C., Irie, K., and Li, J.J. (2000). Clb/Cdc28 kinases promote nuclear export of the replication initiator proteins Mcm2-7. *Curr Biol* *10*, 195-205.
- Nguyen, V.Q., Co, C., and Li, J.J. (2001). Cyclin-dependent kinases prevent DNA re-replication through multiple mechanisms. *Nature* *411*, 1068-1073.

- Nishitani, H., Lygerou, Z., Nishimoto, T., and Nurse, P. (2000). The Cdt1 protein is required to license DNA for replication in fission yeast. *Nature* 404, 625-628.
- Nyberg, K.A., Michelson, R.J., Putnam, C.W., and Weinert, T.A. (2002). Toward maintaining the genome: DNA damage and replication checkpoints. *Annu Rev Genet* 36, 617-656.
- Osborn, A.J., and Elledge, S.J. (2003). Mrc1 is a replication fork component whose phosphorylation in response to DNA replication stress activates Rad53. *Genes Dev* 17, 1755-1767.
- Quinn, L.M., Herr, A., McGarry, T.J., and Richardson, H. (2001). The Drosophila Geminin homolog: roles for Geminin in limiting DNA replication, in anaphase and in neurogenesis. *Genes Dev* 15, 2741-2754.
- Saintigny, Y., Delacote, F., Vares, G., Petitot, F., Lambert, S., Averbek, D., and Lopez, B.S. (2001). Characterization of homologous recombination induced by replication inhibition in mammalian cells. *Embo J* 20, 3861-3870.
- Sanchez, Y., Desany, B.A., Jones, W.J., Liu, Q., Wang, B., and Elledge, S.J. (1996). Regulation of RAD53 by the ATM-like kinases MEC1 and TEL1 in yeast cell cycle checkpoint pathways. *Science* 271, 357-360.
- Sauer, K., Knoblich, J.A., Richardson, H., and Lehner, C.F. (1995). Distinct modes of cyclin E/cdc2c kinase regulation and S-phase control in mitotic and endoreduplication cycles of Drosophila embryogenesis. *Genes Dev* 9, 1327-1339.
- Saxena, S., Yuan, P., Dhar, S.K., Senga, T., Takeda, D., Robinson, H., Kornbluth, S., Swaminathan, K., and Dutta, A. (2004). A dimerized coiled-coil domain and an



- adjoining part of geminin interact with two sites on Cdt1 for replication inhibition. *Mol Cell* *15*, 245-258.
- Schwab, M., Lutum, A.S., and Seufert, W. (1997). Yeast Hct1 is a regulator of Clb2 cyclin proteolysis. *Cell* *90*, 683-693.
- Sogo, J.M., Lopes, M., and Foiani, M. (2002). Fork reversal and ssDNA accumulation at stalled replication forks owing to checkpoint defects. *Science* *297*, 599-602.
- Sun, Z., Fay, D.S., Marini, F., Foiani, M., and Stern, D.F. (1996). Spk1/Rad53 is regulated by Mec1-dependent protein phosphorylation in DNA replication and damage checkpoint pathways. *Genes Dev* *10*, 395-406.
- Tada, S., Li, A., Maiorano, D., Mechali, M., and Blow, J.J. (2001). Repression of origin assembly in metaphase depends on inhibition of RLF-B/Cdt1 by geminin. *Nat Cell Biol* *3*, 107-113.
- Toh, G.W., and Lowndes, N.F. (2003). Role of the *Saccharomyces cerevisiae* Rad9 protein in sensing and responding to DNA damage. *Biochem Soc Trans* *31*, 242-246.
- Uhlmann, F., Wernic, D., Poupart, M.A., Koonin, E.V., and Nasmyth, K. (2000). Cleavage of cohesin by the CD clan protease separin triggers anaphase in yeast. *Cell* *103*, 375-386.
- Vas, A., Mok, W., and Leatherwood, J. (2001). Control of DNA rereplication via Cdc2 phosphorylation sites in the origin recognition complex. *Mol Cell Biol* *21*, 5767-5777.
- Vaziri, C., Saxena, S., Jeon, Y., Lee, C., Murata, K., Machida, Y., Wagle, N., Hwang, D.S., and Dutta, A. (2003). A p53-dependent checkpoint pathway prevents rereplication. *Mol Cell* *11*, 997-1008.

- Verreault, A. (2003). Histone deposition at the replication fork: a matter of urgency. *Mol Cell* 11, 283-284.
- Visintin, R., Prinz, S., and Amon, A. (1997). CDC20 and CDH1: a family of substrate-specific activators of APC-dependent proteolysis. *Science* 278, 460-463.
- Ward, I.M., and Chen, J. (2001). Histone H2AX is phosphorylated in an ATR-dependent manner in response to replicational stress. *J Biol Chem* 276, 47759-47762.
- Weinert, T.A., Kiser, G.L., and Hartwell, L.H. (1994). Mitotic checkpoint genes in budding yeast and the dependence of mitosis on DNA replication and repair. *Genes Dev* 8, 652-665.
- Wilmes, G.M., Archambault, V., Austin, R.J., Jacobson, M.D., Bell, S.P., and Cross, F.R. (2004). Interaction of the S-phase cyclin Clb5 with an "RXL" docking sequence in the initiator protein Orc6 provides an origin-localized replication control switch. *Genes Dev* 18, 981-991.
- Wohlschlegel, J.A., Kutok, J.L., Weng, A.P., and Dutta, A. (2002). Expression of geminin as a marker of cell proliferation in normal tissues and malignancies. *Am J Pathol* 161, 267-273.
- Wuarin, J., Buck, V., Nurse, P., and Millar, J.B. (2002). Stable association of mitotic cyclin B/Cdc2 to replication origins prevents endoreduplication. *Cell* 111, 419-431.
- Yanow, S.K., Lygerou, Z., and Nurse, P. (2001). Expression of Cdc18/Cdc6 and Cdt1 during G2 phase induces initiation of DNA replication. *Embo J* 20, 4648-4656.
- Zhong, W., Feng, H., Santiago, F.E., and Kipreos, E.T. (2003). CUL-4 ubiquitin ligase maintains genome stability by restraining DNA-replication licensing. *Nature* 423, 885-889.

Zhu, W., Chen, Y., and Dutta, A. (2004). Rereplication by depletion of geminin is seen regardless of p53 status and activates a G2/M checkpoint. *Mol Cell Biol* 24, 7140-7150.

**Table 1.** Strains used in this study

Strain	Source	Genotype
YJL310	(Detweiler and Li, 1998)	<i>leu2-3,112 ura3-52 trp1-289 bar1Δ::LEU2</i>
YJL3244	(Nguyen <i>et al.</i> , 2001)	<i>orc2-cdk6A orc6-cdk4A leu2 ura3-52::pGAL1, URA3) trp1-289 ade2 ade3 MCM7-2NLS bar1Δ::LEU2 cdc20::pMET3-HA3-CDC20, TRP1}</i>
YJL3248	(Nguyen <i>et al.</i> , 2001)	<i>orc2-cdk6A orc6-cdk4A ura3-52::pGAL1-Δntcdc6, URA3} trp1-289 leu2 ade2 ade3 MCM7-2NLS bar1Δ::LEU2 cdc20::pMET3-HA3-CDC20, TRP1}</i>
YJL3604	This study	<i>rad53Δ::kanMX6 sml1Δ::TRP1 orc2-cdk6A orc6-cdk4A ura3-52::pGAL1-Δntcdc6, URA3} trp1-289 leu2 ade2 ade3 MCM7-2NLS bar1Δ::LEU2</i>
YJL3607	This study	<i>rad53Δ::kanMX6 sml1Δ::TRP1 orc2-cdk6A orc6-cdk4A leu2 ura3-52::pGAL1, URA3} trp1-289 ade2 ade3 MCM7-2NLS bar1Δ::LEU2</i>
YJL5048	This study	<i>orc2-cdk6A orc6-cdk4A ura3-52::pGAL1-Δntcdc6, URA3} trp1-289 leu2 ade2 ade3 MCM7-2NLS bar1Δ::LEU2 rad53::RAD53-</i>

		<i>2HA6HIS, TRP1}</i>
YJL5055	This study	<i>orc2-cdk6A orc6-cdk4A leu2 ura3-52::pGAL1, URA3} trp1-289 ade2 ade3 MCM7-2NLS bar1Δ::LEU2 rad53::RAD53-2HA6HIS, TRP1}</i>
YJL5060	This study	<i>orc2-cdk6A orc6-cdk4A ura3-52::pGAL1-Δntcdc6, URA3} trp1-289 leu2 ade2 ade3 MCM7-2NLS bar1Δ::LEU2 rad53::RAD53-2HA6HIS, TRP1} rad9Δ::kanMX</i>
YJL5065	This study	<i>orc2-cdk6A orc6-cdk4A leu2 ura3-52::pGAL1, URA3} trp1-289 ade2 ade3 MCM7-2NLS bar1Δ::LEU2 rad53::RAD53-2HA6HIS, TRP1} rad9Δ::kanMX</i>
YJL5085	This study	<i>orc2-cdk6A orc6-cdk4A ura3-52::pGAL1, URA3} trp1-289 leu2 ade2 ade3 MCM7-2NLS bar1Δ::LEU2 rad53::RAD53-2HA6HIS, TRP1} mrc1Δ::kanMX</i>
YJL5087	This study	<i>orc2-cdk6A orc6-cdk4A ura3-52::pGAL1-Δntcdc6, URA3} trp1-289 leu2 ade2 ade3 MCM7-2NLS bar1Δ::LEU2 rad53::RAD53-2HA6HIS, TRP1} mrc1Δ::kanMX</i>
YJL5132	This study	<i>orc2-cdk6A orc6-cdk4A leu2 ura3-52::pGAL1, URA3} trp1-289 ade2 ade3 MCM7-2NLS</i>

		<i>bar1Δ::LEU2 ddc2::{DDC2 GFP, kanMX}</i>
YJL5135	This study	<i>orc2-cdk6A orc6-cdk4A leu2 ura3-52::{pGAL1-Δntcdc6, URA3} trp1-289 ade2 ade3 MCM7-2NLS bar1Δ::LEU2 ddc2::{DDC2 GFP, kanMX}</i>
YJL5408	This study	<i>rad53Δ::kanMX6 sml1Δ::TRP1 orc2-cdk6A orc6-cdk4A ura3-52::{pGAL1-Δntcdc6, URA3} trp1-289 leu2 ade2 ade3 MCM7-2NLS bar1Δ::LEU2 cdc20::{pMET3-HA3-CDC20, NatMX}</i>
YJL5411	This study	<i>orc2-cdk6A orc6-cdk4A ura3-52::{pGAL1-Δntcdc6, URA3} trp1-289 leu2 ade2 ade3 MCM7-2NLS bar1Δ::LEU2 rad53::{RAD53-2HA6HIS, TRP1} rad9Δ::kanMX cdc20::{pMET3-HA3-CDC20, NatMX}</i>
YJL5441	This study	<i>orc2-cdk6A orc6-cdk4A ura3-52::{pGAL1-Δntcdc6, URA3} trp1-289 leu2 ade2 ade3 MCM7-2NLS bar1Δ::LEU2 rad53::{RAD53-2HA6HIS, TRP1} mrc1Δ::kanMX cdc20::{pMET3-HA3-CDC20, NatMX}</i>

**Table 2.** Oligonucleotides used in this study

Oligo	Purpose	Sequence
OJL1404	<i>DDC2-</i> <i>GFP</i>	AAAGGTACGTGGGACAAGAC
OJL1405	<i>DDC2-</i> <i>GFP</i>	AGACAGCAACACACATCTAG
OJL1110	<i>sml1Δ</i>	CTCGCATCGATAAGGATCACGTTCTTCTGC
OJL1111	<i>sml1Δ</i>	GCGACCTCGAGGAAGACATTGCGGGTTCAAG
OJL1002	<i>rad53Δ</i>	GAGAGAATAGTGAGAAAAGATAGTGTTACACAA CATCAACCGGATCCCCGGGTTAATTAA
OJL1003	<i>rad53Δ</i>	CTCTTAAAAAGGGGCAGCATTTTCTATGGGTATT TGTCCTGAATTCGAGCTCGTTTAAAC
OJL1487	<i>rad9Δ</i>	GCTCCCCATCAAATAAGGTC
OJL1488	<i>rad9Δ</i>	TATGTGTCGTCCCAGTACTC
OJL1497	<i>mrc1Δ</i>	AGACAAACA ACTAAGGAAGTTCGTTATTCGCTT TTGAACTTATCACCAAATATTTTAGTGCGGATCC CCGGGTTAATTAA
OJL1498	<i>mrc1Δ</i>	CGACTACTTCAAGACAGCTTCTGGAGTTCAATCA ACTTCTTCGGAAAAGATAAAAAACCACATCGAT GAATTCGAGCTCG

**Figure 1.** Induction of re-replication rapidly blocks cell proliferation.

(A) Checkpoint deficient strains are capable of re-replicating. Cells with the indicated genotypes plus *pMET3-HA3-CDC20 orc2-cdk6A orc6-cdk4A MCM7-2NLS* were grown in medium containing 3% raffinose plus 0.05% dextrose. Metaphase arrest was induced by adding 2mM methionine, to transcriptionally deplete Cdc20p, and 15  $\mu$ g/ml nocodazole. 2% galactose was then added and samples were taken hourly for flow cytometry. Vertical lines indicate the median DNA content for the zero and three hour time points.

(B) Constitutive induction of re-replication prevents cell proliferation. Cells with the indicated genotypes plus *orc2-cdk6A orc6-cdk4A MCM7-2NLS* were grown on plates containing 2% dextrose and serially diluted into S broth with five-fold dilutions. The dilutions were plated on medium containing either 2% dextrose, which represses re-replication, or 2% galactose, which induces re-replication in strains containing *pGAL1- $\Delta$ ntdc6*.

(C) Transient induction of re-replication rapidly inhibits colony forming potential. Cells with the indicated genotypes plus *orc2-cdk6A orc6-cdk4A MCM7-2NLS* were grown in medium containing 3% raffinose plus 0.05% dextrose and arrested in metaphase with addition of 15  $\mu$ g/ml nocodazole. 2% galactose was added for the indicated number of hours to allow for transient induction of re-replication and cells were then plated on medium containing 2% dextrose to score colony forming units (CFU). For each strain, the CFU is expressed as a percentage of the CFU present at time 0 hour. Error bars show standard error of the mean from two experiments.



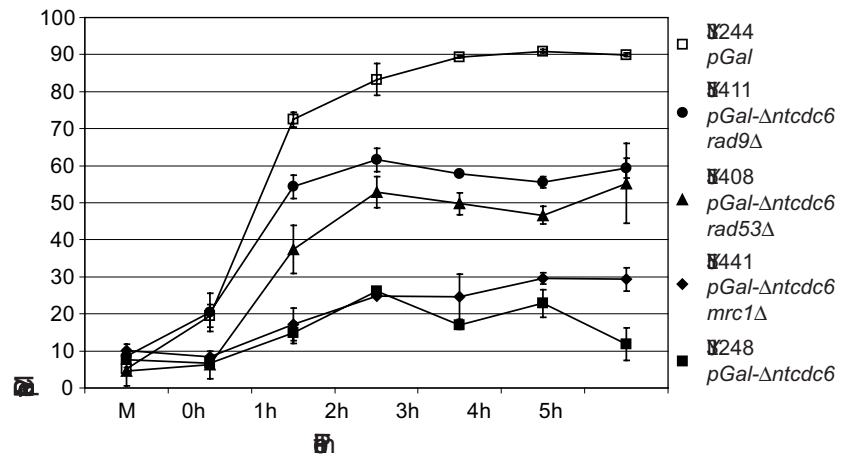


**Figure 2.** Re-replication induces a Rad53-dependent checkpoint response

(A) Re-replication induces a metaphase arrest that is dependent in part on *RAD53* and *RAD9*. Cells with the indicated genotypes plus *pMET3-HA3-CDC20 orc2-cdk6A orc6-cdk4A MCM7-2NLS* were arrested in metaphase by transcriptional depletion of Cdc20p in medium containing 3% raffinose and 2mM methionine (M). 2% galactose was added for two hours to allow the induction of re-replication followed, at time 0h, by release from the Cdc20p depletion arrest by transfer of cells to medium lacking methionine but containing 2% galactose and alpha factor. At hourly intervals following the release, DAPI stained cells were scored (n = 300) as pre- or post-metaphase. The percentage of post metaphase cells are shown for each strain, along with the standard error of the mean.

(B) Re-replication induces phosphorylation of Rad53p. Cells containing the indicated genotypes plus *RAD53-HA orc2-cdk6A orc6-cdk4A MCM7-2NLS* were grown in medium containing 3% raffinose plus 0.05% dextrose and arrested in metaphase with 15 µg/ml nocodazole. 2% galactose was added to allow the induction of re-replication and at the indicated times samples were harvested for immunoblot analysis of Rad53p-HA. The hypophosphorylated protein is indicated by Rad53 and the hyperphosphorylated protein is indicated by Rad53-P.

9  
A



B

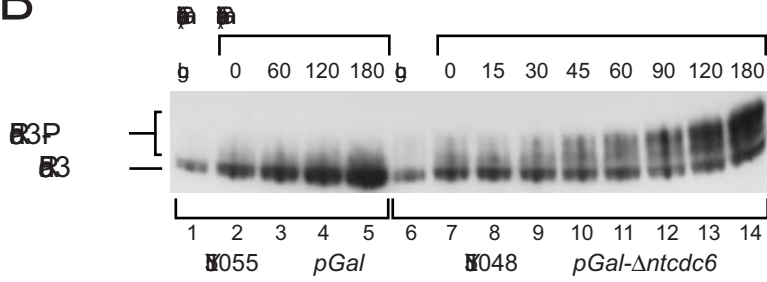


**Figure 3.** Subnuclear Ddc2p foci consistent with DNA damage are formed when re-replication is induced.

(A) HU induced replication stress does not induce subnuclear Ddc2p foci to the same extent as DNA damage. YJL5135 (*ddc2:DDC2-GFP pGAL1- $\Delta$ ntcdc6 orc2-cdk6A orc6-cdk4A MCM7-2NLS*) growing in medium containing 2% dextrose was arrested in metaphase with 15  $\mu$ g/ml nocodazole followed by treatment with 20 $\mu$ g/ml phleomycin to induce DNA damage. A parallel culture was arrested in G1 phase with alpha factor and released from the arrest into 0.2M HU to induce replication stress. At hourly intervals following either phleomycin addition or release into HU, cells were scored for subnuclear GFP foci and the number of cells with zero foci, one focus or two or more foci were quantified. Representative images at 0 and 3 hour are shown. Error bars show standard error of the mean from two experiments (n = 60-120 per experiment).

(B) Re-replication induces Ddc2p foci. YJL5135 and YJL5132 (*ddc2:DDC2-GFP pGAL1 orc2-cdk6A orc6-cdk4A MCM7-2NLS*) growing in medium containing 3% raffinose plus 0.05% dextrose were arrested in metaphase by the addition of 15  $\mu$ g/ml nocodazole. 2% galactose was added to induce re-replication in YJL5135 and at 30 min intervals the number of foci per cell was quantified (n = 60-120 per experiment).

Representative images and quantification are shown as in (A).

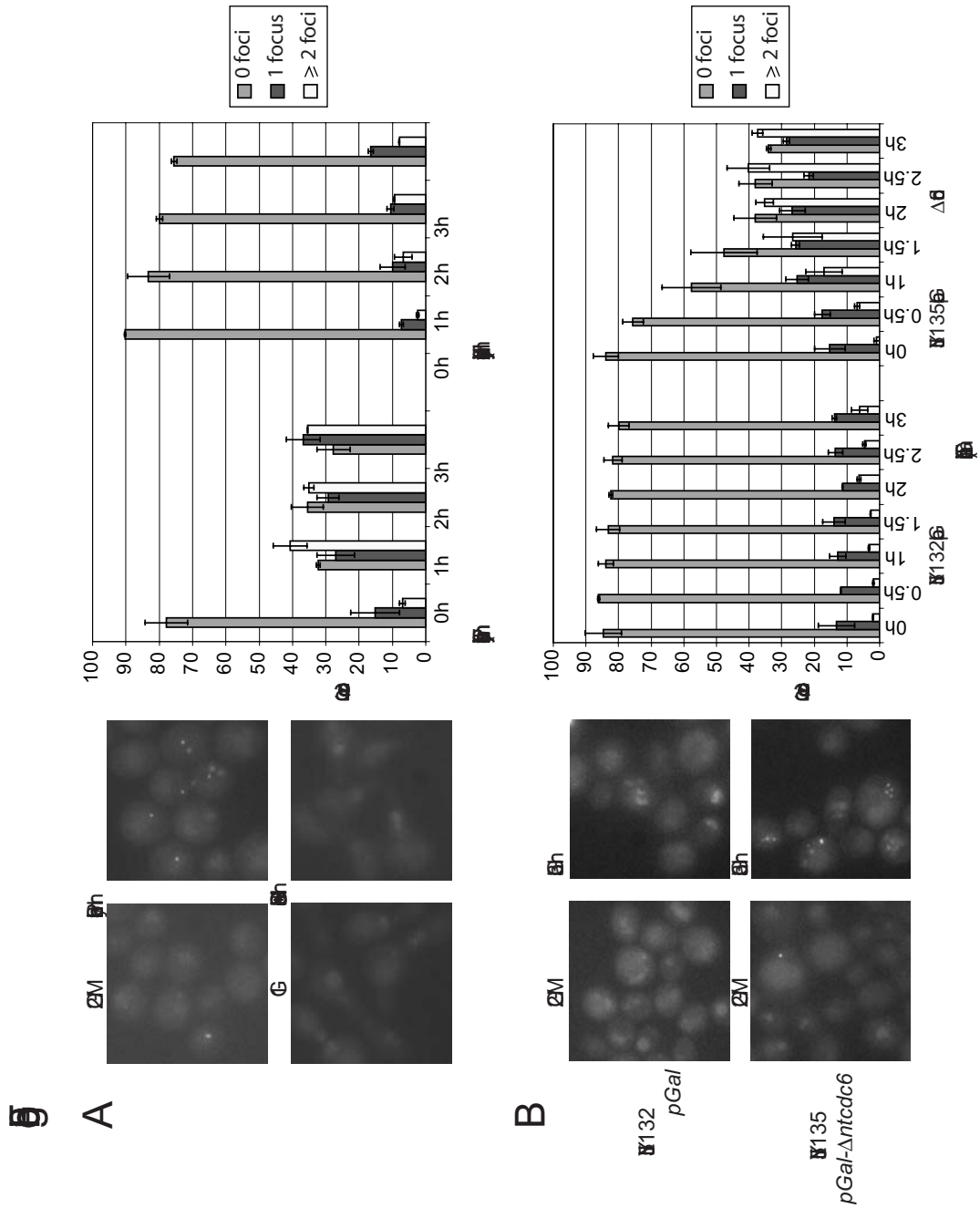


**Figure 4.** The checkpoint response induced by re-replication is dependent on Rad9p and not Mrc1p.

(A) Cells with the indicated genotypes plus *orc2-cdk6A orc6-cdk4A MCM7-2NLS* were grown in 3% raffinose plus 0.05% dextrose and arrested in metaphase by the addition of 15 µg/ml nocodazole. 2% galactose was then added and at the indicated times samples were harvested for immunoblot analysis of Rad53p-HA. The hypophosphorylated protein is indicated by Rad53 and the hyperphosphorylated protein is indicated by Rad53-P.

(B) The *rad9Δ* cells are capable of responding to stalled re-replication forks. YJL5060 (*rad9Δ pGAL1-Δntcdc6 orc2-cdk6A orc6-cdk4A MCM7-2NLS*) grown in medium containing 3% raffinose plus 0.05% dextrose was arrested at metaphase with 15 µg/ml nocodazole and split into three cultures: 0.2M HU and 2% dextrose was added to the first culture; 0.2M HU and 2% galactose was added to the second; and 2% galactose was added to the third. Immunoblot analysis was performed as in (A).

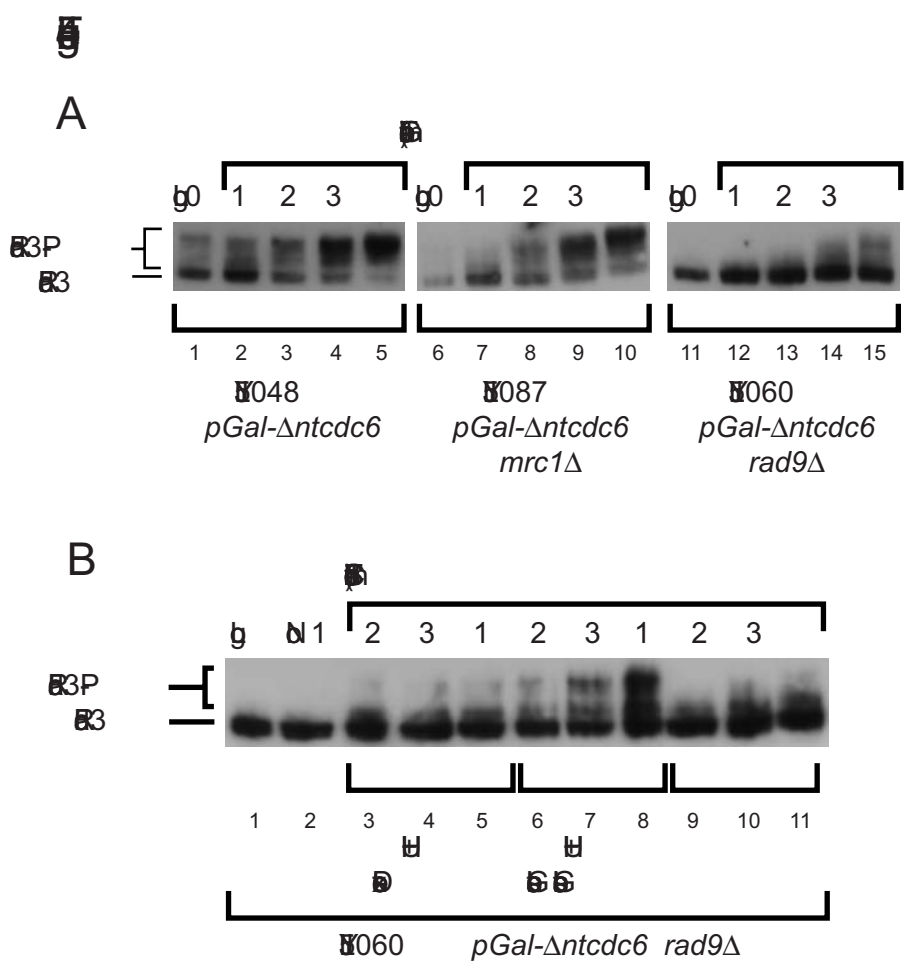


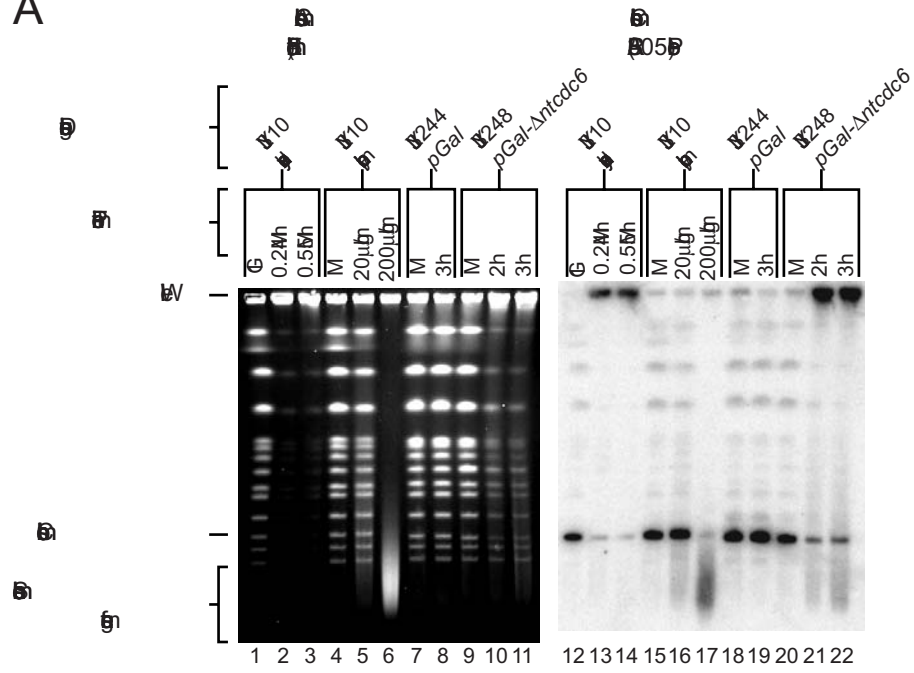
**Figure 5.** Re-replication induces double-stranded breaks.

(A) Re-replication generates sub-chromosomal fragments. (lanes 1-11) PFGE stained with ethidium bromide. (lanes 12-22) Southern blot of PFGE probed with ARS305 fragment to detect chromosome III. (lanes 1-3, 12-14) YJL310 (*CDC6 ORC2 ORC6 MCM7*) was arrested in G1 phase with alpha factor then released from the arrest into the indicated amounts of HU for the indicated times. (lanes 4-6, 15-17) YJL310 was arrested in metaphase with 15 µg/ml nocodazole then treated for two hours with the indicated amount of phleomycin. (lanes 7-8, 18-19) YJL3244 (*pGAL1 orc2-cdk6A orc6-cdk4A MCM7-2NLS pMET3-HA3-CDC20*) was arrested in metaphase in medium containing 3% raffinose and 2mM methionine. Once arrested galactose was added to 2%. (lanes 9-11, 20-22) YJL3248 (*pGAL1-Δntcdc6 orc2-cdk6A orc6-cdk4A MCM7-2NLS pMET3-HA3-CDC20*) was treated as for YJL3244. DNA from equivalent numbers of cells were loaded in each lane, except twice as many cells were loaded in lanes 1-3 and 12-14 to compensate for their G1 or nearly G1 DNA content.

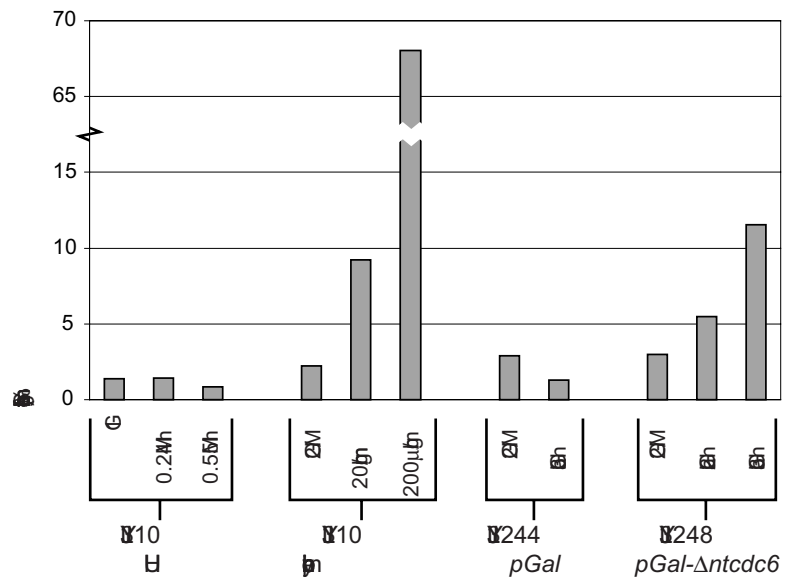
(B) Quantification of sub-chromosomal fragment from southern blot in (A). The intensity of subchromosomal signal is shown as a percent of the total signal for each lane.



9  
A



B



## **CHAPTER 4**

### **Loss of DNA Replication Control is a Potent Inducer of Gene Amplification**

**Eukaryotic cells use a multitude of overlapping mechanisms to ensure that their DNA is virtually never re-replicated within a single cell cycle <sup>1</sup>. This extensive regulation is thought to protect cells from heritable genomic changes that could, in principle, arise from re-replication. Direct evidence for such genomic alterations has been lacking, however. Here we show in the budding yeast *Saccharomyces cerevisiae* that re-replication arising from loss of DNA replication control induces a high frequency of gene amplification, a genomic alteration often linked to cancers. The amplified units, or amplicons, consist of large internal chromosomal segments up to several hundred kilobases long that are bounded by repetitive sequences and intrachromosomally arrayed in direct head-to-tail orientation. The high incidence of these segmental amplifications appears to be specific to re-replication, as they are not observed with appreciable frequency when S phase DNA replication is impaired or DNA is directly damaged. While similarly arrayed amplicons in direct repeat have been observed in tumors <sup>2</sup>, these structures have eluded explanation by the prevailing breakage-fusion-bridge (BFB) model for gene amplification, which predicts formation of indirect repeats adjacent to telomeric deletions <sup>3</sup>. We thus propose that loss of replication control should be considered a potential source of the genomic instability associated with carcinogenesis.**

Many proteins involved in the initiation of eukaryotic DNA replication are tightly regulated to minimize the probability that re-initiation within a single cell cycle occurs at any of the hundreds to thousands of replication origins in a genome. Although such exquisitely tight control is presumed to be necessary because re-replication could conceivably pose a threat to genome stability, this premise has never been

experimentally tested. Hence, re-replication has not been seriously considered as a source of genomic instability, either on an evolutionary time scale or the more accelerated time scale associated with carcinogenesis.

Our recently acquired ability to disrupt replication control in budding yeast<sup>4,5</sup> has allowed us to examine whether re-replication can promote heritable genomic alterations. Because re-replication synthesizes extra gene copies, we have first asked whether re-replication can induce gene amplification, a heritable increase in the copy number of genes. Notably, gene amplification of known or suspected oncogenes is associated with many tumors<sup>2</sup>.

The mechanism behind many gene amplification events is poorly understood<sup>2</sup>. Gene amplifications can be intrachromosomal or extrachromosomal and the amplified structures can be quite diverse. The most molecularly defined model for intrachromosomal gene amplification, the breakage-fusion-bridge (BFB) model (see Supplemental Figure 1) leads to the following three structural features: (1) amplicons in inverted orientation, (2) deletion of DNA telomeric to the amplified region, and (3) mitotic bridges arising from bipolar tension on dicentric chromosomes<sup>3</sup>. Such structural hallmarks have been documented most carefully in cell culture systems where gene amplification is induced by drug selection, but they have also been observed in some tumors<sup>2,6</sup>.

An increasing number of tumors, however, have been shown to contain amplified structures incompatible with the BFB model. For example, some of the classic examples of amplified oncogenes in tumors, such as MYCN in neuroblastomas<sup>7</sup> and ERBB2 in breast, ovarian and gastric cancers<sup>8</sup> are arrayed in direct repeats. We show here that re-

replication induced gene amplification can account for intrachromosomal amplicons arranged in direct repeat and provides a new gene amplification paradigm that can complement the BFB model.

To detect gene amplification arising from DNA re-replication in the budding yeast *Saccharomyces cerevisiae*, we adapted a colony color assay that monitors the copy number of an *ade3-2p* reporter gene. In this assay, cells with a single copy of *ade3-2p* allele turn pink, and cells with two or more copies turn red<sup>9</sup>. To examine the effect of re-replicating this reporter gene, we constructed an *ade3-2p* reporter cassette containing *ade3-2p* and *ARS317*, the primary origin that re-initiates replication in strains deregulated for Mcm2-7 and Cdc6 (*MC2A* strain background)<sup>5</sup>. We integrated the cassette at either 567 kb or 1089 kb from the left end of chromosome IV and deleted *ARS317* from its endogenous locus. Re-initiation of *ARS317* is conditional in the resulting strains (induced by galactose and repressed by dextrose), allowing us to examine the consequences of a transient pulse of re-replication at a defined genomic locus.

In Fig 1B we confirm that re-replication of the *ade3-2p* cassette is efficient and dependent on *ARS317*. Cells arrested in G2/M with nocodazole were induced to re-replicate by addition of galactose for three hours then harvested to examine their DNA re-replication by array comparative genomic hybridization (aCGH) against DNA from a non-replicating reference strain. In the resulting re-replication profiles, peak position indicates the site of re-initiation, peak height represents the efficiency of re-initiation, and peak width reflects the size distribution of the re-replication bubbles<sup>5</sup>. Re-initiation to approximately 3C was observed where the *ade3-2p* reporter cassette was integrated on

chromosome IV (Fig 1B), which is similar to the efficiency observed for *ARS317* at its endogenous locus <sup>5</sup>.

Following three hours of induced re-replication, we plated single cells onto medium that repressed further re-initiation and allowed proper color development of the resulting colonies. We reasoned that, in some cells or their immediate descendants, the re-replication bubble containing a duplication of *ade3-2p* would be converted to a stable heritable structure, causing all subsequent progeny to turn red. Fig 1C shows an example of a colony with a quarter red sector that presumably arose when one cell acquired a stable duplication of *ade3-2p* at the four-cell stage. In order to focus on stable duplications that occurred soon after re-replication was induced, we scored pink colonies with half, quarter and eighth red sectors. We then colony purified cells from the red sectors of these colonies to analyze their genomic structure.

Galactose induction of re-replication in *MC2A* cells with the *ade3-2p* cassette integrated 567 kb from the left end of chromosome IV (YJL6558) caused a dramatic increase in red sectors to 3.6% of all colonies (Fig 2A). No increase was observed in congeneric strains lacking the inducible Cdc6 and thus not re-replicating in galactose containing media (YJL6974). Moreover, re-replicating cells containing an integrated *ade3-2p* cassette lacking *ARS317* (YJL6555) showed only a modest increase in sectoring, suggesting re-initiation from the cassette is necessary for efficient sector formation. The few red sectors induced in cells with a cassette lacking *ARS317* were likely due to sporadic and inefficient re-replication that occurs throughout the genome in the *MC2A* strain <sup>5</sup>. Re-replication also induced significant colony sectoring when the *ade3-2p* cassette was located 1089kb from the left end of chromosome IV (Supplemental Fig 2A).

We selected 24 red sectors induced by re-replication from the *ade3-2p* cassette at 567kb to determine their extent and amount of amplification using aCGH. Genomic DNA from these red sector cells was hybridized against genomic DNA from a reference strain with a non-amplified genome (Fig 2B). Of the 24 red sectors, 20 had at least two copies of the chromosomal segment spanning the *ade3-2p* cassette, confirming that gene amplification had occurred in most of the sectored colonies. Since none of our amplified chromosomal segments contained telomeres or centromeres, we describe them as segmental amplifications, which must be integrated in an existing chromosome to be stably maintained and detected in our colony-sectored screen.

The boundaries of the amplified regions appeared to coincide with Ty elements or LTR sequences (long terminal repeat segments that remain after Ty excision) that have been mapped in the *Saccharomyces* Genome Database<sup>10</sup>. These dispersed repetitive elements have been found at the junctions of many deletions and translocations observed in *S. cerevisiae*<sup>11</sup>, and such junctions are thought to arise from homologous recombination between these elements. Eighteen of the 20 amplified regions were bounded by the nearest Ty elements to either side of the *ade3-2p* cassette. The remaining amplified regions were bounded at one or both ends by a more distal LTR or Ty element.

When the *ade3-2p* cassette was integrated at 1089kb from the left end of chromosome IV (YJL6561), 16 of the 24 red sectors induced by re-replication had segmental amplifications spanning the cassette (Supplemental Fig 2B). Although the boundaries of these amplifications were more varied than those derived from YJL6558, they retained three shared features. First, the boundaries enclosed amplified segments on the order of 100-300 kb long, roughly the width of the re-replication peaks. Second, all

but one boundary mapped near a Ty or LTR element. Third, there was a preference for elements that were close to the *ade3-2p* cassette, where re-replication initiates. These properties are consistent with a scenario in which segmental amplifications arise from homologous recombination of re-replicated Ty or LTR elements.

To determine within which chromosomes the segmental amplifications were integrated, we separated chromosomes using pulsed field gel electrophoresis (PFGE) and probed for the presence of the *ADE3* gene (Fig 3A). This probe hybridizes to both the endogenous mutant *ade3* allele on chromosome VII as well as the *ade3-2p* cassette originally integrated in chromosome IV (Fig 3A, lanes 1 and 26, parental strains). The additional amplified segments are large enough to noticeably decrease the mobility of the host chromosome. Of the 24 red sectors derived from YJL6558, the 20 that showed segmental amplification by aCGH all showed an increase in chromosome IV size consistent with the size and copy number of the amplicons. (Fig 3A, lanes 2-25). Importantly, no other chromosome besides IV (site of *ade3-2p* cassette) and VII (site of endogenous *ade3*) were detected by the *ADE3* probe, indicating that all amplified segments were integrated in chromosome IV.

To determine the precise position of these amplified segments in chromosome IV, we tested the hypothesis that these segments are arranged in tandem at the original locus. Tandem duplications can be arranged in three possible arrangements: head to tail, head to head and tail to tail, each generating a unique set of junctions and boundaries that can be distinguished by PCR (Fig. 3B). Of the 20 red sectors containing an amplification of the *ade3-2p* cassette, 19 generated PCR products consistent with a tandem head-to-tail duplication at the original locus. Moreover, the sizes of the PCR products were



consistent with the expected presence of Ty or LTR elements at the amplicon boundaries, an expectation confirmed by sequencing (data not shown). Similar PCR analysis of the amplification structures induced by re-replication from the 1089 kb locus also indicated a head-to-tail orientation of duplicate amplicons (data not shown). Thus, re-replication can induce segmental amplification with the amplicons in direct repeat and bounded by Ty or LTR elements.

Defects in S phase replication due to partial depletion of replication proteins or insertion of palindromic DNA structures have been implicated in gene duplication or amplification events<sup>12,13</sup>. The frequency of these amplification events ( $5 \times 10^{-4}$  and  $3 \times 10^{-5}$ , respectively) is at, or lower than, the background of our sectoring assay, and the resulting amplification structures (extrachromosomal elements, chromosome arm duplications and inverted repeats) are very different from those we characterized. Nonetheless, these observations raise the question of whether re-replication induced gene amplification is simply a secondary consequence of disrupted replication or DNA damage, particularly because the re-replication surrounding *ARS317* in the *MC2A* background is limited (Fig 1B) and because re-replication leads to DNA damage<sup>1,14</sup>. To address this question, we asked whether either S phase disruption or DNA damage could induce detectable gene amplification in our sectoring screen

To disrupt S phase replication we used mutants that affect various steps of replication. Diploid strains homozygous for the temperature sensitive alleles *cdc6-1*, *cdc7-1*, *cdc9-1*, or *cdc17-1* were shifted to either nonpermissive (36° C for 3 hours) or semi-permissive (30° C for 6 hours) conditions. We also treated cycling cells with hydroxyurea, a drug that depletes nucleotides, for 3 hr (0.2M) or 6 hr (0.1M). Little, if

any, increase in red sector formation was observed in the sectoring assay after these treatments (Fig 4). To induce DNA damage we treated diploid cells for 3 hr with two different concentrations of the DNA damaging agent phleomycin before assaying for red sectors (Fig 5A). Although DNA damage did cause a modest increase in the frequency of red sectors, most of the sectors appeared qualitatively less red than those due to re-replication (data not shown), and microarray CGH on 24 of the sectors showed that none displayed any segmental duplication of chromosome IV (Fig 5B). Thus the estimated frequency of actual head to tail gene amplification events shows little induction by DNA damage (Fig 5C). Together, these data indicate that the high frequency of tandem direct gene amplification events is specific to re-replication.

What is it about re-replication that gives it a special propensity to generate segmental amplifications in direct tandem repeat? One possibility is that re-replicating forks are particularly susceptible to breakage and re-replication bubbles provide an optimal context for break repair to create direct repeat amplifications. Figure 6 shows a working model that incorporates these ideas. In this model re-replication past repetitive elements at opposite ends of a bubble followed by breaks in trans at the two forks could lead to homologous recombination between the two opposing elements. Such a recombination event would convert the two parallel re-replicated arms into serial direct repeats bounded by repetitive elements. Future experiments to test this and related models will need to detect and structurally characterize the broken chromosomal intermediates predicted by the models.

Our observation that re-replication is a potent inducer of gene amplification suggest that loss of replication control may be a more prominent contributor to

carcinogenesis than previously appreciated. Interestingly, elevated expression of replication proteins has been observed in a number of cancers<sup>15</sup>. Although this elevation could simply be secondary to the increased proliferation of tumorigenic cells, our results raise the possibility that this elevation might have a causative role. Encouraging such speculation is the observation that overexpression of the replication protein, Cdt1, which can induce re-replication in humans, *Drosophila melanogaster*, *Xenopus laevis*, *Caenorhabditis elegans*<sup>16-20</sup>, somehow promotes carcinogenesis in mice<sup>21,22</sup>. Although re-replication was not readily apparent in these mouse cells, we note that only barely detectable levels of re-replication may be capable of promoting carcinogenesis, as overt re-replication leads to massive cell death<sup>14,23-25</sup>. Finally, our experimental design and sectoring assay was best suited for detecting intrachromosomal amplifications. Alterations of the design and assay may reveal other types of genomic instability induced by re-replication such as extrachromosomal amplifications, segmental deletions, and missegregation (from re-replication of centromeres).

Increases in gene copy number are also important for evolution, as gene duplication allows for functional divergence of the duplicates<sup>26</sup>. An estimated 30 to 60% of eukaryotic genes arose from gene duplication events<sup>27</sup>, and some of these events may have been similar to the segmental duplications we observed in this report. In addition, the recent observation that as much as 12% of the human genome displays copy number variation (CNV) within a set of <300 individuals<sup>28</sup>, has raised the possibility that copy number increases (and decreases) may be an important source of phenotypic variation, the substrate for evolutionary selection. The mechanism by which many of these CNVs are generated is completely unknown, since precise structures for most have not been

determined. Nonetheless, we suggest that sporadic re-replication should be considered as a possible driving force in evolution and phenotypic variation as well as carcinogenesis

## **Methods**

Strains (Supplemental Table 1) and plasmids (Supplemental Table 2) were constructed as described in Supplemental Methods. Oligonucleotide sequences are described in Supplemental Table 3. Cells were grown in or on YEP or synthetic complete (SC) medium<sup>29</sup> supplemented with 2% dextrose (wt/vol) or 3% raffinose (wt/vol) + 0.05% dextrose (wt/vol). All experiments were performed at 30°C except where noted.

To obtain reproducible induction of re-replication, cells were inoculated from a fresh unsaturated culture containing 2% dextrose into a culture containing 3% raffinose + 0.05% dextrose and grown for 12–15 h the night before the experiment. After cells were arrested in G2/M with 15ug/ml nocodazole, the GAL1 promoter (pGAL1) was induced by addition of 2% galactose for 3 hours. To perturb S phase replication, the indicated mutant strains were grown overnight in YEPD at 23°C, then shifted to 36°C or 30°C for 3 or 6 hours, respectively or wild type strain was grown in YEPD at 30°C overnight then 0.2M or 0.1M hydroxyurea was added for 3 or 6 hours, respectively. To induce DNA damage, cells were grown in YEPD at 30°C overnight then 0.2ug/ml or 2ug/ml phleomycin was added for 3 hours.

To score the frequency of red sectors, ~200 colonies were plated onto SDC plates containing 0.5x adenine. Temperature sensitive strains were grown for 7 days at 23°C and other strains were grown at 30°C for 5 days, then 23°C for 3 days to allow color to

develop. Plates were randomized and scored blind. Red sectors were counted if: 1) the sectors were greater than 1/8 of the colony, 2) darker red than the neighboring colonies (ie, not a pink sector in a nearly white colony) and 3) the junctions between the red sector and pink colony were largely straight, to minimize sectors due to poor growth. The total viable colonies were counted for each time point and the total sector counts were normalized to this number.

Comparative genomic hybridization (aCGH) profiles were obtained as described<sup>5</sup> without smoothing applied. For aCGH screening of sectors, DNA from 1.5ml of saturated YEPD culture was prepared using the MasterPure Yeast DNA Purification Kit (Epicentre). 40ul (80%) of each DNA sample was labeled with Cy5 and 1.5ug of purified DNA from YJL6032 was labeled with Cy3 essentially as described<sup>5</sup> but samples were cleaned up as described (PLEISS, ref). Samples were hybridized as described<sup>5</sup>.

Cells were prepared for pulsed field gel electrophoresis as described<sup>14</sup>. Plugs were cut in half and loaded on a 1% SeaKem LE agarose (wt/vol) gel in 1x TAE (40 mM Tris, 40 mM acetate, and 2 mM EDTA, pH 8.0). The gel was electrophoresed in 14°C 1x TAE on a CHEF DR-III system with a switch time of 500 s, run time of 48 h, voltage of 3 V, and angle of 106°. The DNA was transferred as described<sup>14</sup> and probed with an ADE3 probe generated with OJL1757 and OJL1758 (Supplemental Table 3).

Use of PCR to analyze novel genomic DNA junctions is described in the Supplemental Methods.

## **Acknowledgements**

We thank Dave Toczyski, Elizabeth Blackburn, Pat O'Farrell, Steve Elledge, Fred Winston and Joyce Hamlin for helpful discussions and comments on the manuscript. This work was supported by grants to J.J.L. from the Sandler Program in Biological Sciences, the ACS (RPG-99-169-01-CCG) and the NIH (RO1 GM59704). B.M.G. was supported by an NSF Predoctoral Fellowship (DGE-0202754) and a DOD Breast Cancer Predoctoral Fellowship (W81XWH-04-1-0409).

## References

1. Blow, J. J. & Dutta, A. Preventing re-replication of chromosomal DNA. *Nat Rev Mol Cell Biol* **6**, 476-86 (2005).
2. Albertson, D. G. Gene amplification in cancer. *Trends Genet* **22**, 447-55 (2006).
3. McClintock, B. The Fusion of Broken Ends of Chromosomes Following Nuclear Fusion. *Proc Natl Acad Sci U S A* **28**, 458-63 (1942).
4. Nguyen, V. Q., Co, C. & Li, J. J. Cyclin-dependent kinases prevent DNA re-replication through multiple mechanisms. *Nature* **411**, 1068-73 (2001).
5. Green, B. M., Morreale, R. J., Ozaydin, B., Derisi, J. L. & Li, J. J. Genome-wide mapping of DNA synthesis in *Saccharomyces cerevisiae* reveals that mechanisms preventing reinitiation of DNA replication are not redundant. *Mol Biol Cell* **17**, 2401-14 (2006).
6. Albertson, D. G., Collins, C., McCormick, F. & Gray, J. W. Chromosome aberrations in solid tumors. *Nat Genet* **34**, 369-76 (2003).
7. Herrick, J. et al. Genomic organization of amplified MYC genes suggests distinct mechanisms of amplification in tumorigenesis. *Cancer Res* **65**, 1174-9 (2005).

8. Kuwahara, Y. et al. Alternative mechanisms of gene amplification in human cancers. *Genes Chromosomes Cancer* **41**, 125-32 (2004).
9. Koshland, D., Kent, J. C. & Hartwell, L. H. Genetic analysis of the mitotic transmission of minichromosomes. *Cell* **40**, 393-403 (1985).
10. Hong EL, B. R., Christie KR, Costanzo MC, Dwight SS, Engel SR, Fisk DG, Hirschman JE, Livstone MS, Nash R, Oughtred R, Park J, Skrzypek M, Starr B, Theesfeld CL, Andrada R, Binkley G, Dong Q, Lane CD, Hitz BC, Miyasato S, Schroeder M, Weng S, Wong ED, Dolinski K, Botstein D, and Cherry JM. (2006).
11. Mieczkowski, P. A., Lemoine, F. J. & Petes, T. D. Recombination between retrotransposons as a source of chromosome rearrangements in the yeast *Saccharomyces cerevisiae*. *DNA Repair (Amst)* **5**, 1010-20 (2006).
12. Narayanan, V., Mieczkowski, P. A., Kim, H. M., Petes, T. D. & Lobachev, K. S. The pattern of gene amplification is determined by the chromosomal location of hairpin-capped breaks. *Cell* **125**, 1283-96 (2006).
13. Lemoine, F. J., Degtyareva, N. P., Lobachev, K. & Petes, T. D. Chromosomal translocations in yeast induced by low levels of DNA polymerase a model for chromosome fragile sites. *Cell* **120**, 587-98 (2005).
14. Green, B. M. & Li, J. J. Loss of rereplication control in *Saccharomyces cerevisiae* results in extensive DNA damage. *Mol Biol Cell* **16**, 421-32 (2005).
15. Gonzalez, M. A., Tachibana, K. E., Laskey, R. A. & Coleman, N. Control of DNA replication and its potential clinical exploitation. *Nat Rev Cancer* **5**, 135-41 (2005).

16. Arias, E. E. & Walter, J. C. Replication-dependent destruction of Cdt1 limits DNA replication to a single round per cell cycle in *Xenopus* egg extracts. *Genes Dev* **19**, 114-26 (2005).
17. Zhong, W., Feng, H., Santiago, F. E. & Kipreos, E. T. CUL-4 ubiquitin ligase maintains genome stability by restraining DNA-replication licensing. *Nature* **423**, 885-9 (2003).
18. Thomer, M., May, N. R., Aggarwal, B. D., Kwok, G. & Calvi, B. R. *Drosophila* double-parked is sufficient to induce re-replication during development and is regulated by cyclin E/CDK2. *Development* **131**, 4807-18 (2004).
19. Maiorano, D., Krasinska, L., Lutzmann, M. & Mechali, M. Recombinant Cdt1 induces rereplication of G2 nuclei in *Xenopus* egg extracts. *Curr Biol* **15**, 146-53 (2005).
20. Li, A. & Blow, J. J. Cdt1 downregulation by proteolysis and geminin inhibition prevents DNA re-replication in *Xenopus*. *Embo J* **24**, 395-404 (2005).
21. Seo, J. et al. Cdt1 transgenic mice develop lymphoblastic lymphoma in the absence of p53. *Oncogene* **24**, 8176-86 (2005).
22. Arentson, E. et al. Oncogenic potential of the DNA replication licensing protein CDT1. *Oncogene* **21**, 1150-8 (2002).
23. Archambault, V., Ikui, A. E., Drapkin, B. J. & Cross, F. R. Disruption of mechanisms that prevent rereplication triggers a DNA damage response. *Mol Cell Biol* **25**, 6707-21 (2005).



24. Wilmes, G. M. et al. Interaction of the S-phase cyclin Clb5 with an "RXL" docking sequence in the initiator protein Orc6 provides an origin-localized replication control switch. *Genes Dev* **18**, 981-91 (2004).
25. Vaziri, C. et al. A p53-dependent checkpoint pathway prevents rereplication. *Mol Cell* **11**, 997-1008 (2003).
26. Presgraves, D. C. Evolutionary genomics: new genes for new jobs. *Curr Biol* **15**, R52-3 (2005).
27. Ball, C. A. & Cherry, J. M. Genome comparisons highlight similarity and diversity within the eukaryotic kingdoms. *Curr Opin Chem Biol* **5**, 86-9 (2001).
28. Redon, R. et al. Global variation in copy number in the human genome. *Nature* **444**, 444-54 (2006).
29. Guthrie, C. & Fink, G. (eds.) *Guide to Yeast Genetics and Molecular Biology* (Academic Press, 1990).

**Figure 1** – Gene amplification assay

A) An *ade3-2p* reporter cassette consisting of the copy number reporter *ade3-2p*, the re-initiating origin *ARS317*, and the selectable marker *kanMX* was inserted into the genomic loci of interest via homologous recombination. Cassettes lacking the origin were inserted in control strains.

B) *ARS317* in the *ade3-2p* cassette is sufficient for re-initiation at ectopic loci. The reporter cassette was integrated at two genomic loci in a strain deleted for the endogenous *ARS317*. Cells were arrested in G2/M phase, galactose was added for 3 hours to induce  $\Delta$ *nt-cdc6-2A*, and genomic DNA was then isolated for replication analysis by array competitive genomic hybridization. Top panel: YJL6557 contains an *ade3-2p* cassette lacking *ARS317* integrated 1089kb from the left end of chromosome IV. Middle panel: YJL6558 contains an *ade3-2p* cassette inserted 567kb from the left end of chromosome IV. Bottom panel: YJL6561 contains an *ade3-2p* cassette inserted 1089kb from the left end of chromosome IV.

C) Schematic of gene amplification screen. Cells were induced to re-replicate for three hours at a G2/M arrest then plated for single colonies on plates that allow *ade2* color development. Shown is an example of a colony where stable heritable amplification of the *ade3-2p* reporter was acquired by one cell at the four-cell stage, resulting in pink colony with a red quarter sector. Colonies with 1/2, 1/4, and 1/8 red sectors were streaked to colony purify red cells. Those sectors that were confirmed by the streaks were quantified and their DNA analyzed further for genomic copy number variation.

Figure 1

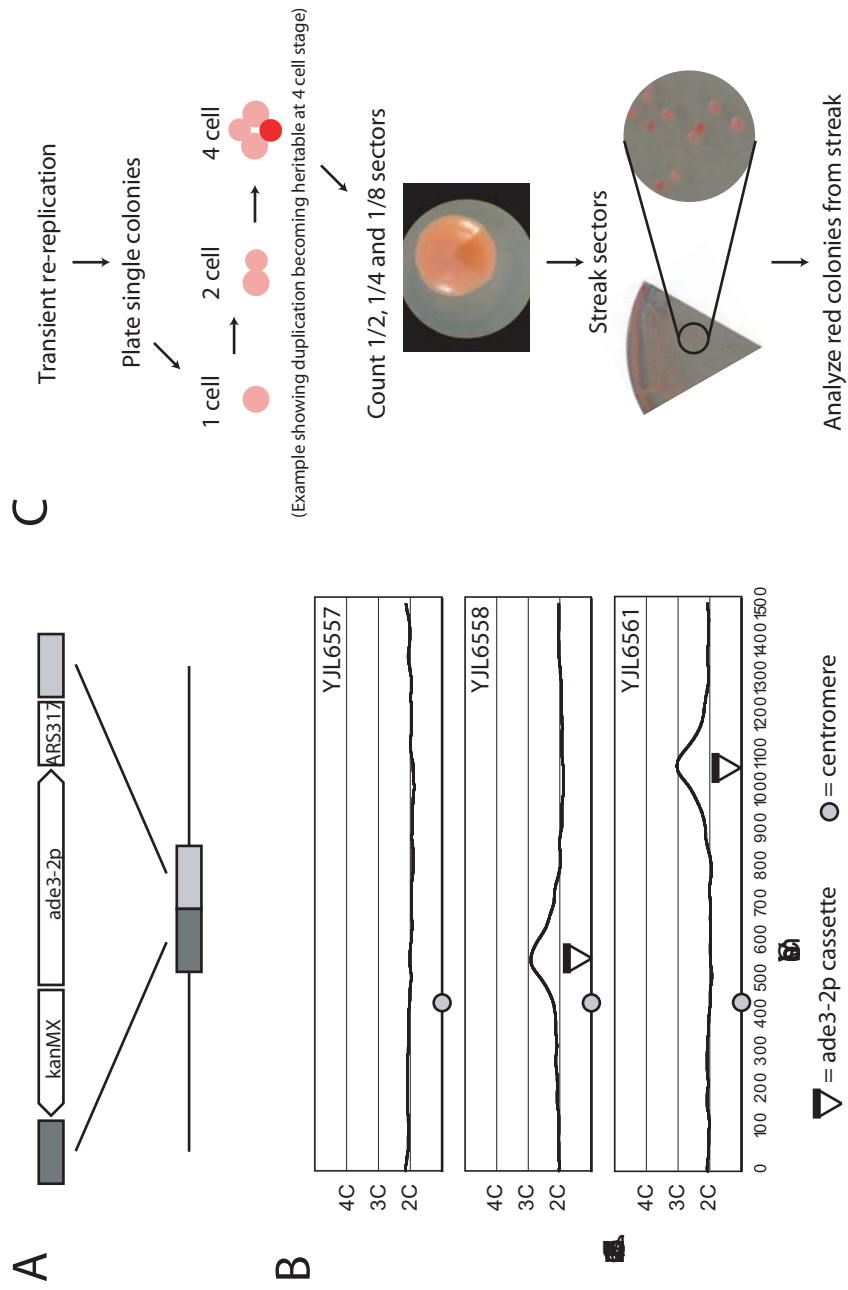


**Figure 2 – Re-replication induces segmental duplications**

A) Re-replication induces gene amplifications. YJL6974, YJL6555, and YJL6558 were assayed for gene amplification frequencies as described in Figure 1C.

All strains were *MCM7-2NLS ars317Δ ade3 ade2 Chromosome IV 567kb::ade3-2p cassette*. Distinguishing alleles are indicated, with *ARS317* referring to the presence of the origin in the *ade3-2p* cassette. The mean and standard error of the mean of at least two independent experiments is shown.

B) Amplification events induced by re-replication involve segmental duplications. 24 sectors identified in Figure 2A from YJL6558 were analyzed by array CGH using non-replicating reference DNA from YJL6032. Four types of copy number variations on chromosome IV (1-4) were observed. For each type, a representative copy number profile and the number of sectors observed is shown. Four sectors showed no evidence of increased *ade3-2p* copy number.

Figure 2

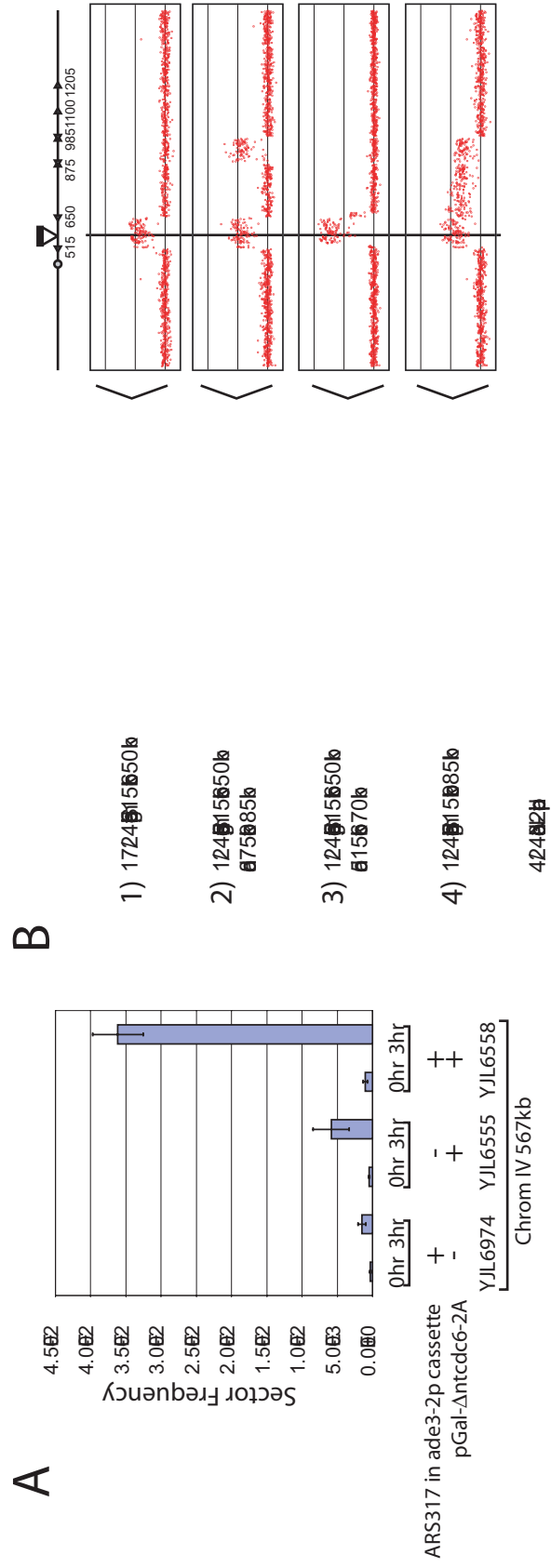


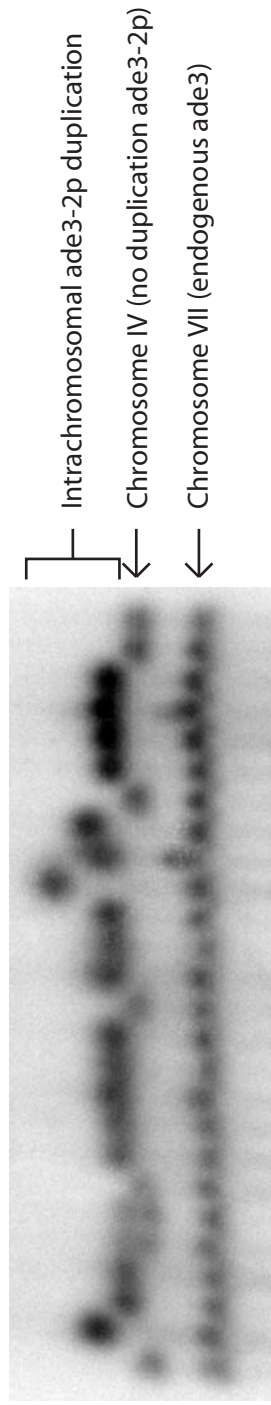
**Figure 3 – Re-replication leads to head to tail gene amplification**

A) Re-replication induces intrachromosomal gene amplifications. Chromosomes from the 24 sectors analyzed by array CGH in Figure 2B were analyzed by PFGE. After transferring to a membrane, the DNA was probed for *ADE3*, which detects both the endogenous *ade3* locus on chromosome VII and the *ade3-2p* reporter gene integrated on chromosome IV. Lane 1 and 26: YJL6558 parental strain before induction of re-replication. Lanes 2-25: Sectorized isolates 1-24 respectively. Doublet pattern for chromosome IV in lanes 5 and 6 is consistent with a partial loss of the segmental amplification from the population.

B) Amplicons are tandemly arrayed in direct head-to-tail orientation. Schematic shows structure of unamplified amplicon unit and the three possible orientations for tandemly duplicated amplicons. Predicted PCR junction fragments spanning the boundaries of each amplicon structure are shown for the various combinations of primers displayed (+ PCR product expected; - no PCR product expected). The parental strain YJL6558 and 20 derivative strains that were shown in Figure 2B to contain segmental duplication of the *ade3-2p* reporter were subject to this PCR analysis. 19 of 20 (all of type 1, type 2, and type 4 from Figure 2B) generated a pattern of PCR products only compatible with tandem amplicons in head-to-tail orientation.

Figure 3

A



Lane: 1 2 3 4 5 6 7 8 9 10 11 12 13 14 15 16 17 18 19 20 21 22 23 24 25 26

B

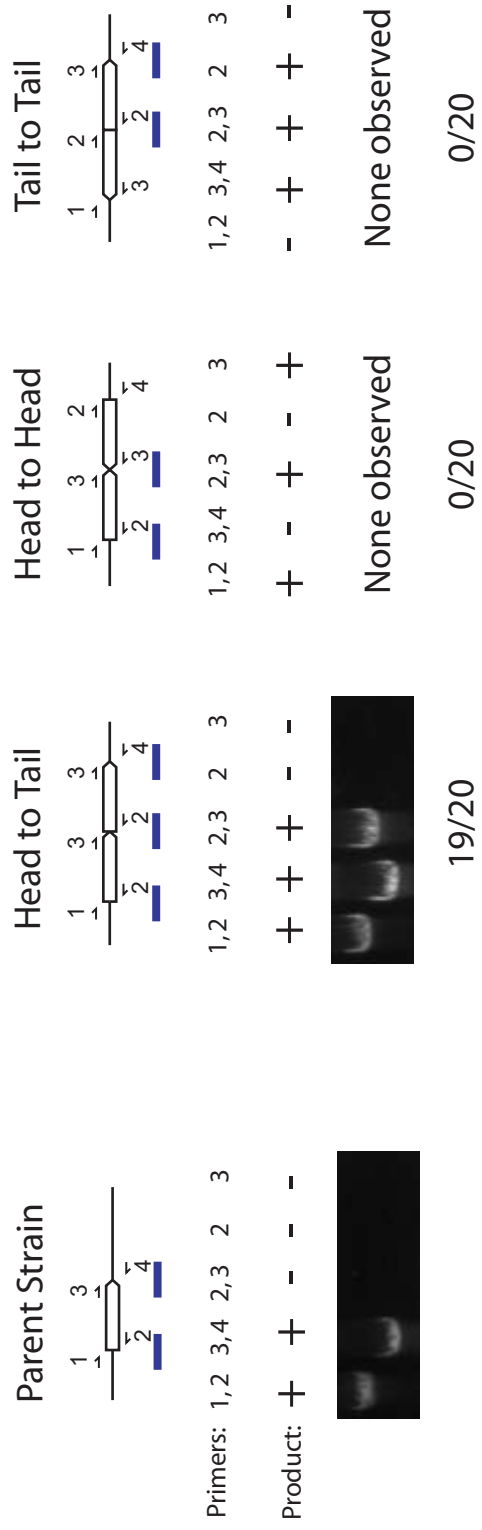


**Figure 4** – Underreplication does not lead to significant gene amplification

A) Diploid strains YJL7002 (WT), YJL7003 (*cdc6-1/cdc6-1*), YJL7085 (*cdc7-1/cdc7-1*), YJL7005 (*cdc9-1/cdc9-1*), and YJL7006 (*cdc17-1/cdc17-1*) were grown exponentially at 23° C then shifted to 36° C for 3 hours or 30° C for 6 hours to perturb replication. The effectiveness of this perturbation was monitored by the percent of cells containing large buds. The frequency of red sectors was determined in at least two independent experiments and the mean and standard error of the mean are shown. The frequency due to re-replication of YJL6558 (described in Figure 2A) is provided for reference.

B) Diploid YJL7007 (WT) grown exponentially at 30 C was treated with hydroxyurea for the times and concentrations shown and analyzed as described in A.



Figure 4

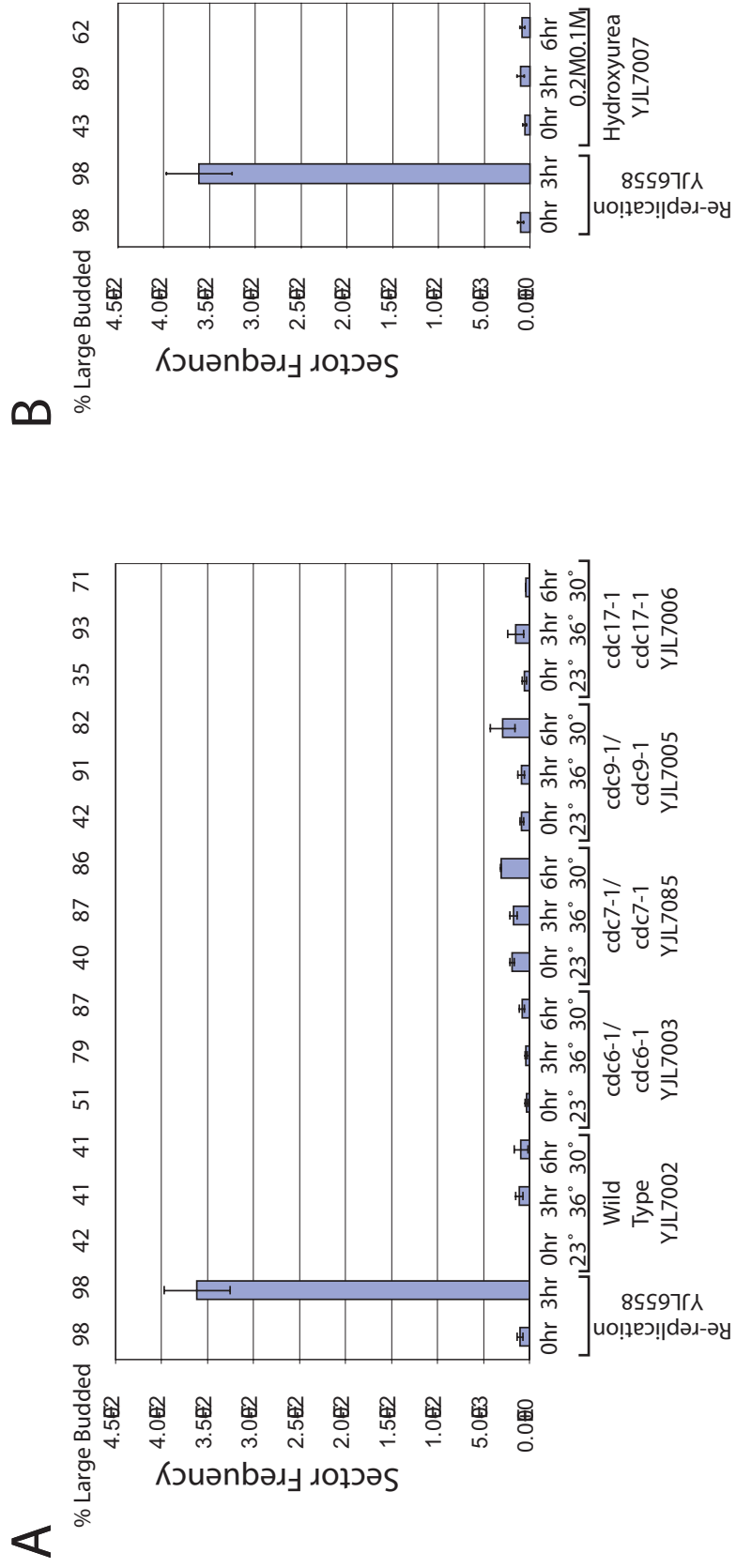


**Figure 5 – DNA damage does not lead to significant gene amplification**

A) DNA damage induces a modest increase in sectoring frequency. Exponentially growing diploid YJL7007 (WT) cells were treated with the indicated concentration of phleomycin for 3 hours and the frequency of red sectors was obtained as described in Figure 1C. The mean and standard error of the mean of at least two independent experiments are shown. The frequency due to re-replication of YJL6558 (described in Figure 2A) is shown for reference.

B) Sectors induced by DNA damage do not contain any segmental amplification spanning the *ade3-2p* reporter gene. 24 red sectors obtained from treatment of YJL7007 with 20  $\mu\text{g/ml}$  phleomycin (described in Figure 5A) were analyzed by array CGH. All displayed the representative copy number profile of chromosome IV shown in the figure.

C) DNA damage does not significantly induce the head to tail gene amplification events that are observed following re-replication. The red sector frequencies induced by re-replication of YJL6558 (from Figure 2A) were multiplied by 19/24, the fraction of sectors that were confirmed to contain a head-to-tail gene amplification in Figure 3B. The red sector frequency induced by phleomycin treatment of YJL7007 were multiplied by 1/24, the minimum fraction of these sectors that could have been observed to have a head-to-tail gene amplification.

Figure 5

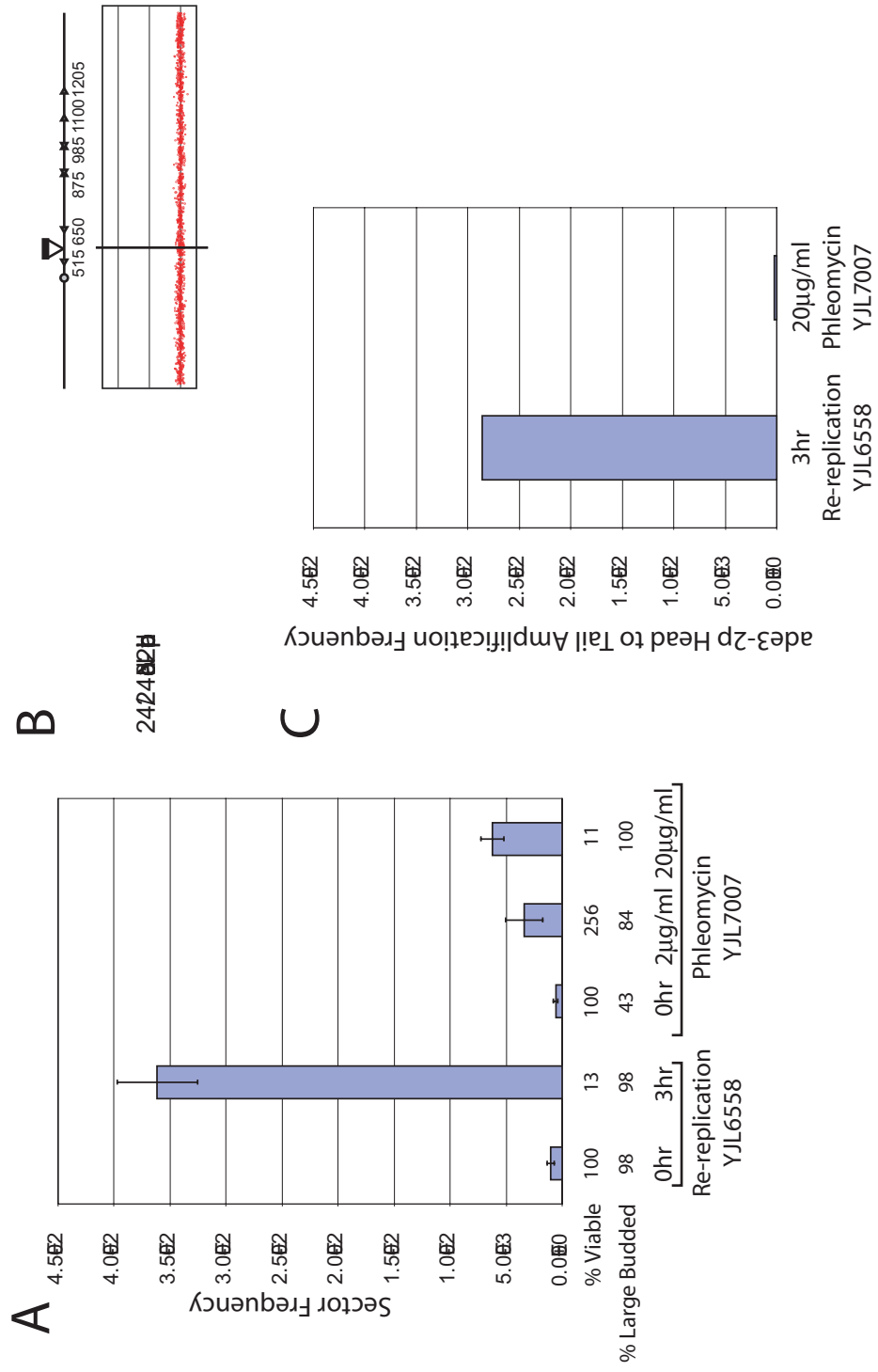
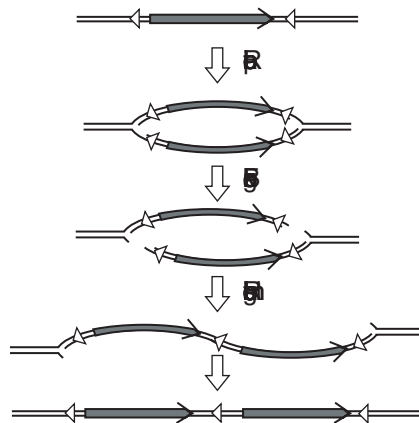


**Figure 6** – Model for re-replication induced gene amplification

Re-replication forms a bubble structure with duplicated regions of DNA. Depending on the DNA sequence, this unstable duplication could include regions of homology to other portions of the replication bubble. If the replication forks break in trans, there will be two free ends, which could promote homologous recombination between repetitive sequences. This recombination could generate a tandem amplification oriented head to tail, precisely the type of structure that we observe after re-replication.

Figure 6



## **CHAPTER 5**

### **Conclusions**

How eukaryotic cells control initiation of DNA replication from hundreds to thousands of origins and prevent reinitiation from those same origins for the remainder of the cell cycle has been a long standing question in biology. In recent years, some of the controls that prevent re-replication have been identified, in our lab and others. When I began the work in this dissertation, little was known about what occurs when these controls are disrupted. Chapters 2 and 6, published in *Molecular Biology of the Cell*<sup>1</sup>, focus on an analysis of re-replication – what regions of DNA reinitiate during different portions of the cell cycle, what regions reinitiate when different control are perturbed and what combinations of perturbations result in re-replication. Chapter 3, also published in *Molecular Biology of the Cell*<sup>2</sup>, then addresses the immediate consequences of re-replication – demonstrating that re-replication leads to DNA damage. Finally, despite considerable speculation that re-replication might lead to genome instability, Chapters 4 and 7 (submitted for publication) will be the first demonstrations that gene amplification is, in fact, a long term consequence of re-replication.

In Chapter 2, I describe work where we refined previously published genome-wide replication assays for budding yeast and made them more amenable for routine and widespread use in the study of DNA replication. This technology development, during which I coded the computational analysis software, facilitated the study of re-replication under a number of conditions. Our first objective was to demonstrate that re-replication occurred from origins of DNA replication used during normal S phase. Previous work had demonstrated that a few selected origins appeared to reinitiate<sup>3</sup>, but we demonstrated that on a genome-wide basis, re-replication primarily occurs from regular S phase origins. This indicates that disrupting the controls of replication initiation results in formation of

re-replication preRCs using similar rules to those used to establish preRCs for use in a normal S phase.

In contrast to the rules used to establish preRCs, which appear to be conserved in normal S phase and re-replication, the efficiency or timing of initiation differs between S phase and re-replication. A number of origins that replicate early in S phase do not appear to re-replicate with any efficiency during re-replication. Additionally, a number of later initiating regions seem to re-replicate quite efficiently. Simple sequence gazing of the efficiently re-replicating origins does not immediately suggest a reason that those origins preferentially reinitiate. However, this analysis is hampered by the error in mapping of origins inherent in our re-replication data. Perhaps coupling more precise identification of origins locations <sup>4</sup> with our re-replication data will allow for recognition of a motif or sequence that predicts whether a sequence is particularly prone to reinitiation.

Another major conclusion from the work presented in Chapters 2 and 6 was that re-replication can be detected after deregulation of only two inhibitory mechanisms. Previous work in our lab <sup>3</sup> had suggested that re-replication could only be observed after deregulation of three separate mechanisms. This led many in the field to assume that the mechanisms that prevent re-replication might be redundant. However, we demonstrate in Chapters 2 and 6 that these mechanisms all contribute to reduce the probability of re-replication. Specifically, we show that re-replication does occur when only two mechanisms are deregulated, but more sensitive assays than those previously applied must be used to detect this re-replication. In particular, use of our array CGH assay was



essential to demonstrate that re-replication was occurring and to pinpoint the primary origin that initiates.

Our observation of re-replication when two mechanisms are deregulated suggests that it might be possible, with the development of even more sensitive assays, to demonstrate that re-replication might be occurring when even a single mechanism is perturbed. It is likely that single cell assays would need to be developed to observe this re-replication. In a population analysis, many cells would fail to re-replicate any given region and would dampen the signal from inefficient re-replication. Perhaps DNA combining<sup>5</sup> would be sensitive enough to allow for identification of the sporadic and highly inefficient re-replication that might arise from disruption of a single mechanism that prevents re-replication. If disruption of a single mechanism is sufficient to induce re-replication, it would increase the likelihood that re-replication might be a pathologically relevant state.

Working under the assumption that re-replication might be occasionally and sporadically occurring in the trillions of cells that make up a human, or occur intermittently during the course of evolution, I next began to address the consequences of disruption of replication control. I initially focused on the immediate consequences and, in Chapter 3, found that re-replication led to a rapid and severe DNA damage response. Cells induced to re-replicate lost viability, activated a DNA damage checkpoint response and experienced chromosomal fragmentation. Importantly, and in contrast to previous work in human cells<sup>6,7</sup>, I demonstrated that this DNA damage response occurred largely in the absence of a replication stress checkpoint. Re-replication led to DNA damage and forks that failed to progress without the cell experiencing canonically stalled forks.

At this point we do not know exactly how exactly re-replication led to DNA damage, but several models could be postulated. One model, described as “forks chasing forks” has been proposed to explain DNA damage and replication fork stalling during re-replication in *Xenopus* extracts<sup>8</sup>. In this proposed situation, a replication fork derived from a second reinitiation event at a single preRC catches the fork from the first reinitiation event. This collision will result in a linear fragment being extruded from replication bubble, and the parental strands of DNA will remain intact. Although we need to address this question more completely, it does not appear that “forks chasing forks” is the sole source of elongation inhibition and DNA damage in our system. Firstly, some of the subchromosomal fragments observed after re-replication (Chapter 3, Figure 5) are larger than would be expected if they arose from extrusion of a single re-replication bubble. Secondly, our lab has demonstrated that when a single round of re-replication is induced, fork elongation is still restrained (Morreale, R unpublished data). Neither of these results can rule out the involvement of the “forks chasing forks” model in DNA damage and fork elongation inhibition, but they suggest that it might not be the only factor.

Another model for the genesis of DNA damage supposes that the first round of S phase replication somehow changes the nature of the chromatin, making replication through that chromatin structure inherently more prone to failure and damage. An obvious candidate for this chromatin change would be the establishment of sister chromatid cohesion which occurs during each S phase<sup>9</sup>. Preliminary re-replication elongation experiments in strains lacking cohesion (Morreale, R unpublished data), or induction of S phase in cells with non degradable cohesion (data not shown), however,

suggest that the presence of cohesion might not significantly alter re-replication elongation. Further experiments with cohesion, and analysis of other candidate chromatin modifications, are needed to determine if the structure of the G2/M DNA facilitates DNA damage and elongation inhibition during re-replication. Understanding the relative importance of these and/or other potential contributors (such as inefficient nucleosome deposition, defective replisome assembly, etc.) to this DNA damage will be an interesting avenue for further work.

Our observation that re-replication leads to cell inviability raises an apparent paradox in our suggestion that re-replication might occur in human cells and cause disease or drive evolution. If, as we (Chapter 3, Figure 1) and others<sup>10-14</sup> have demonstrated, re-replication leads to cell death or apoptosis, how can one propose that these cells can survive to develop altered function? This paradox can be resolved if the extent of loss of viability correlates with the extent of re-replication. In fact, re-replication primarily from a single origin of DNA replication (in the MC<sub>2A</sub> strain) allows for a much higher percentage of viable cells (~15%, Chapter 4, Figure 5) than re-replication from numerous origins (in the OMC strain, ~2%, Chapter 3, Figure 1). Given that rare re-replication might be more likely to occur than rampant re-replication, and that rare re-replication is likely to be more survivable, we expect that any pathologically relevant re-replication will occur from only a few origins.

In light of this expectation, I determined the long term genomic consequences of re-replication in the MC<sub>2A</sub> strain, which primarily re-replicates from a single origin. We focused initially on gene amplification, and specifically gene duplication. As described in Chapter 4, I adapted a color sectoring assay that enables cells with two copies of a

gene (*ade3-2p*) to be distinguished from cells with one copy on the basis of their color. The starting strain, with one copy of *ade3-2p*, is pink but when a gene duplication event occurs, the resulting cells with two copies of *ade3-2p* are red. Once the system was established, I demonstrated that re-replication led to gene duplication of genes near the region induced to re-replicate. The boundaries of these breakpoints were almost exclusively retrotransposable Ty elements or their remnants, called long terminal repeats (LTRs). Ty elements and LTRs have been found at the breakpoints of many genomic rearrangements in yeast<sup>15</sup> and are thought to simply provide a substrate for homologous recombination. Importantly, inhibition of S phase replication or DNA damage resulted in gene amplification rates considerably lower than those observed after re-replication.

When the structures of the re-replication induced amplicons were determined, it was clear that in the majority of amplicons, the duplicated DNA was arranged in a head to tail orientation at the site of the original gene. This orientation, and the fact that nearly all of the amplicons are located on the same chromosome as the original gene, suggests a model for the genesis of this amplification. A replication bubble that extends past two homologous regions, one in each direction, could experience breakage of the parent molecules in trans (Figure 1). Misalignment of the two homologous regions with each other and repair by homologous recombination would result in duplication of a region in head to tail orientation. It remains to be determined why replication perturbations do not lead to a similar set of circumstances, but perhaps cohesion established during normal S phase prevents the misalignment required for this mechanism.

Gene amplification or duplication has been shown to be important for evolution, as it is thought that 30 to 60% of eukaryotic genes arose from gene duplication events<sup>16</sup>.

This is not surprising, since gene duplication allows one (or both) of the copies of a gene to evolve new function. Additionally, copy number variation has been shown to be surprisingly prevalent in human populations – as much as 12% of the human genome shows copy number variation among individuals<sup>17</sup>. It is thought that this copy number variation can lead to phenotypic variability, potentially helping to explain what makes each of us unique. Regions of copy number variation are often associated with repetitive sequences<sup>17</sup>, which is what I observed with gene duplication events induced by re-replication. Perhaps, then, re-replication might contribute DNA copy number changes which lead to evolutionary diversity or phenotypic variability.

Tumor formation can be considered evolution on a very short time scale since tumor cells develop new functions that contribute to their ability to proliferate. Some tumors have been shown to have amplicons with certain similarities to re-replication induced amplicons, such as a head to tail orientation<sup>18,19</sup>. However, in those two cases some dissimilarities exist – for example, when MYCN is amplified in head to tail orientation it appears to first exist as an extrachromosomal element before integration into the genome. Although no tumor has yet been shown to have amplicons exactly like those observed in our strains, the vast majority of amplicons have not been characterized in sufficient structural detail to address this issue. Even though no currently described amplicons in tumors precisely match the structures we observe, we maintain that it is quite possible that loss of re-replication control could lead to gene amplification in precursor tumor cells.

It is important to note that the assay described in Chapter 4 enabled me to identify gene duplication events, but many amplicons seen in tumors have many copies of the

amplified genes. An additional assay will be needed to look for high copy number amplifications, and one based on copper and formaldehyde resistance has recently been described <sup>20</sup>. In very initial experiments using this system, I was able to observe high copy number gene amplification after a single round of re-replication (data not shown). As multiple, successively more stringent, selection steps were required to isolate these amplification events, it is likely that re-replication led to a gene amplification structure that predisposed the cell to high copy number amplification. The frequency of these events and the mechanisms by which they are generated will be an important area of future study.

There are numerous genomic changes other than gene amplification, such as loss of heterozygosity, translocations and aneuploidy, which are intimately involved in tumor formation <sup>21</sup>. It will be very interesting to assay for the induction of many of these sorts of genomic changes after re-replication. In fact, if re-replication was induced from an origin on Chromosome III (a small chromosome), disomy of Chromosome III was observed in nearly 10% of the cells (data not shown). It is possible that this was simply due to re-replication of the entire chromosome, but it raises the intriguing possibility that re-replication through a centromere (which appeared to occur in this case) might somehow lead to aneuploidy. Further experiments are needed to characterize these potential consequences of re-replication.

Finally, it would be illuminating to extend my work into mammalian cell lines and animals. It has been shown that overexpression of Cdt1 under certain conditions can cause re-replication <sup>10</sup> and under other conditions can cause tumors in mice <sup>22,23</sup>. These data do not demonstrate a causative link between re-replication and tumors, but it would

be very interesting to look for evidence of re-replication under the conditions that cause tumors in mice. If re-replication could be observed, then looking for re-replication induced gene amplification would be a clear next step. With these sorts of experiments, it would be possible to unequivocally demonstrate that re-replication could contribute to tumor formation.

In the work presented here, I have made progress in the goal of understanding re-replication and its potential role in tumorigenesis. I have helped to advance our understanding of how re-replication is prevented and the consequences of failure to maintain the controls. I have demonstrated that re-replication leads to cell inviability, DNA damage and gene amplification. We thus propose that re-replication might be an important source of the genome instability important for tumor formation and evolution.

## References

1. Green, B. M., Morreale, R. J., Ozaydin, B., Derisi, J. L. & Li, J. J. Genome-wide mapping of DNA synthesis in *Saccharomyces cerevisiae* reveals that mechanisms preventing reinitiation of DNA replication are not redundant. *Mol Biol Cell* **17**, 2401-14 (2006).
2. Green, B. M. & Li, J. J. Loss of rereplication control in *Saccharomyces cerevisiae* results in extensive DNA damage. *Mol Biol Cell* **16**, 421-32 (2005).
3. Nguyen, V. Q., Co, C. & Li, J. J. Cyclin-dependent kinases prevent DNA re-replication through multiple mechanisms. *Nature* **411**, 1068-73 (2001).

4. Xu, W., Aparicio, J. G., Aparicio, O. M. & Tavaré, S. Genome-wide mapping of ORC and Mcm2p binding sites on tiling arrays and identification of essential ARS consensus sequences in *S. cerevisiae*. *BMC Genomics* **7**, 276 (2006).
5. Pasero, P., Bensimon, A. & Schwob, E. Single-molecule analysis reveals clustering and epigenetic regulation of replication origins at the yeast rDNA locus. *Genes Dev* **16**, 2479-84 (2002).
6. Zhu, W., Chen, Y. & Dutta, A. Rereplication by depletion of geminin is seen regardless of p53 status and activates a G2/M checkpoint. *Mol Cell Biol* **24**, 7140-50 (2004).
7. Melixetian, M. et al. Loss of Geminin induces rereplication in the presence of functional p53. *J Cell Biol* **165**, 473-82 (2004).
8. Davidson, I. F., Li, A. & Blow, J. J. Deregulated replication licensing causes DNA fragmentation consistent with head-to-tail fork collision. *Mol Cell* **24**, 433-43 (2006).
9. Nasmyth, K. Disseminating the genome: joining, resolving, and separating sister chromatids during mitosis and meiosis. *Annu Rev Genet* **35**, 673-745 (2001).
10. Vaziri, C. et al. A p53-dependent checkpoint pathway prevents rereplication. *Mol Cell* **11**, 997-1008 (2003).
11. Thomer, M., May, N. R., Aggarwal, B. D., Kwok, G. & Calvi, B. R. *Drosophila* double-parked is sufficient to induce re-replication during development and is regulated by cyclin E/CDK2. *Development* **131**, 4807-18 (2004).



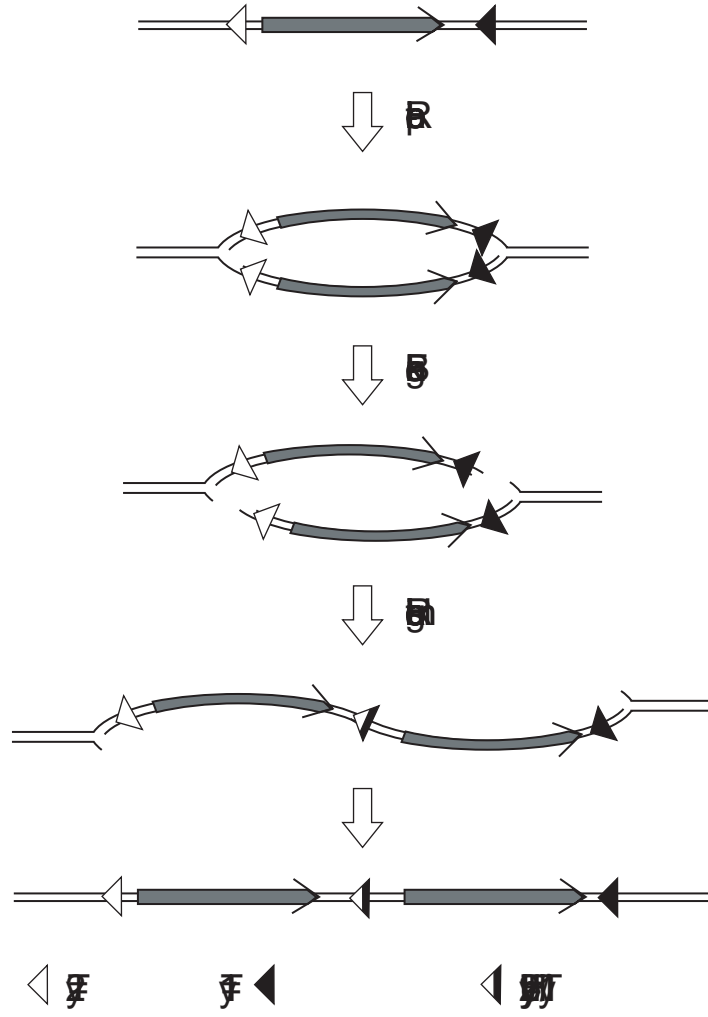
12. Jallepalli, P. V., Brown, G. W., Muzi-Falconi, M., Tien, D. & Kelly, T. J. Regulation of the replication initiator protein p65cdc18 by CDK phosphorylation. *Genes Dev* **11**, 2767-79 (1997).
13. Wilmes, G. M. et al. Interaction of the S-phase cyclin Clb5 with an "RXL" docking sequence in the initiator protein Orc6 provides an origin-localized replication control switch. *Genes Dev* **18**, 981-91 (2004).
14. Yanow, S. K., Lygerou, Z. & Nurse, P. Expression of Cdc18/Cdc6 and Cdt1 during G2 phase induces initiation of DNA replication. *Embo J* **20**, 4648-56 (2001).
15. Mieczkowski, P. A., Lemoine, F. J. & Petes, T. D. Recombination between retrotransposons as a source of chromosome rearrangements in the yeast *Saccharomyces cerevisiae*. *DNA Repair (Amst)* **5**, 1010-20 (2006).
16. Ball, C. A. & Cherry, J. M. Genome comparisons highlight similarity and diversity within the eukaryotic kingdoms. *Curr Opin Chem Biol* **5**, 86-9 (2001).
17. Redon, R. et al. Global variation in copy number in the human genome. *Nature* **444**, 444-54 (2006).
18. Herrick, J. et al. Genomic organization of amplified MYC genes suggests distinct mechanisms of amplification in tumorigenesis. *Cancer Res* **65**, 1174-9 (2005).
19. Kuwahara, Y. et al. Alternative mechanisms of gene amplification in human cancers. *Genes Chromosomes Cancer* **41**, 125-32 (2004).
20. Narayanan, V., Mieczkowski, P. A., Kim, H. M., Petes, T. D. & Lobachev, K. S. The pattern of gene amplification is determined by the chromosomal location of hairpin-capped breaks. *Cell* **125**, 1283-96 (2006).

21. De Lange, T. Telomere-related genome instability in cancer. *Cold Spring Harb Symp Quant Biol* **70**, 197-204 (2005).
22. Seo, J. et al. Cdt1 transgenic mice develop lymphoblastic lymphoma in the absence of p53. *Oncogene* **24**, 8176-86 (2005).
23. Arentson, E. et al. Oncogenic potential of the DNA replication licensing protein CDT1. *Oncogene* **21**, 1150-8 (2002).

**Figure 1** Potential mechanism of gene amplification induced by re-replication

Re-replication results in an unstable replication bubble which will not be stably inherited. In this model, we presume that some sort of replication fork difficulty leads to breakage at each of the two replication forks. When these breaks occur in the parental strands in trans, two broken ends will be exposed. If the cell is not capable of repairing this damage properly, by essentially recreating the fork structure or by homologous recombination between appropriate regions, repair might result in a genomic rearrangement. In our experimental system, the re-replicating origin is flanked by regions of high homology, Ty elements. Resection of the broken end to these homologous regions could allow the homologous recombination machinery to repair the damage through creation of a hybrid Ty molecule. This error in choice of homology will result in a head to tail gene amplification structure, which can be stably propagated. Re-replication might be uniquely poised to cause these gene amplification events due to the combination of duplication of regions by replication and induction of DNA damage.

5



## **CHAPTER 6**

### **Supplemental data for Chapter 2**

## SUPPLEMENTAL MATERIALS AND METHODS

### Plasmids

All plasmids are described in Table 1. Only pJL1488 (*pGAL1-Δntcdc6-cdk2A*) was constructed in this study. It contains the sequence 5'-TATGAGCGGCCGC-3' followed by *CDC6* from +139 to +1983 inserted in the *SmaI* site of pJL806 downstream of the *GAL1* promoter. This plasmid expresses a truncated Cdc6 with amino acids 2-47 replaced by amino acids S-G-R and with S354A and S372A alanine substitutions at the two remaining CDK consensus phosphorylation sites (S/T-P-X-K/R). The S354A mutation was marked with an *NheI* restriction site by introducing silent nucleotide substitutions T1059a and T1060g. The S372A mutation was marked with a *NarI* restriction site by introducing silent nucleotide substitutions T1113g, T1114g, and T1116g. Amino acid and base substitutions are listed relative to the first amino acid and nucleotide, respectively, of the wild type *CDC6* ORF (+1); the starting amino acid or nucleotide is on the left, and the substitution is on the right.

### Strain construction

All strains (Table 2) with the exception of YJL5038 were derived from YJL1737 (*MATa orc2-cdk6A orc6-cdk4A leu2 ura3-52 trp1-289 ade2 ade3 bar1Δ::LEU2*) (Nguyen *et al.*, 2001). The *orc2-cdk6A* and *orc6-cdk4A* alleles encode mutant proteins in which alanine is substituted for the phosphoacceptor serines or threonines at all full CDK consensus phosphorylation sites (residues 16, 24, 70, 174, 188, and 206 for *orc2-cdk6A*, and residues 106, 116, 123, and 146 *orc6-cdk4A*). Plasmids pMP933 (*ORC2*,

*URA3/EcoNI*), pJL737 (*ORC6, URA3/SphI*), pJL1206 (*MCM7-2NLS, URA3/AspI*), pKI1260 (*MCM7-2nls3A/AspI*) (Nguyen *et al.*, 2001) and pPP117 (*cdc7-1, URA3/ClaI*) (Hollingsworth *et al.*, 1992) were used in 2-step gene replacements at their respective chromosomal loci. YIp22 (*pMET3-HA3-CDC20, TRP1/MscI*) (Uhlmann *et al.*, 2000) was used in a one-step gene replacement at the *CDC20* locus. Plasmids pJL806 (*pGAL1, URA3/StuI*), pJL1488 (*pGAL1- $\Delta$ ntcdc6-cdk2A, URA3/StuI*), and pJL1489 (*pGAL1- $\Delta$ ntcdc6, URA3/StuI*) (Nguyen *et al.*, 2001) were inserted at the *URA3* locus by one step integration.

*ARS316, ARS317* and *ARS318* were deleted using PCR fragments containing KanMX6 or NatMX4 that were amplified, respectively, from pFA6a (Wach *et al.*, 1994) or pAG25 (Goldstein and McCusker, 1999) using oligonucleotide primers shown in Table 3. The *ars316 $\Delta$*  removes a 1.19 kb sequence containing *ARS316* and replaces it with a KanMX6 cassette (Poloumienko *et al.*, 2001). The *ars317 $\Delta$*  removes a 99 bp sequence containing the ARS consensus sequence (ACS) and the ABF1 binding site and replaces it with a KanMX6 cassette. The *ars318 $\Delta$*  removes an 89 bp sequence containing the ARS consensus sequence (ACS) and the ABF1 binding site and replaces it with a NatMX6 cassette.

YJL5038 (*MAT $\alpha$  his3 $\Delta$ ::KanMX leu2 $\Delta$ 0 met15 $\Delta$ 0 ura3 $\Delta$ 0 bar1 $\Delta$ ::NatMX4 can1 $\Delta$ ::pMFA1-HIS3::pMF $\alpha$ 1-LEU2*) was derived from a cross between YJL4161 (YD02458, *MAT $\alpha$  his3 $\Delta$ ::KanMX4 leu2 $\Delta$ 0 met15 $\Delta$ 0 ura3 $\Delta$ 0*, from the Saccharomyces Genome Deletion Project) (Winzeler *et al.*, 1999) and YJL4954 (*MAT $\alpha$  bar1 $\Delta$ ::NatMX4 can1 $\Delta$ ::pMFA1-HIS3::pMF $\alpha$ 1-LEU2 his3 $\Delta$ 1 leu2 $\Delta$ 0 lys2 $\Delta$ 0 ura3 $\Delta$ 0 met15 $\Delta$ 0*). YJL4954 was generated by deleting *BARI* in Y3655 (*MAT $\alpha$  can1 $\Delta$ ::pMFA1-HIS3::pMF $\alpha$ 1-LEU2*

*his3Δ1 leu2Δ0 lys2Δ0 ura3Δ0 met15Δ0*) (Tong *et al.*, 2004) using a PCR fragment containing NatMX4 amplified from pAG25 (Goldstein and McCusker, 1999) using oligonucleotide primers shown in Table 3.

## 2-D Gel Electrophoresis

Neutral-neutral two-dimensional (2D) gel analysis was performed essentially as described at <http://fangman-brewer.genetics.washington.edu>. The DNA preparation described there is a slight modification of the one used in Huberman *et al.* (Huberman *et al.*, 1987). The following modifications to the previous protocols were made. Thirty micrograms of DNA was digested with *ClaI* and *BglIII* for analysis of ARS317. Digested DNA was then enriched for replication intermediates with BND cellulose as follows. 4 g BND cellulose (Sigma B6385) was boiled in 20 ml water in a 50 ml conical tube for 5 min then spun at 2,000 rpm for 2 min in a SX4750 rotor using a GS-6 centrifuge (Beckman). The BND cellulose was washed once with 20 ml water and twice with NET (1 M NaCl, 1 mM EDTA, 10 mM Tris, pH 8.0) buffer. 1 ml packed column volume of BND cellulose suspension was placed in a disposable chromatography column (BioRad 731-1550) for each sample and washed with 5 ml of NET buffer. 5 M NaCl was added to each DNA digest to a final concentration of 1 M and the DNA was loaded on the column by passing the sample through twice. The column was washed with 5 ml NET and eluted with 3 ml 50 °C NET plus 1.8% caffeine. 3 ml isopropanol was added to the eluate, mixed by inversion and placed on ice for 30 min. The samples were spun for 30 min at 10,000 rpm at 4 °C, and the pellet was washed with ice cold 70% ethanol before being air-dried and resuspended in 40 µl TE. Loading dye (final concentrations: 2% w/v Ficoll



400, 0.01 M EDTA, 2% w/v SDS, 0.025% w/v bromophenol blue, 0.025% xylene cyanol) was added to the pellet and the entire sample was loaded on the gel.

For direct comparison, up to four samples were electrophoresed in the second dimension in quadrants of a single large gel and transferred using the high-salt downward capillary transfer method (Ausubel *et al.*, 2000) together to a single membrane GeneScreen Plus nitrocellulose membrane (NEN) and cross-linked with 0.12 J of UV light in a UV Stratalinker 1800 (Stratagene). The ARS317 probe was generated by PCR amplification of yeast genomic DNA using primers OJL1607 and OJL1608 (Table 3). This probe was labeled with the MegaPrime DNA labeling kit (Amersham Pharmacia), hybridized with ExpressHyb (Clontech) per the manufacturer's instructions and detected on a Storm 860 PhosphorImager (Molecular Dynamics).

#### Array Design and Fabrication

PCR products representing every ORF and intergenic region were designed and amplified as previously described (DeRisi *et al.*, 1997; Iyer *et al.*, 2001). Intergenic regions larger than 1.5 kb were amplified in segments of at most 1.5 kb. Each of the PCR products was resuspended in 3X SSC and robotically arrayed onto poly-L-lysine coated glass slides as previously described (DeRisi *et al.*, 1997). The remaining poly-L-lysine was then blocked as previously described (DeRisi *et al.*, 1997) (protocol is available at <http://derisilab.ucsf.edu/core/resources/index.html>) with the following modifications. The hydration step was omitted and instead slides were incubated in 3X SSC 0.2% SDS at 65°C for 5 min. Slides were washed successively with H<sub>2</sub>O and 95% ethanol, and then

dried by centrifugation for 2 min at 500 rpm in a SX4750 rotor using a GS-6 centrifuge (Beckman) and processed as described previously.

#### Genomic DNA preparation for CGH

450 ml of culture was mixed with 2.25 ml of 20% sodium azide and added to 50 ml of frozen,  $-80^{\circ}\text{C}$ , 0.2 M EDTA, 0.1% sodium azide. Cells were pelleted, washed with 50 ml  $4^{\circ}\text{C}$  TE (10 mM TrisCl 1 mM EDTA pH 7.5) and stored frozen at  $-80^{\circ}\text{C}$ . Pellets were resuspended in 4 ml Lysis buffer (2% Triton X-100, 1% SDS, 100 mM NaCl, 10 mM Tris-Cl, 1 mM EDTA pH8.0) and mixed with 4 ml of phenol:CHCl<sub>3</sub>:isoamyl alcohol (25:25:1) and 8 ml 0.5 mm glass beads (BioSpec Products, Inc., Bartlesville, OK). The suspension was vortexed seven times for 2 min separated by 2 min intervals at room temperature until greater than 95% of the cells lysed. The lysate was diluted with 8 ml phenol:CHCl<sub>3</sub>:isoamyl alcohol and 8 ml TE, and then centrifuged at 18,500 x g for 15 min at RT. After collecting the aqueous phase, the interphase was re-extracted with 8 ml TE, and the second aqueous phase from this re-extraction pooled with the first. The combined aqueous phases were extracted with an equal volume of CHCl<sub>3</sub>. The bulk of the RNA in the extract was selectively precipitated by addition of 0.01 volume 5 M NaCl to 50 mM and 0.4 volumes isopropanol and centrifugation at 12,000 x g for 15 min at RT. The RNA pellet was discarded and an additional 0.4 volumes of isopropanol was added to the supernatant. The sample was pelleted, washed with 70% ethanol, dried, and resuspended with 5.3 ml 10 mM Tris-Cl, (pH 8) 1 mM EDTA 1 M NaCl. RNase A (Qiagen, Valencia, CA) was added to 225  $\mu\text{g}/\text{ml}$  followed by incubation at  $37^{\circ}\text{C}$  for 30 min. Proteinase K was then added to 350

$\mu\text{g/ml}$  followed by incubation at  $55\text{ }^{\circ}\text{C}$  for 30 min. Finally, 0.6 ml of 10% (w/v) Cetyltrimethylammonium Bromide (CTAB) in 1 M NaCl (prewarmed to  $65\text{ }^{\circ}\text{C}$ ) was added and the sample was incubated for 20 min at  $65\text{ }^{\circ}\text{C}$  before being extracted with 8 ml  $\text{CHCl}_3$  and centrifuged at  $6000 \times g$  for 15 min at RT. The DNA in the aqueous phase was precipitated with 0.8 volumes isopropanol at RT, washed with 70% ethanol, dried, and resuspended in 10 ml Qiagen buffer QBT. DNA was loaded and purified on a Qiagen Genomic-tip 100/G column as per the manufacturer's instructions (Qiagen, Valencia, CA). The eluted DNA was precipitated with 0.8 volumes isopropanol at  $4\text{ }^{\circ}\text{C}$ , washed with 70% ethanol, dried, and resuspended in  $250\ \mu\text{l}$  2 mM Tris pH 7.5. This highly purified genomic DNA (OD 260/280 1.82-1.86) was sheared by sonication with a Branson Sonifier 450 to an average fragment size of 500 bp. Isolating DNA of this purity is important for generating reproducible replication profiles.

#### Labeling and Hybridization

5  $\mu\text{g}$  of sheared genomic DNA was randomly primed with 10  $\mu\text{g}$  of  $\text{N}_9$  nonomer by boiling for 5 min, then cooling on ice for 5 min. 5-(3-Aminoallyl)-2'-deoxyuridine 5'-triphosphate (Sigma A0410, St. Louis, MO) was incorporated into the primed genomic DNA in a 50  $\mu\text{l}$  reaction containing 10 mM TrisHCl pH 7.5, 5 mM  $\text{MgCl}_2$ , 7.5 mM dithiothreitol, 120  $\mu\text{M}$  dATP, 120  $\mu\text{M}$  dCTP, 120  $\mu\text{M}$  dGTP, 20  $\mu\text{M}$  dTTP, 100  $\mu\text{M}$  5-(3-Aminoallyl)-2'-deoxyuridine 5'-triphosphate, and 5 U Klenow fragment. The reaction was incubated at  $37\text{ }^{\circ}\text{C}$  for 4 hr, and the DNA was purified using the DNA Clean and Concentrator kit (Zymo Research, Orange, California). 15-40 nmol of Cy3 and Cy5 (Amersham, Piscataway, NJ) were then separately coupled to the appropriate DNA with

0.1 M  $\text{NaHCO}_3$ , pH 9.0 for 1 hr (Bozdech *et al.*, 2003), and the fluorescently labeled DNA purified using the DNA Clean and Concentrator kit (Zymo Research, Orange, California). For most hybridizations, the replicating or re-replicating DNA was labeled with Cy5 and the non-replicating control DNA was labeled with Cy3.

Cy3 and Cy5 labeled DNA were pooled in a 40  $\mu\text{l}$  mixture containing 3X SSC, 25 mM HEPES pH 7.0, and 0.25% SDS. Samples denatured for 2 min at 100°C and hybridized under a glass mSeries Lifterslip (Erie Scientific 25x40I-M-5227, Portsmouth, NH) to a microarray for 18-24 hours at 63°C. Microarrays were washed successively in 0.85X SSC, 0.02% SDS and 0.035X SSC immediately before scanning. The microarrays were spun dry and scanned with a GenePix 4000B scanner (Axon Instruments Union City, California) in an enclosed chamber where atmospheric ozone was maintained below 10 ppb using two OI-45 Ozone Interceptors (Ozone solutions, Sioux Center, Iowa). Reducing Cy5 exposure to atmospheric ozone during the final drying and scanning is essential for obtaining reproducible replication profiles.

### Data analysis

Genepix Pro 4.0 software (Axon Instruments, Union City, CA) was used for micorarray image analysis and quantification. Data were filtered to remove features that had (1) obvious defects, (2) saturated pixels, (3) regression  $R^2$  values less than 0.5, or (4) fewer than 55% of their pixels with fluorescence intensity greater than 2 standard deviations above background. Data was also filtered to remove 1572 features that contain repetitive sequences from the analysis. The median of the ratios for each element was used for the raw Cy5/Cy3 value.

The raw ratios were normalized by multiplying each value by a scalar normalization factor chosen so that the average of the normalized values was equal to the DNA content of the cells. DNA content was calculated from the median of the flow cytometry profile after correcting for signal increase due to mitochondrial replication (detailed information on the calculation of DNA content is provided below). The raw data were then binned and smoothed essentially as described (Raghuraman *et al.*, 2001). In short, a moving median was calculated over a 10 kb window for every 0.5 kb location along the genome. If a given 10 kb window did not contain any raw data points after filtering it was defined as a no data zone and the binned value from the previous window was used for smoothing purposes. The binned data were then smoothed using Fourier Convolution Smoothing essentially as described (Raghuraman *et al.*, 2001). However, the equation for  $k(S)$  was incorrectly provided in part II.3 of the supplemental information of that paper. The correct equation is as follows (personal communication, Collingwood D.):

$$k(S) = \left\{ \exp(-2^{-S} n^2) : n \text{ is an integer satisfying } \left\lfloor \frac{T}{2} \right\rfloor \leq n \leq T - 1 - \left\lfloor \frac{T}{2} \right\rfloor \right\}$$

In Raghuraman *et al.* (Raghuraman *et al.*, 2001) the optimal value for S was computationally determined for each chromosome for each experiment. While this was effective for replication profiles, we found that predetermined values for S resulted in better re-replication profiles. Thus, for all G2/M and G1 release re-replication profiles, the following values for S were used for each chromosome: I: 8, II: 9.75, III: 8.25, IV: 12, V: 9, VI: 8, VII: 10.5, VIII: 9, IX: 8.75, X: 9.5, XI: 9.25, XII: 10.5, XIII: 10.25, XIV: 9.75, XV: 10.75, XVI: 10.25.

In most cases, two hybridizations were performed from each of two independent genomic DNA preparations. For presentation purposes, the resulting four replication profiles were averaged into one composite profile. Table S2 contains the value at each chromosomal locus for each of the composite profiles in this manuscript. In the final replication profiles, no data regions as described above are presented as gaps in the profiles.

### Peak Finding

In order to identify potential origins, all local maxima in the smoothed data were identified and filtered based on two parameters, slide and drop. The maxima that satisfy our slide and drop parameters define the origin list. Due to the very different nature of replication and re-replication, some peak finding parameters were different between the two types of profiles. Solely for peak finding purposes, the re-replication data were normalized to half of their DNA content, in order to use the same range of parameters as are used during replication.

The drop value is a semi global measure of peak height. For each maximum, drop is the difference between the Cy5/Cy3 ratio of that maximum and the lowest Cy5/Cy3 value within 15kb (replication) or 200kb (re-replication) on either side of that maximum. The slide value (Glynn *et al.*, 2004) is a local measure of peak height and is the difference between the Cy5/Cy3 ratio of the maxima being considered and the closest local minima on either side of the maxima. The total slide is the sum of the left slide and the right slide. For replication profiles, a local maxima was identified as a potential origin if the following conditions all apply: 1) the drop value was greater than 0.05, 2) the

left slide was greater than 0.005, 3) the right slide was greater than 0.005 and 4) the total slide was greater than 0.05 (replication) or 0.02 (re-replication). .

To identify a list of origins for a given experimental condition, duplicate microarrays were performed for each of two independent genomic DNA preparations, and the sets of potential origins from the four individual microarrays were merged as follows. Hierarchical clustering (average linkage) was used to identify locations where several individual microarray experiments had potential origins. If three of the four microarray experiments recorded a potential origin in a 15 kb region (replication) or two of the four within 20 kb (re-replication), the locations of those potential origins were averaged and reported as the origin position for the merged dataset. Table S3 contains the list of identified origins for all experiments for which peak finding was performed.

### Scatter Plot

The locations of 351 pro-ARSs from all the budding yeast chromosomes except chromosomes IV and XI were obtained from Wyrick *et al.* (Wyrick *et al.*, 2001). These chromosomes were excluded because some of the strains used in our study have duplications of portions of these chromosomes. These genomic alterations do not have any effect on the extent or origin usage of either replication or re-replication (data not shown). For each pro-ARS, the normalized Cy5/Cy3 ratio of that chromosomal locus for replication or re-replication was plotted against the ratio at that locus of the other profile being compared. The linear regression formula and  $R^2$  value are shown on the plot.

## Normalization of Replication and Re-replication Profiles by Quantification of Flow Cytometry Data

Flow cytometry was used to calculate the DNA content in each experiment. The genomic replication profiles and re-replication profiles were then normalized to the calculated DNA content. Quantification of absolute DNA content in *Saccharomyces cerevisiae* is complicated by fact that roughly 10% of the total DNA in a yeast cell is mitochondrial. Furthermore, cell cycle independent mitochondrial DNA replication causes the peak of flow cytometry profile to gradually increases in cell cycle arrested yeast (Pichler *et al.*, 1997). This complicates the quantification of the absolute DNA content by flow cytometry in synchronized yeast cultures. The following calculations were used to correct for the increase in the flow cytometry peak due to mitochondrial replication and thus determine the actual DNA content from the observed flow cytometry peak.

### *Replication: G1 into 0.1MHU*

First, the absolute increase in fluorescent intensity due to the duplication of the yeast genome was calculated for each strain. The fluorescence intensity for the G1 peak ( $p_{Asyn}^{1C}$ ) and the G2 peak ( $p_{Asyn}^{2C}$ ) were determined from the asynchronous sample collected for each strain at the beginning of each experiment. The values for the G1 and G2 peaks in asynchronous samples were determined by applying the cell cycle model described by Watson *et al.* (Watson *et al.*, 1987) using the computer software FlowJo (Tree Star, Inc., Ashland, OR). The peak value for cell cycle synchronized samples was determined by



taking the median of the flow cytometry graph. The difference ( $\Delta p$ ) between these two peaks was the signal increase due to a single round of replication.

$$\Delta p = p_{Asyn}^{2C} - p_{Asyn}^{1C} \quad (1)$$

When cells are cell cycle arrested, mitochondria continue to replicate their DNA. Thus, the fluorescent intensity continues to increase in the absence of ongoing genomic DNA replication. Thus, the peak of the G1 synchronized cells ( $p_0^{1C}$ ) is greater than the G1 peak in the asynchronous population ( $p_{Asyn}^{1C}$ ). Therefore, when all the cells in a population reach the G1 arrest, the subsequent G2 peak will no longer be twice value of the G1 peak. The subsequent G2 peak will be G1 plus the increase due to duplication of the genomic DNA ( $\Delta p$ ). For cells arrested in G1 with  $\square$  factor the calculated 2C value at time 0 ( $c_0^{2C}$ ) was:

$$c_0^{2C} = p_0^{1C} + \Delta p \quad (2)$$

Cells were subsequently released from the G1 arrest into G2 in the presence of hydroxyurea to slow S phase and nocodazole to arrest cells in the subsequent G2. The calculated value of the G2 peak was confirmed by the measured position of peak when the cells reached the nocodazole arrest. The rightward shift in the flow cytometry peak due to genomic independent (mitochondrial) replication was reduced in the presence of hydroxyurea. It has previously been shown that mitochondrial DNA copy number is

sensitive to nucleotide levels, which could explain the lack of further shift (Taylor *et al.*, 2005).

To calculate the extent of replication following synchronous release from  $\square$  factor an equation relating DNA content to the flow cytometry peak was generated using the measured G1 peak ( $p_0^{1C}$ ) and calculated G2 peak ( $c_0^{2C}$ ) as endpoints. In other words, since it is possible to correlate flow cytometry peak value to DNA content at 1C and 2C, a line connecting those points would enable us to determine the DNA content represented by any measured flow cytometry peak value between those two points. Thus, a linear regression line of the form  $d = mp + b$  was generated where  $d$  is the DNA content,  $p$  is the median of the flow cytometry peak for a sample,  $m$  is the slope and  $b$  is the intercept. For a given time point ( $t$ ) the median of the flow cytometry data ( $p_t$ ) was used to calculate the DNA content ( $d_t$ ). This value was then used as the normalization factor for the corresponding genomic replication profile. The DNA content of the G1 peak ( $d_{1C}$ ) was one and the G2 peak ( $d_{2C}$ ) was two.

$$d_t = \overbrace{\left( \frac{d_{2C} - d_{1C}}{c_0^{2C} - p_0^{1C}} \right)}^m p_t + \overbrace{\left[ d_{1C} - \left( \frac{d_{2C} - d_{1C}}{c_0^{2C} - p_0^{1C}} \right) p_0^{1C} \right]}^b \quad (3)$$

#### *Re-replication: G2/M*

A similar approach was used to correct for the shift in the flow cytometry peak due to mitochondrial replication during G2 arrest and induction of re-replication. For each re-replicating strain containing *pGAL1-Δntcdc6* there was a complementary *pGAL1* control strain. This *pGAL1* control did not re-replicate but did experience the genomic re-

replication independent shifting of the flow cytometry peak. Thus, its shift could be used to correct for re-replication independent shift in the re-replicating strain. At a given time point this shift ( $s_t^{pGAL1}$ ) was the difference of the median of the flow cytometry data of the *pGAL1* control at the start the experiment ( $p_0^{2C,pGAL1}$ ) and the median at the time of interest ( $p_t^{pGAL1}$ ):

$$s_t^{pGAL1} = p_t^{pGAL1} - p_0^{2C,pGAL1} \quad (4)$$

The corrected value of the re-replicating strain's flow cytometry peak ( $f_t^{rerep}$ ) at a given time was calculated by subtracting  $s_t^{pGAL1}$  from the median of the measured flow cytometry peak in the re-replicating strain ( $p_t^{rerep}$ ).

$$f_t^{rerep} = p_t^{rerep} - s_t^{pGAL1} \quad (5)$$

As in the S phase experiments, the absolute increase in fluorescent intensity due to the duplication of the genome ( $\Delta p^{rerep}$ ) was calculated using the G1 peak ( $p_{Asyn}^{1C,rerep}$ ) and G2 peak ( $p_{Asyn}^{2C,rerep}$ ) from the asynchronous sample of the *pGAL1- $\Delta ntc6$*  re-replicating strains.

$$\Delta p^{rerep} = p_{Asyn}^{2C,rerep} - p_{Asyn}^{1C,rerep} \quad (6)$$

Next, the value of a hypothetical 4C peak ( $c_0^{4C,rerep}$ ) was calculated by adding twice  $\Delta p^{rerep}$  to the measured value of the G2/M arrested peak ( $p_0^{2C,rerep}$ ).

$$c_0^{4C,rerep} = p_0^{2C,rerep} + 2(\Delta p^{rerep}) \quad (7)$$

A linear regression line  $d = mf + b$  was generated similar to the S phase experiment above where  $d$  is the DNA content,  $f$  is the corrected median of the FACS peak for a sample,  $m$  is the slope and  $b$  is the intercept. For a given time point ( $t$ ) the corrected median of the flow cytometry data ( $f_t^{rerep}$ ) was used to calculate the DNA content ( $d_t$ ). This value was then used as the normalization factor for the corresponding genomic re-replication profile. The DNA content of the G2 peak ( $d_{2C}$ ) was two and the hypothetical 4C peak ( $d_{4C}$ ) was four.

$$d_t = \left[ \frac{d_{4C} - d_{2C}}{c_0^{4C,rerep} - p_0^{2C,rerep}} \right] f_t^{rerep} + \left[ d_{2C} - \left( \frac{d_{4C} - d_{2C}}{c_0^{4C,rerep} - p_0^{2C,rerep}} \right) p_0^{2C,rerep} \right] \quad (8)$$

#### *Re-replication: G1 into G2/M*

As in the S phase experiments, the absolute increase in fluorescent intensity due to the duplication of the genome ( $\Delta p$ ) was calculated using the G1 peak ( $p_{Asyn}^{1C}$ ) and G2 peak ( $p_{Asyn}^{2C}$ ) from asynchronous samples of both the *pGAL1* control and *pGAL1- $\Delta$ ntcdc6* re-replicating strains.

$$\Delta p^{pGAL1} = p_{Asyn}^{2C,pGAL1} - p_{Asyn}^{1C,pGAL1} \quad (9)$$

$$\Delta p^{rerep} = p_{Asyn}^{2C,rerep} - p_{Asyn}^{1C,rerep} \quad (10)$$

In this type of experiment the flow cytometry peak for the *pGAL1* control will increase for two reasons: genomic replication and genomic independent (mitochondrial) replication. The flow cytometry peaks in the *pGAL1-Δntcdc6* re-replicating strains will increase for up to three reasons: genomic replication, genomic independent (mitochondrial) replication and potentially re-replication. The value of the subsequent G2 peak ( $c_0^{2C,pGAL1}$ ), which accounts for genomic replication, was calculated for the *pGAL1* control and *pGAL1-Δntcdc6* re-replicating strain.

$$c_0^{2C,pGAL1} = p_0^{1C,pGAL1} + \Delta p^{pGAL1} \quad (11)$$

$$c_0^{2C,rerep} = p_0^{1C,rerep} + \Delta p^{rerep} \quad (12)$$

The value of the fluorescence increase due to genomic replication independent (mitochondrial) shifting ( $s_t^{pGAL1}$ ) was calculated from the *pGAL1* control strain by subtracting the calculated value of G2 peak ( $c_0^{2C,pGAL1}$ ) from the median of the flow cytometry data at the cells were harvested ( $p_t^{pGAL1}$ ).

$$s_t^{pGAL1} = p_t^{pGAL1} - c_0^{2C,pGAL1} \quad (13)$$

The shift ( $s_t^{pGAL1}$ ) was then used to correct the observed flow cytometry peak of the re-replicating strain such that the peak value would reflect only the increases due to genomic replication and re-replication. The corrected value of the flow cytometry peak ( $f_t^{rerep}$ ) was determined by subtracting  $s_t^{pGAL1}$  from the measured median of the flow cytometry data in the re-replicating strain ( $p_t^{rerep}$ ).

$$f_t^{rerep} = p_t^{rerep} - s_t^{pGAL1} \quad (14)$$

Next, the value of a hypothetical 4C peak ( $c_0^{4C,rerep}$ ) was calculated by adding three times  $\Delta p^{rerep}$  to the measured value of the G1 arrested peak ( $p_0^{1C,rerep}$ ).

$$c_0^{4C,rerep} = p_0^{1C,rerep} + 3(\Delta p^{rerep}) \quad (15)$$

Finally, a linear regression line  $d = mf + b$  was generated similar to the above experiments where  $d$  is the DNA content,  $f$  is the corrected median of the FACS peak for a sample,  $m$  is the slope and  $b$  is the intercept. For a given time point ( $t$ ) the corrected median of the flow cytometry data ( $f_t^{rerep}$ ) was used to calculate the DNA content ( $d_t$ ). This value was then used as the normalization factor for the corresponding genomic re-replication profile. The DNA content of the G2 peak ( $d_{2C}$ ) was two and the hypothetical 4C peak ( $d_{4C}$ ) was four.

$$d_t = \overbrace{\left( \frac{d_{4C} - d_{2C}}{c_0^{4C, rerep} - c_0^{2C, rerep}} \right)}^m f_t^{rerep} + \overbrace{\left[ d_{2C} - \left( \frac{d_{4C} - d_{2C}}{c_0^{4C, rerep} - c_0^{2C, rerep}} \right) c_0^{2C, rerep} \right]}^b \quad (16)$$

*Re-replication: G1 into HU*

The DNA content for re-replication induced from G1 into hydroxyurea was calculated as in the S phase experiments (Replication: G1 into HU) in the absence of induction of re-replication.

## REFERENCES

- Ausubel, F.M., Brent, R., Kingsbury, R.E., Moore, D.D., Seidman, J.G., Smith, J.A., and Struhl, K. (2000). *Current Protocols in Molecular Biology*. John Wiley & Sons, Inc.: New York.
- Bozdech, Z., Zhu, J., Joachimiak, M.P., Cohen, F.E., Pulliam, B., and DeRisi, J.L. (2003). Expression profiling of the schizont and trophozoite stages of *Plasmodium falciparum* with a long-oligonucleotide microarray. *Genome Biol* 4, R9.
- DeRisi, J.L., Iyer, V.R., and Brown, P.O. (1997). Exploring the metabolic and genetic control of gene expression on a genomic scale. *Science* 278, 680-686.

- Glynn, E.F., Megee, P.C., Yu, H.G., Mistrot, C., Unal, E., Koshland, D.E., DeRisi, J.L., and Gerton, J.L. (2004). Genome-wide mapping of the cohesin complex in the yeast *Saccharomyces cerevisiae*. *PLoS Biol* 2, E259.
- Goldstein, A.L., and McCusker, J.H. (1999). Three new dominant drug resistance cassettes for gene disruption in *Saccharomyces cerevisiae*. *Yeast* 15, 1541-1553.
- Hollingsworth, R.E., Jr., Ostroff, R.M., Klein, M.B., Niswander, L.A., and Sclafani, R.A. (1992). Molecular genetic studies of the Cdc7 protein kinase and induced mutagenesis in yeast. *Genetics* 132, 53-62.
- Huberman, J.A., Spotila, L.D., Nawotka, K.A., el-Assouli, S.M., and Davis, L.R. (1987). The in vivo replication origin of the yeast 2 microns plasmid. *Cell* 51, 473-481.
- Iyer, V.R., Horak, C.E., Scafe, C.S., Botstein, D., Snyder, M., and Brown, P.O. (2001). Genomic binding sites of the yeast cell-cycle transcription factors SBF and MBF. *Nature* 409, 533-538.
- Nguyen, V.Q., Co, C., and Li, J.J. (2001). Cyclin-dependent kinases prevent DNA re-replication through multiple mechanisms. *Nature* 411, 1068-1073.
- Pichler, S., Piatti, S., and Nasmyth, K. (1997). Is the yeast anaphase promoting complex needed to prevent re-replication during G2 and M phases? *Embo J* 16, 5988-5997.
- Poloumienko, A., Dershowitz, A., De, J., and Newlon, C.S. (2001). Completion of replication map of *Saccharomyces cerevisiae* chromosome III. *Mol Biol Cell* 12, 3317-3327.
- Raghuraman, M.K., Winzeler, E.A., Collingwood, D., Hunt, S., Wodicka, L., Conway, A., Lockhart, D.J., Davis, R.W., Brewer, B.J., and Fangman, W.L. (2001). Replication dynamics of the yeast genome. *Science* 294, 115-121.



- Taylor, S.D., Zhang, H., Eaton, J.S., Rodeheffer, M.S., Lebedeva, M.A., O'Rourke T, W., Siede, W., and Shadel, G.S. (2005). The conserved Mec1/Rad53 nuclear checkpoint pathway regulates mitochondrial DNA copy number in *Saccharomyces cerevisiae*. *Mol Biol Cell* *16*, 3010-3018.
- Tong, A.H., Lesage, G., Bader, G.D., Ding, H., Xu, H., Xin, X., Young, J., Berriz, G.F., Brost, R.L., Chang, M., Chen, Y., Cheng, X., Chua, G., Friesen, H., Goldberg, D.S., Haynes, J., Humphries, C., He, G., Hussein, S., Ke, L., Krogan, N., Li, Z., Levinson, J.N., Lu, H., Menard, P., Munyana, C., Parsons, A.B., Ryan, O., Tonikian, R., Roberts, T., Sdicu, A.M., Shapiro, J., Sheikh, B., Suter, B., Wong, S.L., Zhang, L.V., Zhu, H., Burd, C.G., Munro, S., Sander, C., Rine, J., Greenblatt, J., Peter, M., Bretscher, A., Bell, G., Roth, F.P., Brown, G.W., Andrews, B., Bussey, H., and Boone, C. (2004). Global mapping of the yeast genetic interaction network. *Science* *303*, 808-813.
- Uhlmann, F., Wernic, D., Poupart, M.A., Koonin, E.V., and Nasmyth, K. (2000). Cleavage of cohesin by the CD clan protease separin triggers anaphase in yeast. *Cell* *103*, 375-386.
- Wach, A., Brachat, A., Pohlmann, R., and Philippsen, P. (1994). New heterologous modules for classical or PCR-based gene disruptions in *Saccharomyces cerevisiae*. *Yeast* *10*, 1793-1808.
- Watson, J.V., Chambers, S.H., and Smith, P.J. (1987). A pragmatic approach to the analysis of DNA histograms with a definable G1 peak. *Cytometry* *8*, 1-8.
- Winzeler, E.A., Shoemaker, D.D., Astromoff, A., Liang, H., Anderson, K., Andre, B., Bangham, R., Benito, R., Boeke, J.D., Bussey, H., Chu, A.M., Connelly, C.,

Davis, K., Dietrich, F., Dow, S.W., El Bakkoury, M., Foury, F., Friend, S.H., Gentalen, E., Giaever, G., Hegemann, J.H., Jones, T., Laub, M., Liao, H., Liebundguth, N., Lockhart, D.J., Lucau-Danila, A., Lussier, M., M'Rabet, N., Menard, P., Mittmann, M., Pai, C., Rebischung, C., Revuelta, J.L., Riles, L., Roberts, C.J., Ross-MacDonald, P., Scherens, B., Snyder, M., Sookhai-Mahadeo, S., Storms, R.K., Veronneau, S., Voet, M., Volckaert, G., Ward, T.R., Wysocki, R., Yen, G.S., Yu, K., Zimmermann, K., Philippsen, P., Johnston, M., and Davis, R.W. (1999). Functional characterization of the *S. cerevisiae* genome by gene deletion and parallel analysis. *Science* 285, 901-906.

Wyrick, J.J., Aparicio, J.G., Chen, T., Barnett, J.D., Jennings, E.G., Young, R.A., Bell, S.P., and Aparicio, O.M. (2001). Genome-wide distribution of ORC and MCM proteins in *S. cerevisiae*: high-resolution mapping of replication origins. *Science* 294, 2357-2360.

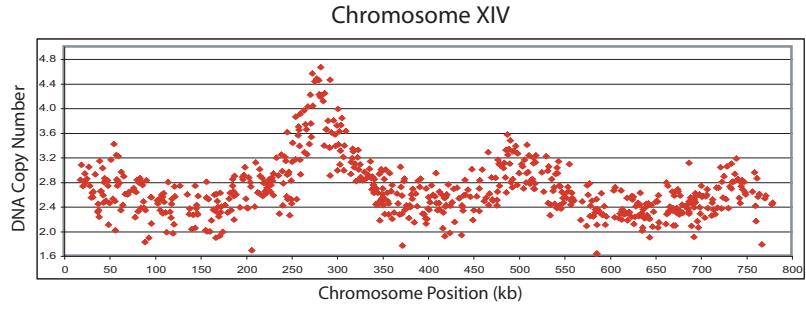
**Table S1.** CGH on spotted microarrays accurately identifies S phase replication origins. Our analysis of the replication of a wild type yeast in the S288c background identified 212 replication origins throughout the genome, which is roughly comparable to the numbers obtained by Rhaguraman *et al.* (Rhaguraman *et al.*, 2001) (332) and Yabuki *et al.* (Yabuki *et al.*, 2002) (260). Origins on chromosome III (Greenfeder and Newlon, 1992; Poloumienko *et al.*, 2001), VI (Yamashita *et al.*, 1997), V (Tanaka *et al.*, 1996) and X (Wyrick *et al.*, 2001) have been systematically mapped by 2-D gel electrophoresis and and/or ARS plasmid assay, and annotated in the Saccharomyces Genome Database (SGD) (Balakrishnan). For each origin that was identified on chromosome III, V, VI, and X, the distance to the closest annotated origin in SGD was determined and the mean of these distances was calculated (This study, four hybridizations). A similar comparison was performed for the other origins identified by three previously published genome-wide analyses of budding yeast origins (Rhaguraman *et al.*, 2001; Yabuki *et al.*, 2002) or potential origins (Wyrick *et al.*, 2001). We note that for screening purposes, our assay can be streamlined even further by using replication profiles from a single microarray (This study, single hybridization.)

	<u>Mean distance</u>
Raghuraman et al. (2001)	6.5 kb
Wyrick et al. (2001)	3.9 kb
Yabuki et al. (2002)	3.5 kb
This study, four hybridizations	3.2 kb
This study, single hybridization	6.1 kb

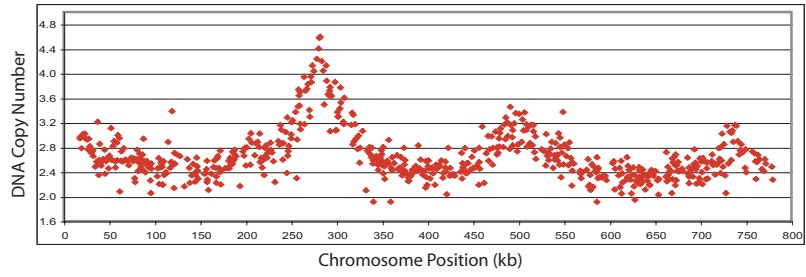
**Figure S1.** Example of raw data from a re-replication microarray experiment. For most experiments, two independent sets of genomic DNA were prepared and each set was competitively hybridized in duplicate. The ratio of signal intensity of Cy5 to Cy3 was calculated for each sequence element on the array and normalized such that the average ratio of all elements was set to the median DNA content of the re-replicating cells. Normalized raw ratios of the four hybridizations from the experiment described in Figure 2B are shown for chromosome XIV (top four panels). These normalized ratios were subjected to local averaging and Fourier convolution smoothing to generate a smoothed profile. The four smoothed profiles were then merged (see Supplemental Methods) to generate a composite re-replication profile (bottom panel).

Supplemental Figure 1

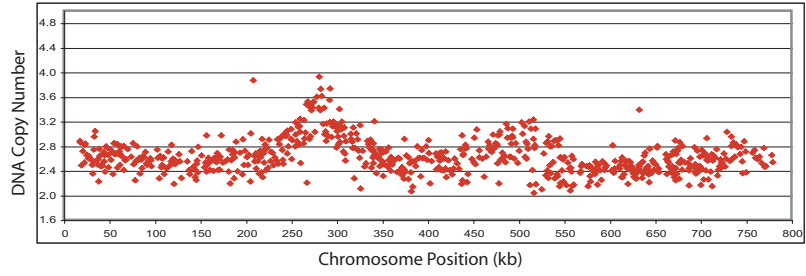
Raw Data for Hybridization 1



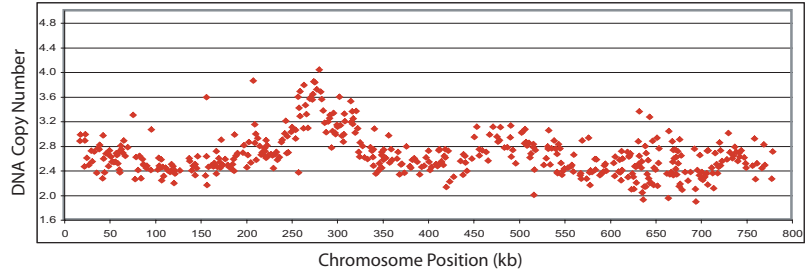
Raw Data for Hybridization 2



Raw Data for Hybridization 3



Raw Data for Hybridization 4



Smoothed profile generated from the 4 hybridizations

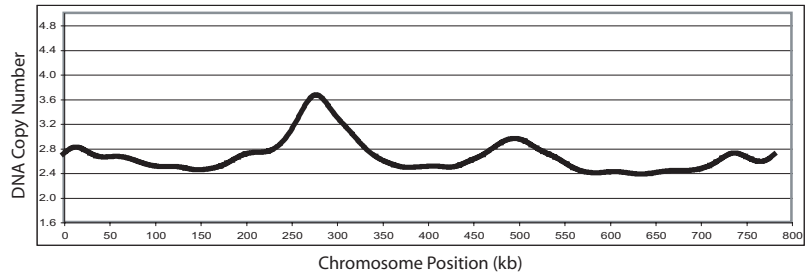


**Figure S2.** Replication profiles generated by comparative genomic hybridization. CGH replication assay was performed on YJL5038, a wild-type yeast strain in the S288c background, in an experiment described in Figure 1B. G1 phase genomic DNA was isolated from cells arrested in alpha factor. S phase genomic DNA was isolated from cells released from an alpha factor arrest in the presence of 100 mM hydroxyurea (HU) for 120 min (DNA content was 1.4 C). The composite replication profiles (blue lines) plus and minus one standard deviation (light gray bands, see Methods) are shown for all sixteen chromosomes. Positions of the 212 origins identified by application of a peak finding algorithm are shown (blue diamonds). Positions of ARSs annotated in the Saccharomyces Genome Database (SGD, (Balakrishnan)) (black open triangles), locations of pro-ARSs mapped by Wyrick *et al.* (Wyrick *et al.*, 2001) (red triangles) and the centromeres (black circles) are marked along the X-axis. Replication profiles derived from Raghuraman *et al.* (Raghuraman *et al.*, 2001) (violet lines) and Yabuki *et al.* (Yabuki *et al.*, 2002) (orange lines) are shown for comparison.

## Supplemental Figure 2

S288c S phase Raghuraman *et al.* Yabuki *et al.*

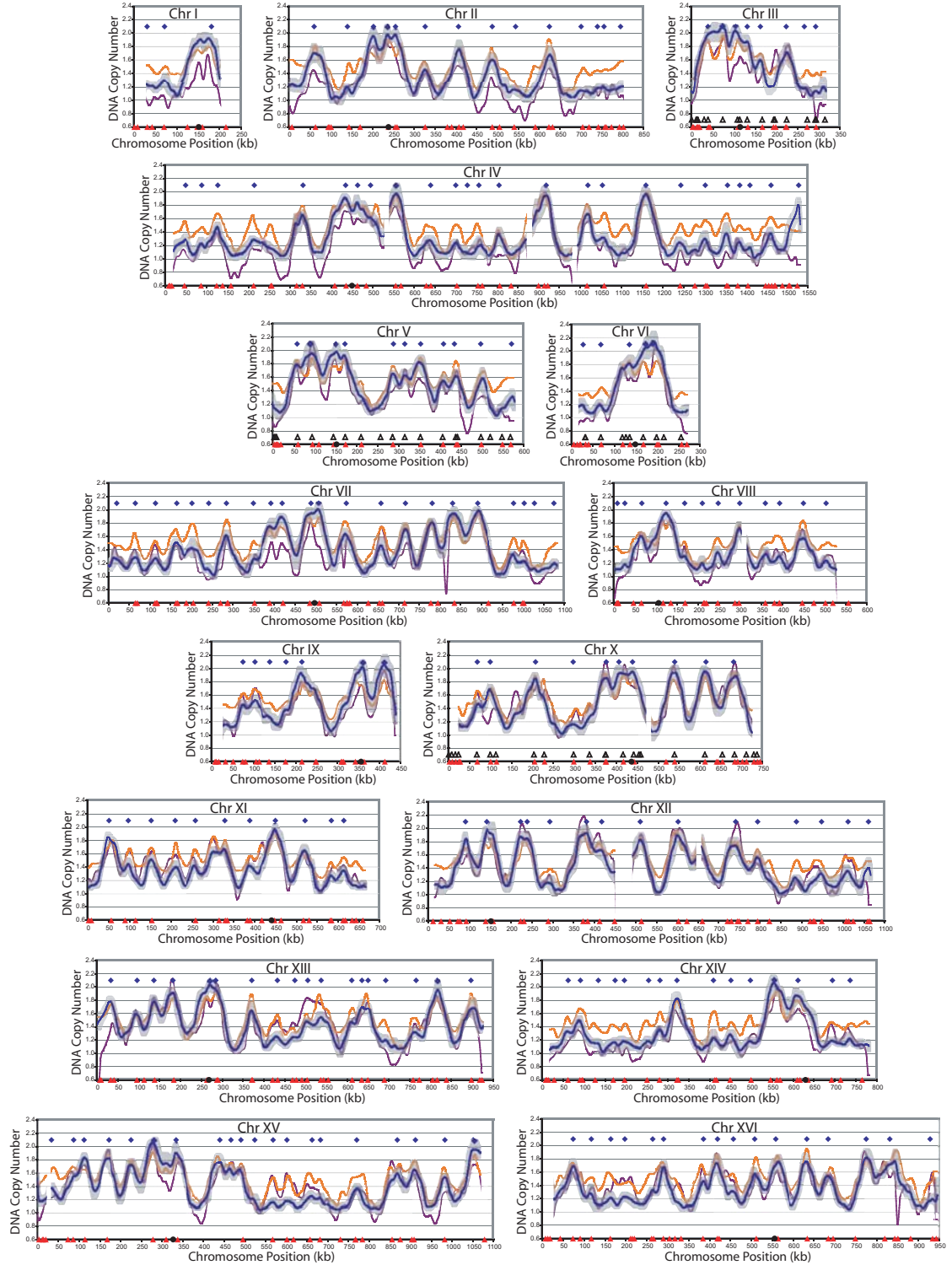


**Figure S3.** The S phase replication profile of the re-replication competent OMC strain and the congenic wild-type strain are similar. S phase replication profiles were generated for the OMC strain YJL3248 (*MCM7-2NLS orc2-cdk6A orc6-cdk4A pGAL1-Δntcdc6 pMET3-HA3-CDC20*) and YJL5834 (*pGAL1*), a wild-type yeast strain in the A364a background, in an experiment described in Figure 1D. S phase OMC cells were harvested 180 min after alpha factor release into HU (DNA content was 1.4 C). S phase A364a cells were harvested 135 min after alpha factor release into HU (DNA content was 1.35 C). The S phase replication profiles for the OMC strain (green lines), S phase replication profiles for the A364a strain (red lines), the positions of the 193 origins identified in the OMC strain (green diamonds), and the positions of the 231 origins identified in the A364a strain (red diamonds) are shown for all sixteen chromosomes. Positions of origins annotated in SGD, (Balakrishnan) (black open triangles), locations of pro-ARSs mapped by Wyrick *et al.* (Wyrick *et al.*, 2001) (red triangles) and the centromeres (black circles) are marked along the X-axis.



### Supplemental Figure 3

A364a S phase      OMC S phase

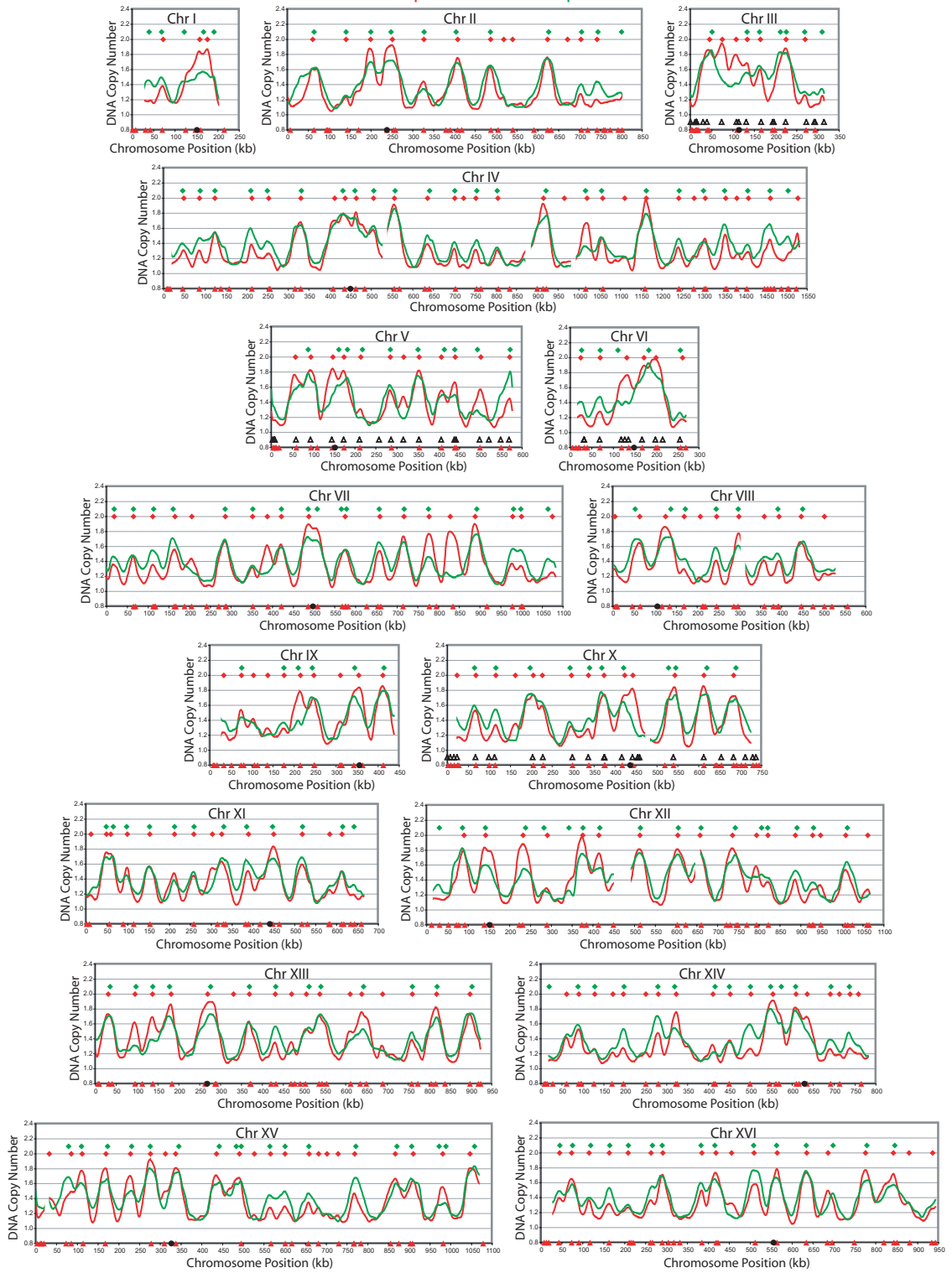


**Figure S4.** Replication timing in the OMC re-replication competent mutant correlates with replication timing in the A364a background. Application of a peak finding algorithm to the S phase replication profiles in Figure S3 identified 193 origins in the OMC strain YJL3248 (*MCM7-2NLS orc2-cdk6A orc6-cdk4A pGAL1- $\Delta$ ntcdc6 pMET3-HA3-CDC20*), and 231 origins in the A364a strain YJL5834 (*pGAL1*). 166 (86%) of the origins identified from the OMC strain had a corresponding origin within 10kb in the wild-type A364a strain. For each of the shared origins, the S phase copy number in the A364a replication profile from Figure S3 was plotted against that for the OMC strain in Figure S3. A linear regression line fitted to these points showed a good correlation, with an  $R^2$  value of 0.58.

## Supplemental Figure 4

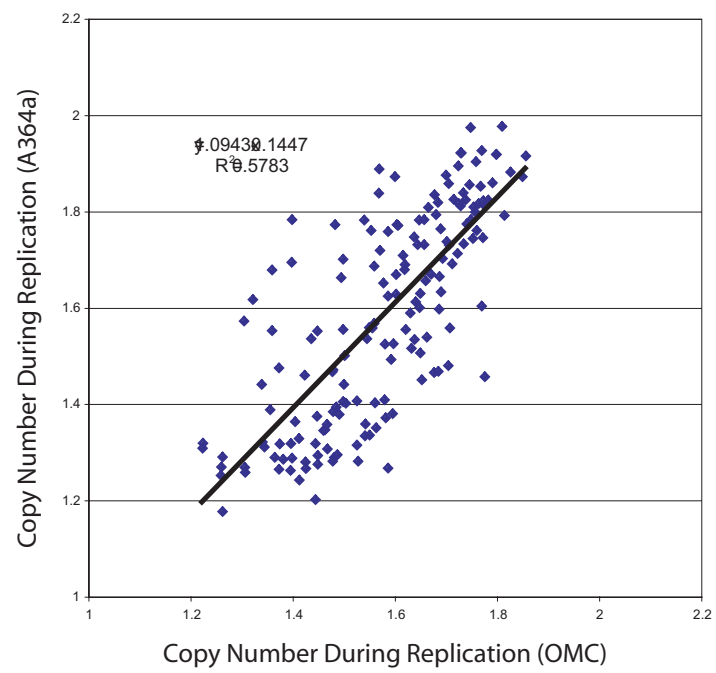


**Figure S5.** Different strain backgrounds have very similar replication timing profiles. The replication profiles (red lines) and identified origins (red diamonds) from the congenic wild-type A364a strain YJL5834 (*pGALI*) from Figure S3 are compared to the replication profiles (blue lines) and identified origins (blue diamonds) from the S288c strain in Figure S2. Positions of origins annotated in SGD (Balakrishnan) (black open triangles), locations of pro-ARSs mapped by Wyrick *et al.* (Wyrick *et al.*, 2001) (red triangles) and the centromeres (black circles) are marked along the X-axis.

# Supplemental Figure 5

S288c S phase      A364a S phase

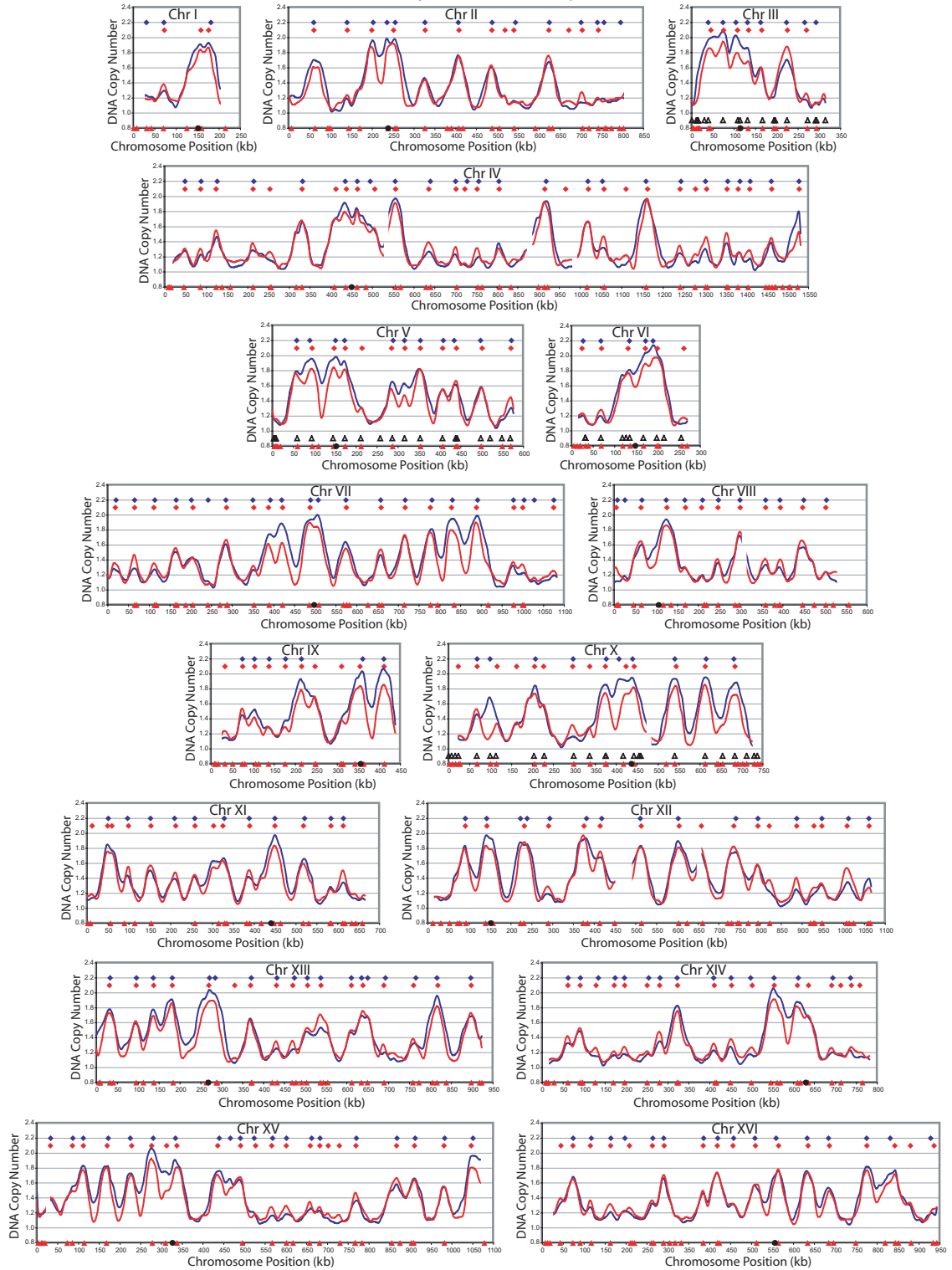


**Figure S6.** Replication timing in the S288c background strongly correlates with replication timing in the A364a background. Application of a peak finding algorithm to the S phase replication profiles in Figure S5 identified 212 origins in the S288c strain, YJL5038 and 231 origins in the A364a strain YJL5834 (*pGALI*). Origin usage during S phase was closely matched between the two strain backgrounds; 193 (92%) of origins identified in the S288c background were within 10kb of origins identified in the A364a background. The mean distance between these corresponding origins was 2.1 kb. For each shared origin, the S phase copy number in the A364a background was plotted against that for the S288c background. A linear regression line fitted to these points showed very strong correlation, with an  $R^2$  value of 0.92.

## Supplemental Figure 6

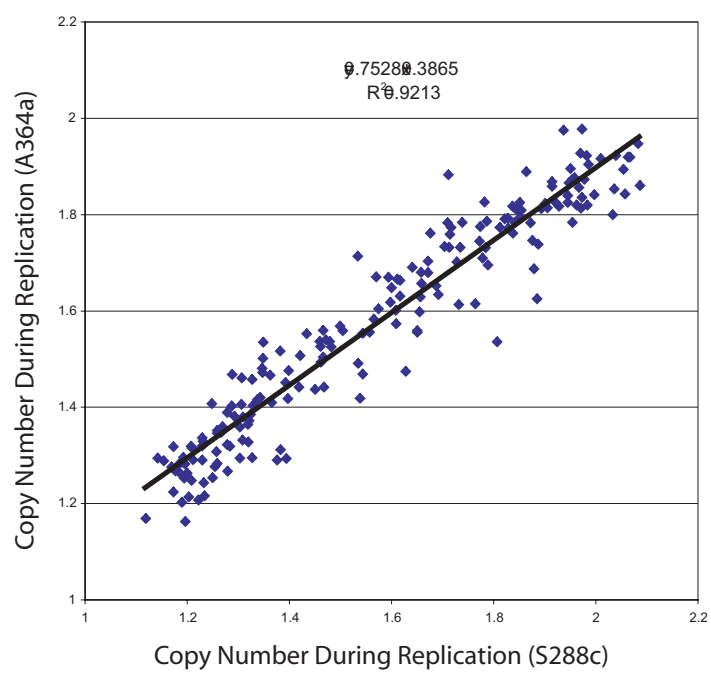


**Figure S7.** Re-replication induced during G2/M phase when ORC, Mcm2-7 and Cdc6 are deregulated. Genomic DNA was purified from the OMC strain YJL3248 (*orc2-cdk6A orc6-cdk4A MCM7-2NLS pGAL1- $\Delta$ ntcdc6 pMET3-HA3-CDC20*) and the control OM strain YJL3244 (*orc2-cdk6A orc6-cdk4A MCM7-2NLS pGAL1 pMET3-HA3-CDC20*) after 3 hr of galactose induction from G2/M arrest in an experiment described in Figure 2 (DNA content for the OMC strain was 2.7 C at 3 hr). The OMC G2/M phase re-replication profiles (blue lines, right axis), the positions of the 106 re-replicating peaks identified by application of a peak finding algorithm (blue diamonds), the OMC S phase replication profile (green line, left axis) and identified origins (green diamonds) replotted from Figure S3 are shown for all sixteen chromosomes. The locations of pro-ARSS mapped by Wyrick *et al.* (Wyrick *et al.*, 2001) (red triangles) and the centromeres (black circles) are marked along the X-axis. In the course of these experiments, we observed that the control OM strain YJL3244 (*orc2-cdk6A orc6-cdk4A MCM7-2NLS pGAL1 pMET3-HA3-CDC20*) contained a duplication of a region of chromosome IV (515kb to 645 kb) and that the OMC strain YJL3248 (*orc2-cdk6A orc6-cdk4A MCM7-2NLS pGAL1- $\Delta$ ntcdc6 pMET3-HA3-CDC20*) had an extra copy of chromosome XI in much of the population. Shown for chromosomes IV and XI are data from a replicate experiment using an isogenic OM strain YJL5493 (*orc2-cdk6A orc6-cdk4A MCM7-2NLS pGAL1 pMET3-HA3-CDC20*) and an isogenic OMC strain YJL3249 (*orc2-cdk6A orc6-cdk4A MCM7-2NLS pGAL1- $\Delta$ ntcdc6 pMET3-HA3-CDC20*), lacking these genomic alterations (yellow lines).



# Supplemental Figure 7

OMC S phase      OMC G2/M

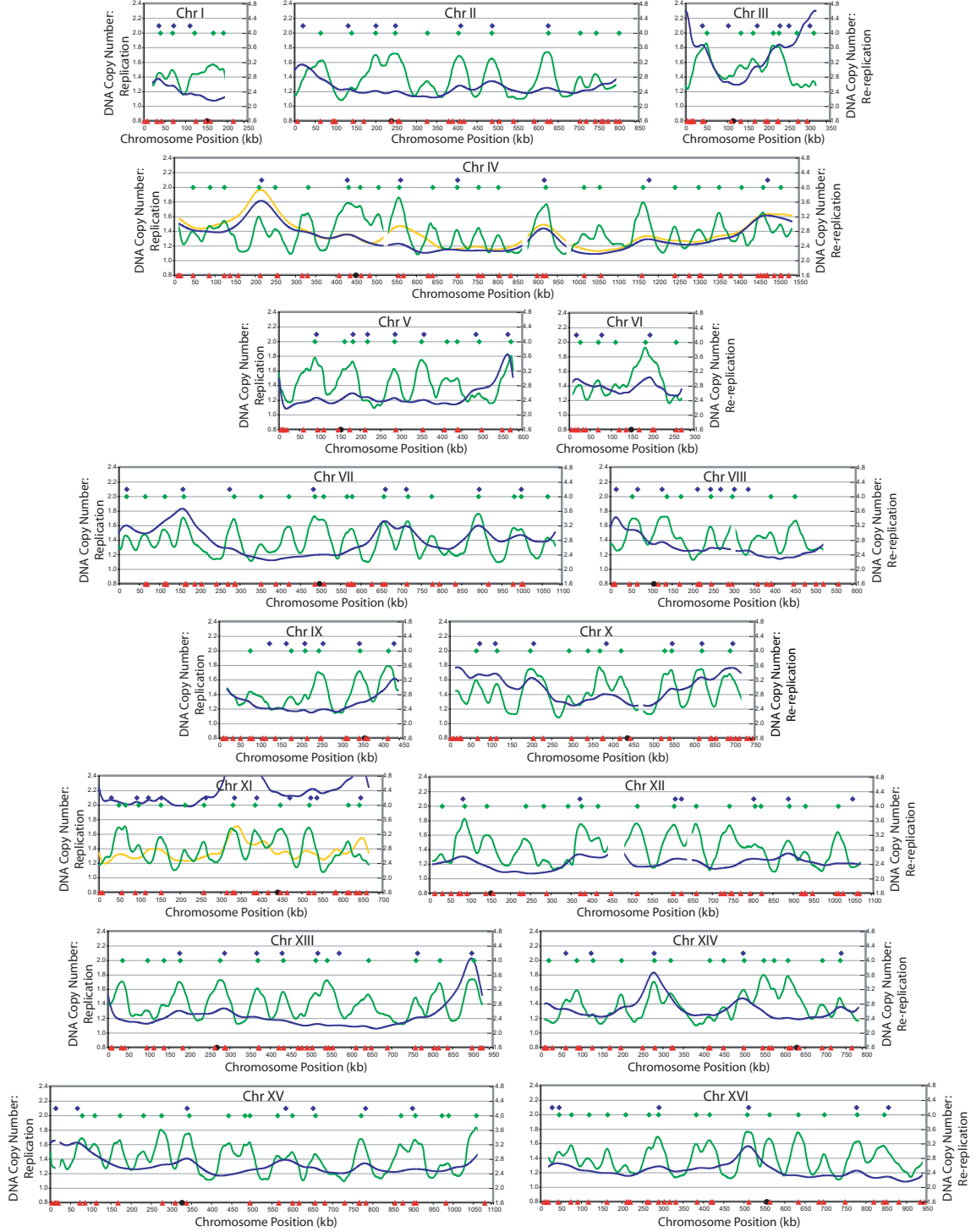


**Figure S8.** The observed mean distance from re-replication peaks to pro-ARSs is highly significant. When re-replication was induced in G2/M, 106 re-replicating origins were identified (Figure S7). The mean distance from those origins to the closest potential S phase origin defined by Wyrick *et al.* (Wyrick *et al.*, 2001) (pro-ARSs) was 7.0 kb. To determine the significance of this value, 106 random chromosomal loci were selected and the mean distance to the closest pro-ARS was calculated. This was repeated 100,000 times and a histogram was generated showing the percent of the random samples with the indicated mean distances. The actual observed mean, which is greatly below the expected random mean, is indicated with an arrow.

Supplemental Figure 8

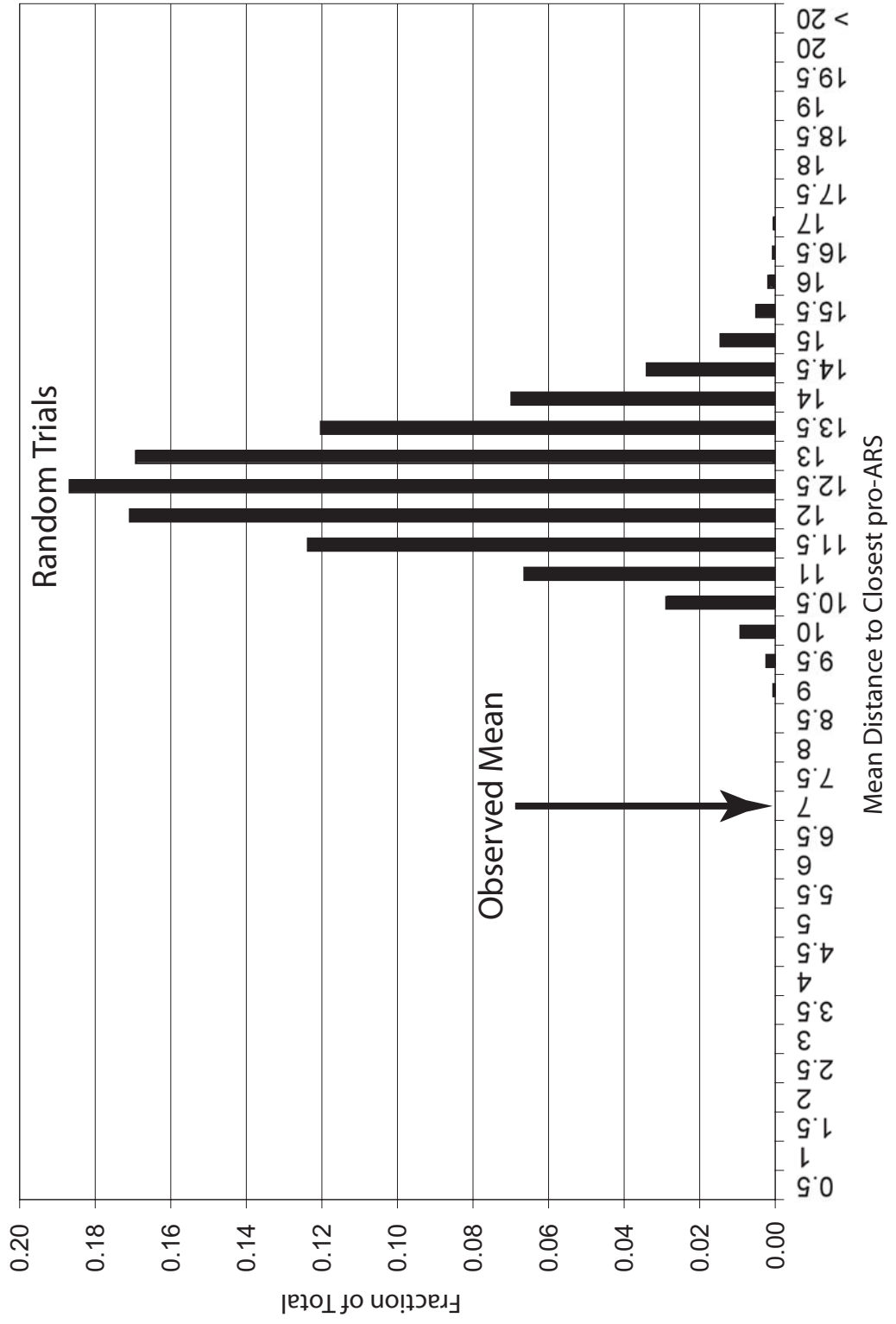


**Figure S9.** OMC cells can re-initiate and re-replicate within S phase. The OMC strain YJL3249 (*orc2-cdk6A orc6-cdk4A MCM7-2NLS pGAL1- $\Delta$ ntcdc6 pMET3-HA3-CDC20*) was induced to re-replicate while still in S phase in an experiment described in Figure 3. The cells were arrested in G1 phase with alpha factor, induced to express  $\Delta$ ntcdc6 by the addition of 2% galactose, then released from the arrest into YEPGal containing 100 mM hydroxyurea (HU) to delay cells from exiting S phase. Genomic DNA from the OMC strain was isolated at the 0 hr (G1 phase) and 4 hr (S phase, DNA content 1.4 C) time points and competitively hybridized against each other. The resulting profiles shown for all sixteen chromosomes reflect copy number increases due to both replication and re-replication. The locations of pro-ARs mapped by Wyrick *et al.* (Wyrick *et al.*, 2001) (red triangles) and the centromeres (black circles) are plotted along the X-axis.

# Supplemental Figure 9

OMC S Re-rep

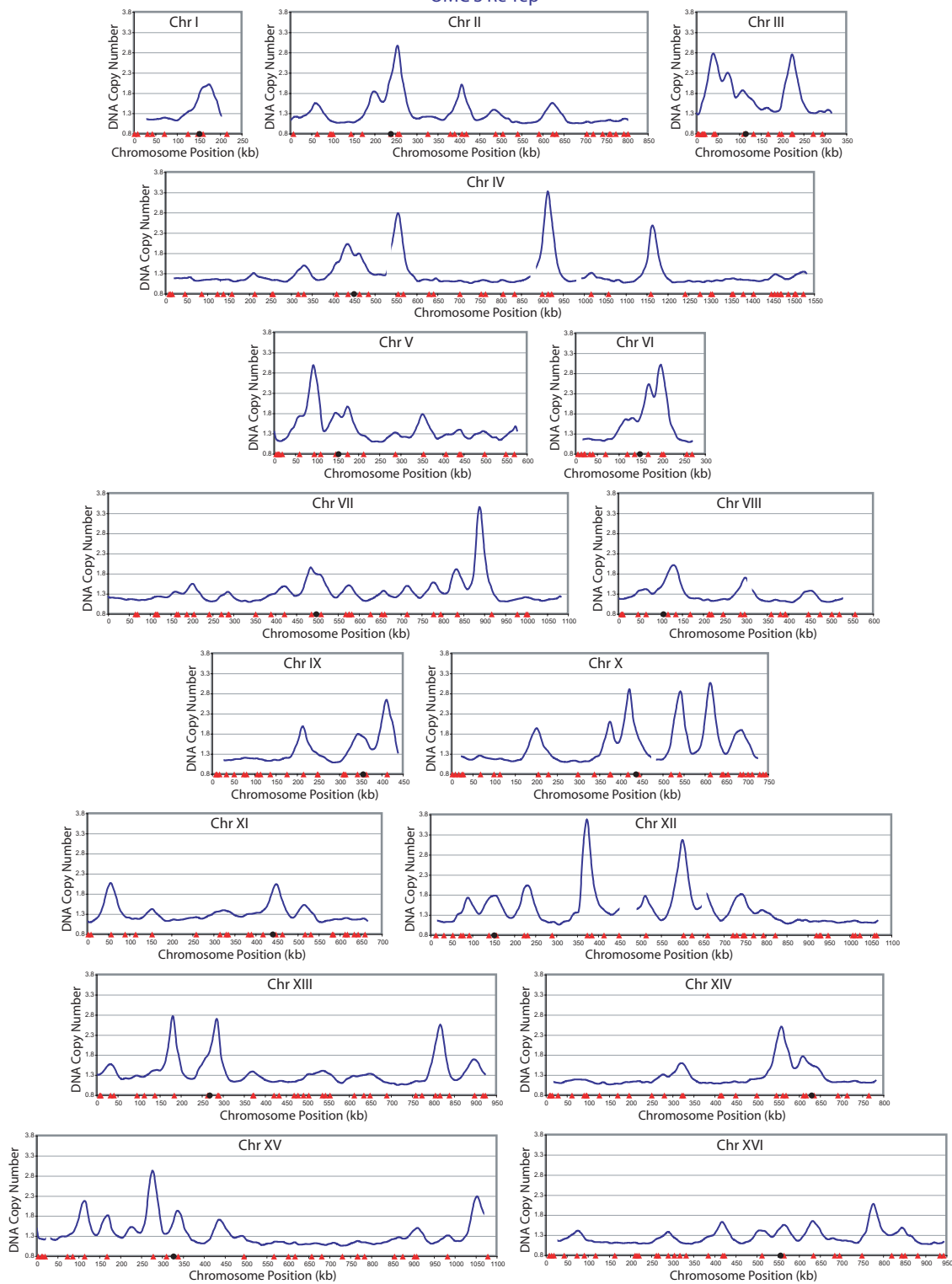


**Figure S10.** Re-replication induced upon release from a G1 arrest when ORC, Mcm2-7 and Cdc6 are deregulated. The OMC strain YJL3248 (*orc2-cdk6A orc6-cdk4A MCM7-2NLS pGAL1- $\Delta$ ntcdc6 pMET3-HA3-CDC20*) was induced to re-replicate during G1 release in an experiment described in Figure 4. Genomic DNA was purified from the OMC strain and the OM strain YJL3244 (*orc2-cdk6A orc6-cdk4A MCM7-2NLS pGAL1 pMET3-HA3-CDC20*) after 3 hr of galactose induction while cells were released from G1 into G2/M phase (DNA content for the OMC strain was 3.2 C at 3 hr). The two DNA preparations were labeled and competitively hybridized against each other to generate the OMC G1 release re-replication profiles shown for all sixteen chromosomes (blue lines) and to identify 87 re-replicating peaks (blue diamonds). The locations of pro-ARs mapped by Wyrick *et al.* (Wyrick *et al.*, 2001) (red triangles) and the centromeres (black circles) are plotted along the X-axis. In the course of these experiments, we observed the same genomic alterations of Chromosome IV and XI described in Figure S7. Shown for chromosomes IV and XI are data from a replicate experiment using an isogenic OM strain YJL5493 (*orc2-cdk6A orc6-cdk4A MCM7-2NLS pGAL1 pMET3-HA3-CDC20*) and an isogenic OMC strain YJL3249 (*orc2-cdk6A orc6-cdk4A MCM7-2NLS pGAL1- $\Delta$ ntcdc6 pMET3-HA3-CDC20*), lacking these genomic alterations (yellow lines).

# Supplemental Figure 10

OMC G1 to G2/M

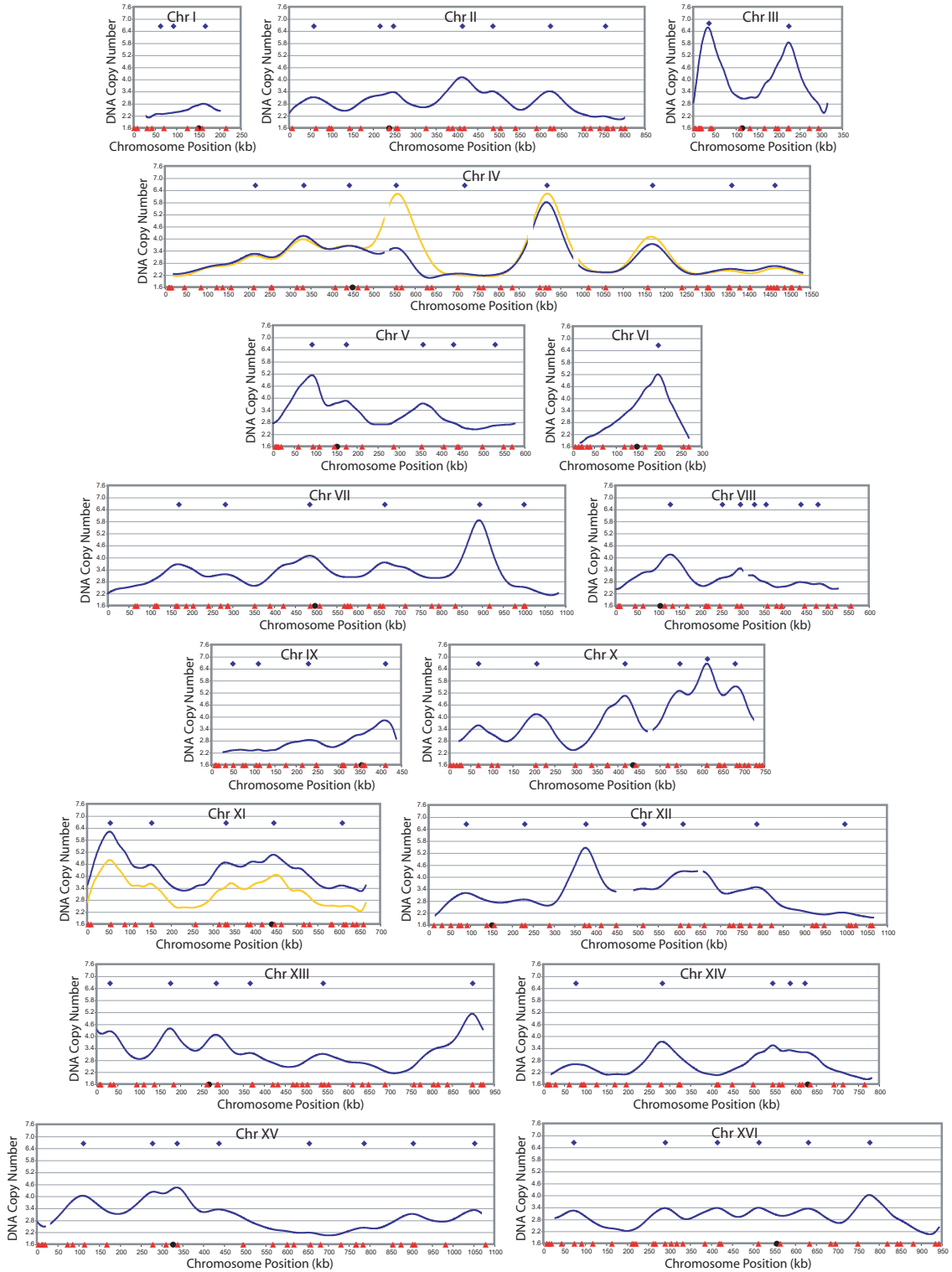


**Figure S11.** Re-replication can be induced when only ORC and Cdc6p are deregulated. The OC strain YJL3240 (*orc2-cdk6A orc6-cdk4A pGAL1- $\Delta$ ntcdc6 pMET3-HA3-CDC20*) and the control O strain YJL4832 (*orc2-cdk6A orc6-cdk4A pGAL1 pMET3-HA3-CDC20*) were induced to re-replicate in G2/M phase or during a G1 release in experiments described in Figures 5A and 5B, respectively. The DNA content of the OC strain was 2.0 C for the G2/M induction and 2.6 C for the G1 release. For each induction protocol, OC and O strain genomic DNA were prepared and competitively hybridized against each other as described in Figure 1A. Shown for all sixteen chromosomes are OC G2/M phase re-replication profiles (blue lines), OC G1 release re-replication profiles (green lines), locations of pro-ARs mapped by Wyrick *et al.* (Wyrick *et al.*, 2001) (red triangles), and centromeres (black circles).



# Supplemental Figure 11

OC G2/M      OC G1 to G2/M

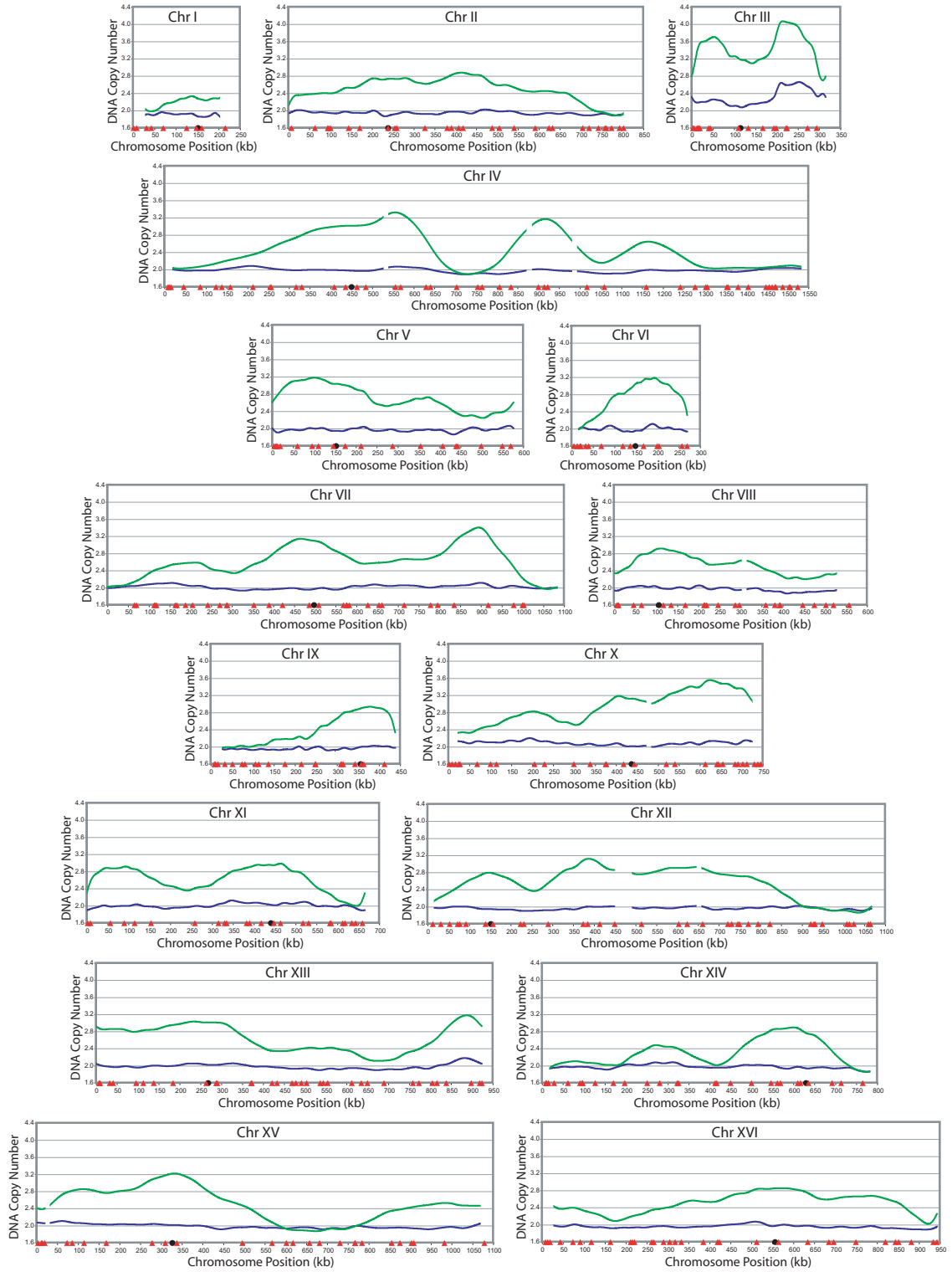


**Figure S12.** Re-replication occurs primarily on a single chromosome when Mcm2-7 and Cdc6 are deregulated. Re-replication in the MC<sub>2A</sub> strain occurs primarily on chromosome III. The MC<sub>2A</sub> strain YJL4489 (*MCM7-NLS pGAL1-Δntcdc6-cdk2A pMET3-HA3-CDC20*) and the control M strain YJL4486 (*MCM7-2NLS pGAL1 pMET3-HA3-CDC20*) were induced to re-replicate in G2/M phase or during a G1 release in experiments described in Figures 6A and 6B, respectively. The DNA content of the MC<sub>2A</sub> strain was 2.0 C for both the G2/M induction and for the G1 release. For each induction protocol, MC<sub>2A</sub> and M strain genomic DNA were prepared and competitively hybridized against each other as described in Figure 1A. Shown for all sixteen chromosomes are MC<sub>2A</sub> G2/M phase re-replication profiles (blue lines), MC<sub>2A</sub> G1 release re-replication profiles (green lines), locations of pro-ARs mapped by Wyrick *et al.* (Wyrick *et al.*, 2001) (red triangles) and the centromeres (black circles).

# Supplemental Figure 12

MC<sub>2A</sub> G2/M      MC<sub>2A</sub> G1 to G2/M

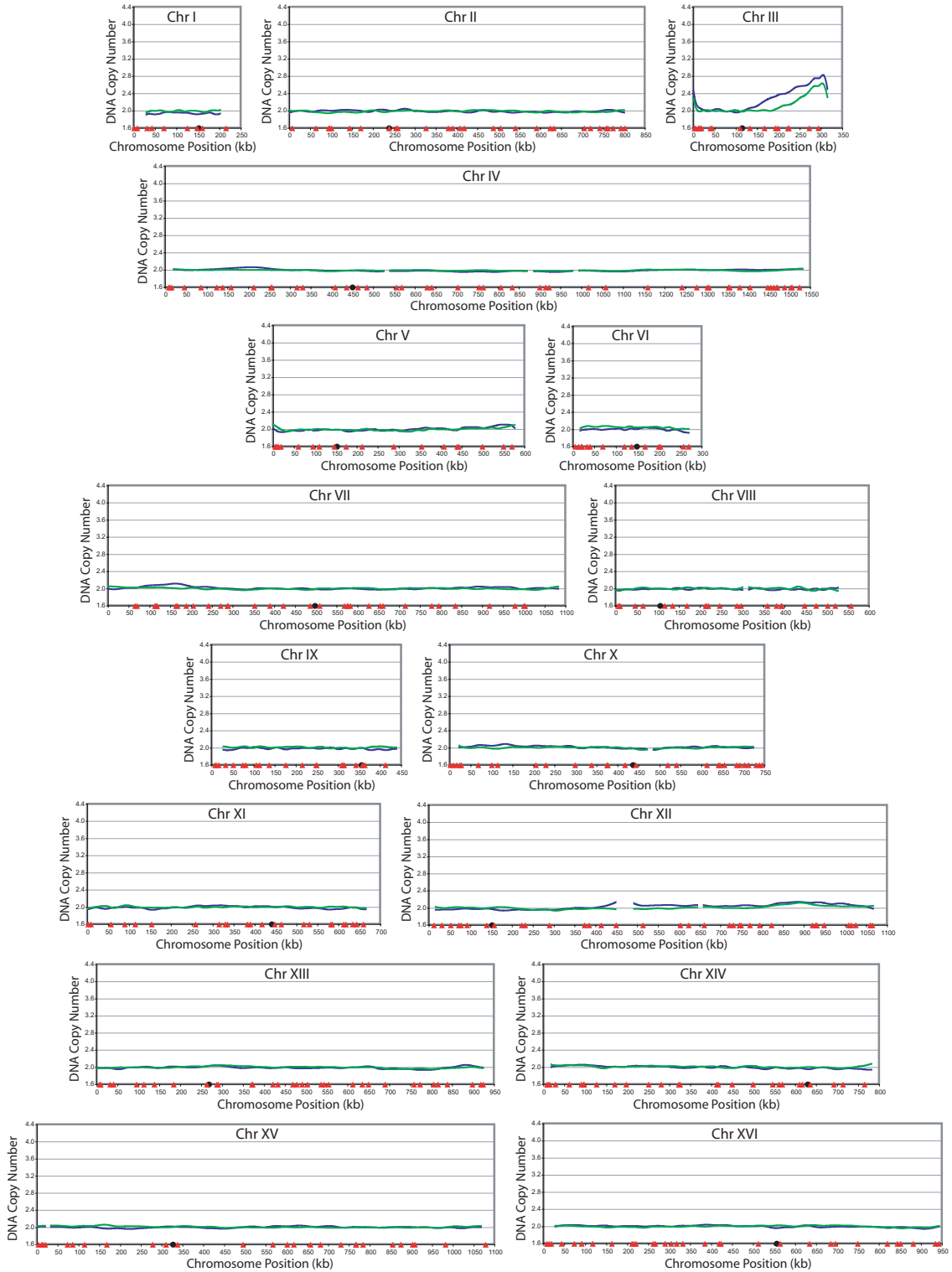
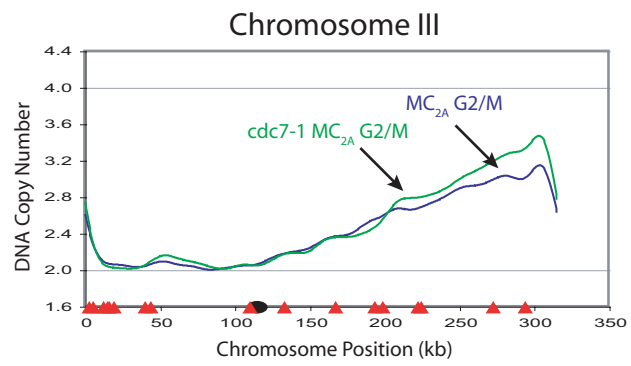


**Figure S13.**  $MC_{2A}$ -*cdc7* strain is competent to re-replicate at the permissive temperature. The  $MC_{2A}$  strain YJL4489 (*MCM7-2NLS pGAL1- $\Delta$ ntcdc6-2A pMET3-HA3-CDC20*), the congenic  $MC_{2A}$ -*cdc7* strain YJL5821 (*MCM7-2NLS pGAL1- $\Delta$ ntcdc6-2A pMET3-HA3-CDC20 cdc7-1*) and their respective controls, the M strain YJL4486 (*MCM7-2NLS pGAL1 pMET3-HA3-CDC20*) and the M-*cdc7* strain YJL5816 (*MCM7-2NLS pGAL1 pMET3-HA3-CDC20 cdc7-1*) were induced with galactose as described in Figure 7C, except that following the initial arrest at 23° C, the arrested cells were maintained at 23° C for 1 hr, before the addition of galactose. Genomic DNA was isolated 4 hr after galactose addition and competitively hybridized ( $MC_{2A}$  versus M and  $MC_{2A}$ -*cdc7* versus M-*cdc7*) as described in Figure 1A. Re-replication profiles for the  $MC_{2A}$  (blue line) and  $MC_{2A}$ -*cdc7* (green line) strains are shown for chromosome III. The locations of pro-ARs mapped by Wyrick *et al.* (Wyrick *et al.*, 2001) (red triangles), and the centromere (black circle) are plotted along the X-axis.

## Supplemental Figure 13



## **CHAPTER 7**

### **Supplemental data for Chapter 4**

## Supplemental Methods

### Plasmids

All plasmids are described in Supplemental Table 2. Plasmids pBJL2890 and pBJL2892 consist of the following fragments of DNA: Homology Left (SacI to StuI of PCR product from OJL1796 and OJL1797 for pBJL2890 and OJL1804 and OJL1805 for pBJL2892), kanMX6 (StuI to XmaI of pFA6a-pGAL1-3HA<sup>1</sup>), *ade3-2p* (XmaI to XbaI of pDK243<sup>2</sup>), *ARS317* (SpeI to XbaI of PCR product from OJL1794 and OJL1795 cloned into pCR2.1 TA TOPO), Homology Right (XbaI to NotI of PCR product from OJL1798 and OJL1799 for pBJL2890 and OJL1806 and OJL1807 for pBJL2892) and vector backbone (NotI to SacI of pRS56). Plasmids pBJL2889 and pBJL2891 consist of the same fragments except they lack the *ARS317* fragment.

### Strains

All strains are described in Supplemental Table 1. YJL6555, YJL6557, YJL6558 and YJL6561 were generated from YJL3758 (*Mat a ORC2-(NotI, SgrAI) ORC6 leu2 ura3-52::pGAL-delntcdc6-cdk2A(6,8), URA3} trp1-289 ade2 ade3 MCM7-2NLS bar1::LEU2*) by the integration of SacI to SalI from pBJL2889, pBJL2890, pBJL2891 or pBJL2892 followed by disruption of the endogenous *ARS317* with a PCR product of natMX from pAG25<sup>3</sup> with OJL1639 and OJL1640. YJL6974 and YJL6977 were generated from YJL3756 (*ORC2-(NotI, SgrAI) ORC6 leu2 ura3-52::pGAL, URA3} trp1-289 ade2 ade3 MCM7-2NLS bar1::LEU2*) by the integration of SacI to SalI from pBJL2890 or pBJL2892 followed by disruption of the endogenous *ARS317* with a PCR

product of natMX from pAG25<sup>3</sup> with OJL1639 and OJL1640. YJL7007 was generated from a mating of YJL3519 (*Mat @ ORC2-(NotI, SgrAI) ORC6 leu2 ura3-52 trp1-289 ade2 ade3 MCM7 bar1::LEU2*) to YJL3516 (*Mat a ORC2-(NotI, SgrAI) ORC6 leu2 ura3-52 trp1-289 ade2 ade3 MCM7 bar1::LEU2*) after integration of SacI to Sall from pBJL2890 into YJL3516. YJL7002 was generated from a mating of 4541-8-1<sup>4</sup> (*Mat @ leu2 ade2 ade3 his7 ura1 can1 sap3 gal1*) integrated with SacI to Sall of pBJL2980 to 4541-8-1 switched to *Mat a* with pSB283<sup>5</sup>. YJL7003 was generated similarly to YJL7002, but 4525-061<sup>4</sup> (*Mat @ cdc6-1 leu2 ade2 ade3 can1 sap3 his7 gal1*) was used instead of 4541-8-1. YJL7005 was generated similarly to YJL7002, but 4528-091<sup>4</sup> (*Mat @ cdc7-1 leu2 ade2 ade3 can1 sap3 ura1 his7 gal1*) was used instead of 4541-8-1. YJL7006 was generated similarly to YJL7002, but 4532-171<sup>4</sup> (*Mat @ cdc17-1 leu2 ade2 ade3 can1 sap3 ura1 his7 gal1*) was used instead of 4541-8-1. YJL7085 was generated similarly to YJL7002, but 4524-1-3<sup>4</sup> (*Mat @ cdc7-1 leu2 ade2 ade3 can1 sap3 ura1 his7 gal1*) was used instead of 4541-8-1.

## Junction PCR

To analyze novel junctions by PCR, DNA was prepared from 1.5ml of saturated culture using a modified Winston Hoffman DNA prep. Cells were pelleted in a screw cap tube and resuspended in 200ul of Winston-Hoffman Lysis buffer (2% Triton X-100, 1% SDS, 100mM NaCl, 10mM Tris.Cl pH8.0, 1mM EDTA pH8.0). 200 ul of glass beads and 200 ul of phenol/chloroform were added and the tubes were vortexed in a Tomy multi mixer (setting of 7) for 10 minutes at room temperature. 450 ul 1x TE was added to each tube, they were mixed well and spun in a microfuge at top speed for 3



minutes. 500 ul of the top layer was transferred to new screw cap tubes containing 10 ul of RNase A (10mg/ml) and incubated at 23°C for 2 hours. 300 ul of phenol/chloroform was added to each tube, they were vortexed in Tomy mixer for 5 minutes and then spun again at top speed for 3 minutes. 400 ul of the top layer was transferred to new Eppendorf tubes containing 300 ul chloroform, vortexed, and spun at top speed for 3 minutes. 300 ul of the top layer was transferred to new Eppendorf tubes containing 3 ul 10N ammonium acetate pH7.0 and 750 ul 100% ethanol. Tubes were vortexed well, then spun at top speed for 7 minutes. The DNA pellet was washed with 300ul of 70% ethanol, dried and resuspended 15 ul TE. 0.5ul of DNA was subjected to PCR with 2.5ul Roche Long Template Buffer, 1.25ul 10uM of each oligo described in Supplemental Table 3, 2.5ul 5mM dNTPs, 0.25 Roche Expand polymerase and up to 25ul H<sub>2</sub>O. The conditions were 94°C for 3m, then 30 cycles of 94°C for 30s, 60°C for 1m, 68°C for 15m, and finally 68°C for 10m.

## References

1. Longtine, M. S. et al. Additional modules for versatile and economical PCR-based gene deletion and modification in *Saccharomyces cerevisiae*. *Yeast* **14**, 953-61 (1998).
2. Koshland, D., Kent, J. C. & Hartwell, L. H. Genetic analysis of the mitotic transmission of minichromosomes. *Cell* **40**, 393-403 (1985).
3. Goldstein, A. L. & McCusker, J. H. Three new dominant drug resistance cassettes for gene disruption in *Saccharomyces cerevisiae*. *Yeast* **15**, 1541-53 (1999).

4. Palmer, R. E., Hogan, E. & Koshland, D. Mitotic transmission of artificial chromosomes in cdc mutants of the yeast, *Saccharomyces cerevisiae*. *Genetics* **125**, 763-74 (1990).
5. Berlin, V., Brill, J. A., Trueheart, J., Boeke, J. D. & Fink, G. R. Genetic screens and selections for cell and nuclear fusion mutants. *Methods Enzymol* **194**, 774-92 (1991).

**Supplemental Table 1** – Strains used in this study

YJL Number	Genotype	Source
YJL6555	ORC2-(NotI, SgrAI) ORC6 leu2 ura3-52:: {pGAL-delIntcdc6-cdk2A(6,8), URA3} trp1-289 ade2 ade3 MCM7-2NLS bar1::LEU2 ChromIV 567kb:: {ade3-2p, kanMX} ars317::natMX	This study
YJL6557	ORC2-(NotI, SgrAI) ORC6 leu2 ura3-52:: {pGAL-delIntcdc6-cdk2A(6,8), URA3} trp1-289 ade2 ade3 MCM7-2NLS bar1::LEU2 ChromIV 1089kb:: {ade3-2p, kanMX} ars317::natMX	This study
YJL6558	ORC2-(NotI, SgrAI) ORC6 leu2 ura3-52:: {pGAL-delIntcdc6-cdk2A(6,8), URA3} trp1-289 ade2 ade3 MCM7-2NLS bar1::LEU2 ChromIV 567kb:: {ade3-2p ARS317, kanMX} ars317::natMX	This study
YJL6561	ORC2-(NotI, SgrAI) ORC6 leu2 ura3-52:: {pGAL-delIntcdc6-cdk2A(6,8), URA3} trp1-289 ade2 ade3 MCM7-2NLS bar1::LEU2 ChromIV 1089kb:: {ade3-2p ARS317, kanMX} ars317::natMX	This study
YJL6974	ORC2-(NotI, SgrAI) ORC6 leu2 ura3-52:: {pGAL, URA3} trp1-289 ade2 ade3 MCM7-2NLS bar1::LEU2 ChromIV 567kb:: {ade3-2p ARS317, kanMX} ars317::natMX	This study
YJL6977	ORC2-(NotI, SgrAI) ORC6 leu2 ura3-52:: {pGAL, URA3}	This study

	trp1-289 ade2 ade3 MCM7-2NLS bar1::LEU2 ChromIV 1089kb::{ade3-2p ARS317, kanMX} ars317::natMX	
YJL7002	leu2/leu2 ade2/ade2 ade3/ade3 gal1/gal1 ura1/ura1 his7/his7 sap3/sap3 can1/can1 ChromIV 567kb/ChromIV 567kb::{ade3- 2p ARS317, kanMX}	This study
YJL7003	cdc6-1/cdc6-1 leu2/leu2 ade2/ade2 ade3/ade3 his7/his7 gal1/gal1 can1/can1 sap3/sap3 ChromIV 567kb/ChromIV 567kb::{ade3-2p ARS317, kanMX}	This study
YJL7005	cdc9-1/cdc9-1 leu2/leu2 ade2/ade2 ade3/ade3 his7/his7 sap3/sap3 gal1/gal1 ura1/ura1 can1/can1 ChromIV 567kb/ChromIV 567kb::{ade3-2p ARS317, kanMX}	This study
YJL7006	cdc17-1/cdc17-1 leu2/leu2 ade2/ade2 ade3/ade3 his7/his7 sap3/sap3 gal1/gal1 ura1/ura1 can1/can1 ChromIV 567kb/ChromIV 567kb::{ade3-2p ARS317, kanMX}	This study
YJL7007	ORC2-(NotI, SgrAI)/ORC2-(NotI, SgrAI) ORC6/ORC6 leu2/leu2 ura3-52/ura3-52 trp1-289/trp1-289 ade2/ade2 ade3/ade3 MCM7/MCM7 bar1::LEU2/bar1::LEU2 ChromIV 567kb/ChromIV 567kb::{ade3-2p ARS317, kanMX}	This study
YJL7085	cdc6-1/cdc6-1 leu2/leu2 ade2/ade2 ade3/ade3 his7/his7 gal1/gal1 can1/can1 sap3/sap3 ChromIV 567kb/ChromIV 567kb::{ade3-2p ARS317, kanMX}	This study

**Supplemental Table 2** – Plasmids used in this study

Name	Description	Source
pBJL2889	ade3-2p, kanMX6 at IV_567	This study
pBJL2890	ade3-2p, kanMX6, ARS317 at IV_567	This study
pBJL2891	ade3-2p, kanMX6 at IV_1089	This study
pBJL2892	ade3-2p, kanMX6, ARS317 at IV_1089	This study
pSB283	pGAL-HO, LEU2, URA3, CEN4	Berlin, 1991 <sup>5</sup>

**Supplemental Table 3** – Oligonucleotides used in this study

Name	Sequence	Purpose
OJL1639	ATTAAACAATGTTTGATTTTTTAAAT CGCAATTTAATACCcggatccccgggtaattaa	<i>ars317::natMX</i>
OJL1640	ATTTTTATGGAAGATTAAGCTCATAA CTTGGACGGGGATCcatcgatgaattcgagctcg	<i>ars317::natMX</i>
OJL1757	CAAAAGCATTCAAGGTCACG	<i>ADE3</i> probe
OJL1758	TCAATTCGCCAATGTTGGTG	<i>ADE3</i> probe
OJL1794	gctcaaatgggtttaaacACTAGTACTTAAAAA AACTG	<i>ARS317</i> for cloning
OJL1795	gctcaaatgggtttaaacCCAGGAGTACCTGCG CTTAT	<i>ARS317</i> for cloning
OJL1796	gctcaaatggaagcttaggcctGTTGGTGTCGGTA AAGAAAA	Homology Left for pBJL2889 and pBJL2890
OJL1797	gctcaaatgggagctcTACAAAATTGGGGAT CATGG	Homology Left for pBJL2889 and pBJL2890
OJL1798	gctcaaatgggcccgcAAATGCCTTGAGA GTTAGCC	Homology Right for pBJL2889 and pBJL2890
OJL1799	gctcaaatggaagctttctagaAGGTGTAGGCTC AAAACATA	Homology Right for pBJL2889 and pBJL2890
OJL1804	gctcaaatggaagcttaggcctGAATAAACAGAC ACTTCCTG	Homology Left for pBJL2891 and pBJL2892
OJL1805	gctcaaatgggagctcATGGAGGAACCTAAGC	Homology Left for

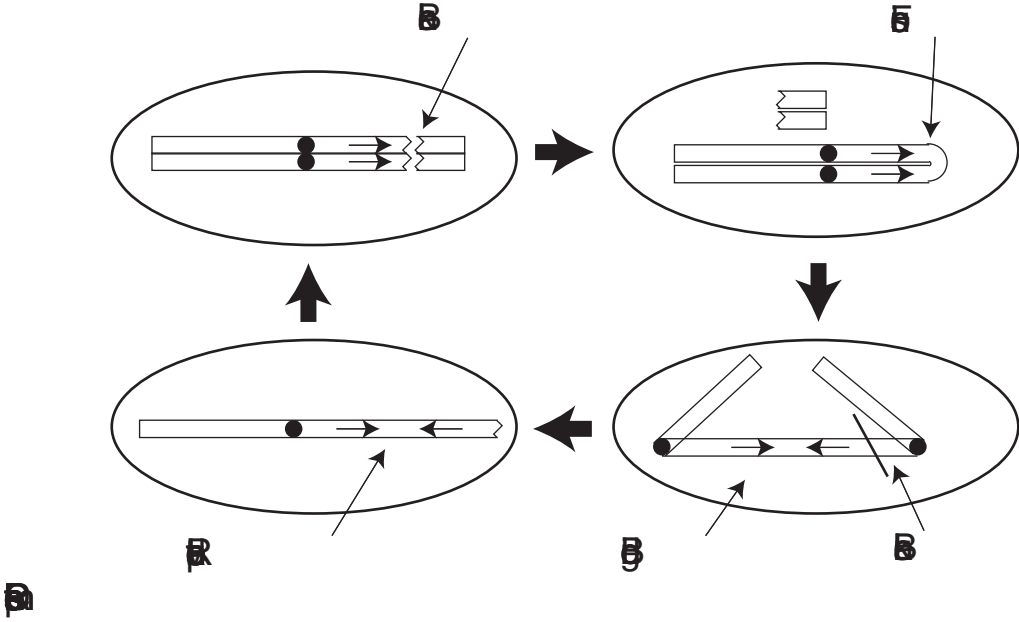
	CTTC	pBJL2891 and pBJL2892
OJL1806	gctcaaatgggcccgcGAGGAGGATCACTT CTGCCC	Homology Right for pBJL2891 and pBJL2892
OJL1807	gctcaaatggaagctttctagaATAGGTGAGGGA ACACCTCA	Homology Right for pBJL2891 and pBJL2892
OJL1955	TCATGCTTTTGAGTAACGGGTAATGA CATACTTAGTGAC	Primer 1 for junction PCR
OJL1956	CTCTTCTTTACAGAAATACAAAAGGC ATGCTGATTGTTGG	Primer 2 for junction PCR
OJL1957	ACTGATGGTTCAACAGAGAAGCCAC AGTTAAAAAAGGTCC	Primer 3 for junction PCR (all sectors but Figure 2B class 4)
OJL1958	TAGGAAAACGTA CTGTGATTTTGAAT ACACTGGAATAGGG	Primer 4 for junction PCR (all sectors but Figure 2B class 4)
OJL1983	TTCACGATCCAAGCACTATTTGCCAT TTTTGTGCCCTTTC	Primer 3 for junction PCR (Figure 2B class 4)
OJL1984	GCGAGGCAGGCACCTAGTCTCTAAAC CCTTCATATTGATC	Primer 4 for junction PCR (Figure 2B class 4)

**Supplemental Figure 1 – Breakage fusion bridge cycles**

A schematic of breakage fusion bridge cycles is shown. Breakage through both sister chromatids, or a break in G1 phase of the cell cycle, (upper left) can result in fusion of the two sisters (upper right). This results in a dicentric chromosome, a mitotic bridge resulting from attempted segregation (lower right), then resolution by breakage. The resulting asymmetric chromosomes result in duplication of the region centromeric to the break and loss of the region telomeric. The amplicon is arranged in an inverted orientation (lower left). Replication of this DNA results in two sister chromatids with a break in each – allowing the structure to be repeated (upper left) until a telomere is captured.



# Supplemental Figure 1



**Supplemental Figure 2** – Re-replication induces segmental duplications at another locus

A) Re-replication induces gene amplifications. YJL6977, YJL6557, and YJL6561 were assayed for gene amplification frequencies as described in Figure 1C.

All strains were *MCM7-2NLS ars317Δ ade3 ade2 Chromosome IV 1089kb::ade3-2p cassette*. Distinguishing alleles are indicated, with *ARS317* referring to the presence of the origin in the *ade3-2p* cassette. The mean and standard error of the mean of at least two independent experiments is shown.

B) Amplification events induced by re-replication involve segmental duplications. Representative sectors identified in Supplemental Figure 2A from YJL6561 were analyzed by array CGH using non-replicating reference DNA from YJL6032.

C) Summary of segmental duplication amplification events induced by re-replication. 24 sectors identified in Supplemental Figure 2A were analyzed by aCGH and schematics of the amplicons are shown. Bold lines indicate the amplified region for each class of amplicon. Asterisks indicate breakpoints of amplicons that appeared to occur at long terminal repeats, rather than full Ty elements. The plus symbol indicates the one breakpoint that does not appear to correspond to a previously described Ty or long terminal repeat.



**Publishing Agreement**

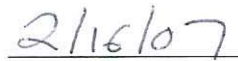
*It is the policy of the University to encourage the distribution of all theses and dissertations. Copies of all UCSF theses and dissertations will be routed to the library via the Graduate Division. The library will make all theses and dissertations accessible to the public and will preserve these to the best of their abilities, in perpetuity.*

***Please sign the following statement:***

*I hereby grant permission to the Graduate Division of the University of California, San Francisco to release copies of my thesis or dissertation to the Campus Library to provide access and preservation, in whole or in part, in perpetuity.*



Author Signature



Date